SEMMELWEIS EGYETEM

DOKTORI ISKOLA

Ph.D. értekezések

2876.

GÖCZ BALÁZS GERGŐ

Neuroendokrinológia
című program

Programvezető: Dr. Fekete Csaba, vezető kutató

Témavezető: Dr. Hrabovszky Erik, vezető kutató

Transcriptomic studies of kisspeptin neurons to reveal the molecular mechanisms of hypothalamic estrogen feedback

PhD thesis

Balázs Gergő Göcz

János Szentágothai Doctoral School of Neurosciences

Semmelweis University

Supervisor:	Erik Hrabovszky, MD, D.Sc
Official reviewers:	Árpád Dobolyi MD, D.Sc
	László Ákos Kovács, MD, Ph.D
Head of the Complex Examination	
Committee:	András Csillag, MD, D.Sc
Members of the Complex Examination	
Committee:	Krisztina Kovács, D.Sc
	Tamás Ruttkay MD, Ph.D

Budapest

2023

Table of contents

4

List of Abbreviations

AP-1	Activator protein 1
ARC	Arcuate nucleus
AVPV	Anteroventral periventricular nucleus of the hypothalamus
cAMP	Cyclic adenosine monophosphate
ChAT	Choline acetyltransferase
CHH	Congenital hypogonadotropic hypogonadism
CPM	Count per million
CPU	Caudate-putamen
DAG	Diacylglycerol
DBD	DNA-binding domain
DCV	Dense-core vesicle
DEPC	Diethylpyrocarbonate
E2	17β-estradiol
EGF	Epidermal growth factor
ERα	Estrogen receptor alpha
ERβ	Estrogen receptor beta
ERE	Estrogen-response element
EtOH	Ethyl alcohol
FDR	False Discovery Rate
FSH	Follicle-stimulating hormone
GABA	γ-Aminobutyric acid
GDP-β-S	G-protein inhibitor Guanosine 50-[β;-thio] diphosphate

GnRH	Gonadotropin-releasing hormone
GPR30	G protein-coupled receptor for estrogen
GPR54	G-protein coupled receptor 54
HPG	hypothalamic-pitutary-gonadal axis
KEGG	Kyoto Encyclopedia of Genes and Genomes
KP	Kisspeptin
KP^{ARC}	Arcuate kisspeptin neurons
KP^{RP3V}	Rostral periventricular area of ventricle III kisspeptin neurons
KYN	Kynurenic acid
LCM	Laser capture microdissection
LBD	Ligand-binding domain
LH	Luteinizing hormone
MAPK	Mitogen-activated protein kinase
MBH	Mediobasal hypothalamus
ME	Median eminence
mER	Membrane-associated estrogen receptor
MS	Medial septal nucleus
NKB	Neurokinin B
ORA	Over-representation analysis
OVLT	Organum vasculosum laminae terminalis
OVX	Surgical ovariectomy
PIC	Picrotoxin
RIN	RNA integrity number

RP3V	Rostral periventricular area of ventricle III
SERT	Serotonin transporter
SPIA	Signaling Pathway Impact Analysis
TAC3	Tachykinin 3
TAC3R	Tachykinin 3 receptor
TF	Transcription factor

1. Introduction

1.1. The central regulation of reproduction in mammals

In mammals, fertility and reproduction are regulated by the hormones of the hypothalamic-pituitary-gonadal (HPG) axis. Hypothalamic gonadotropin-releasing hormone (GnRH) neurons, which represent the uppermost element of this axis, release their neurohormone product GnRH into the portal circulation of the anterior pituitary in the form of secretory pulses. There is a notable similarity between mammals in the pattern of pulsatile GnRH secretion, with a pulse produced hourly during the follicular/diestrous phase and every 3-4 hours after ovulation during the luteal/estrous phase of the cycle (1).
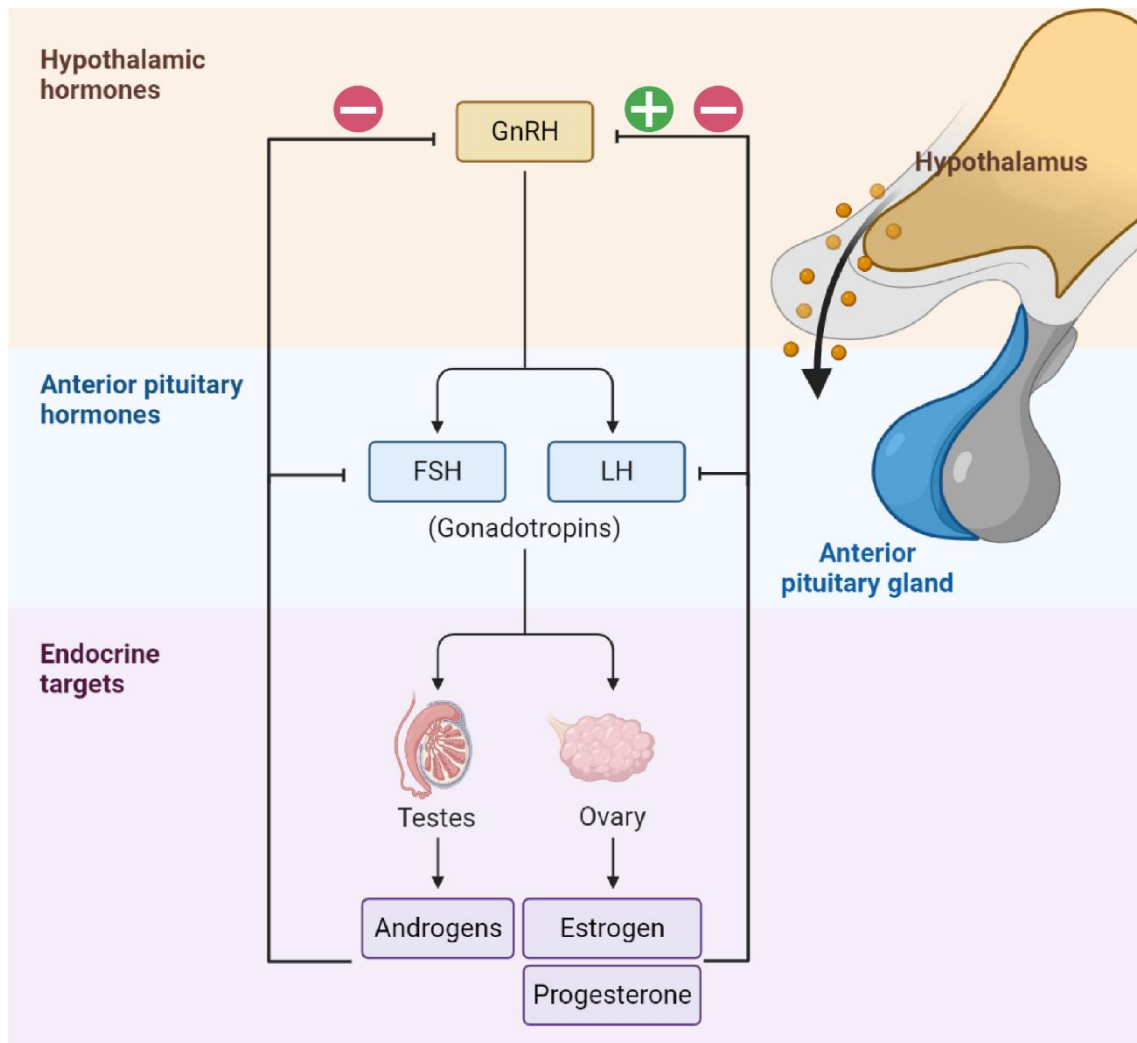
Figure 1. Role of sex steroids in the feedback regulation of the hypothalamic-pituitary-gonadal axis. *In mammals, the neuroendocrine regulation of reproduction can*

occur in three hierarchical levels: the hypothalamus, the pituitary gland, and the gonads (ovaries in females and testes in males). The hypothalamus releases GnRH into the portal circulation of the pituitary gland, which, in turn, stimulates the secretion of luteinizing hormone (LH) and follicle-stimulating hormone (FSH) from the adenohypophysis. These two gonadotrop hormones then stimulate gametogenesis and the production of sex steroids, such as estrogens and progestogens in females and testosterone in males. Among estrogens, 17β-estradiol (E2) is the most potent hormone. E2 regulates target cells in reproductive as well as non-reproductive organs and also exerts negative and positive feedback effects at higher levels of the axis. Modified from Biorender.

The synthesis and secretion of the two adenohypophysial gonadotropic hormones, LH and FSH, depend on the secretion pattern of GnRH. In the absence of pulsatile GnRH release, the secretion of FSH and LH also stops. FSH and LH act in the gonads and stimulate gametogenesis and the production of sex steroid hormones, including androgens, estrogens and progesterone. (2-4) Sex hormones regulate various biological functions throughout the body via acting on sex steroid receptor expressing target cells. They play essential roles in the hypothalamic regulation of reproduction, energy balance, internal temperature, circadian rhythms, and stress responses (5).

Gonadal sex steroids in males and for most of the reproductive cycle also in females, exert inhibitory effects on the hormone release of GnRH neurons. In females, this negative feedback effect is exerted mostly by estrogens and becomes interrupted shortly in the middle of the reproductive cycle by the positive feedback effect of a sustained increase in serum estrogen levels. This shift from negative to positive estrogen feedback leads to increased GnRH neuron activity, resulting in a preovulatory surge of GnRH and LH (6-8).

1.2.   The GnRH neuronal system

GnRH neurons are a peculiar group of cells as they originate from outside the central nervous system. GnRH neurons develop in the medial part of the nasal placode and migrate to the preoptic area and the mediobasal hypothalamus before birth (5, 9). A defect in the prenatal migration of GnRH neurons results in hypogonadotropic hypogonadism. In this disorder, sexual maturation is absent or partial (10). GnRH neurons in mice and rats are sparsely distributed in several areas, including the Diagonal band of Broca, the

medial septum, the medial preoptic area, the organum vasculosum laminae terminalis (OVLT), and the median preoptic nucleus. The number of these neurons is extremely small, ranging from 1000 to 1500 (11). The GnRH neurons in humans is even less compact than in rodents, with a considerable proportion of cell bodies located in the posterior hypothalamus, which includes the infundibular nucleus (also known as the arcuate nucleus; ARC) (12).

The primary target areas of GnRH fiber projections are the OVLT and the outer zone of the median eminence (ME), regions lacking the blood-brain barrier (13, 14). In the ME, GnRH is secreted from the axon terminals into the fenestrated capillaries of the pituitary portal circulation. Portal veins carry GnRH to the anterior lobe of the pituitary where it binds to GnRH receptors and stimulates the production and secretion of the gonadotropic hormones (LH and FSH) (15-17). GnRH fiber projections are dendrite-like in that they are relatively large in diameter and receive a significant number of synaptic inputs. On the other hand, these fibers also exhibit axonal characteristics and are capable of conducting action potentials to the GnRH neurosecretory terminals located in the ME. Because of their dual characteristics, GnRH fibers targeting the ME are often referred to as dendrons (16, 18).

1.2.1. Pulsatile secretion of GnRH/LH

Pulsatile GnRH and LH secretion first appears in late fetal life after GnRH neuronal migration from the nasal cavity into the brain has been completed. After birth, GnRH secretion increases temporarily, inducing a short-lived steroid synthesis in the gonads, especially in males. After this 'minipuberty' (lasting 3-6 months in humans), the pulsatile secretion of GnRH (and LH) becomes abolished and inhibited until the onset of puberty. The exact background of the prepubertal inhibition and pubertal reawakening of the GnRH/LH pulse generator are still largely unknown (19). The rhythmic pattern of GnRH release has been demonstrated by various strategies, including the portal bleeding method and perfusion techniques that measure GnRH in the ME (20, 21). These studies establish a strong temporal relationship between pulsatile GnRH secretion and pulsatile LH secretion and also find that a single pulse occurs every 45 to 60 minutes during the late follicular phase of the ovarian cycle, whereas the frequency slows considerably following ovulation (in the luteal phase in primates) (1). The GnRH pulse is sharp and rapid,

mimicking a "square wave" and consists of a 50-fold increase in GnRH secretion within two minutes. Then it reaches a plateau phase for the next 4 to 5 minutes, before GnRH secretion suddenly declines over three minutes (22, 23).

The mechanism of pulse generation is not fully understood. Two major hypotheses raised in the literature propose the involvement of intrinsic and extrinsic mechanisms, (1). According to the intrinsic pulse generation concept, the interconnected GnRH neurons temporarily synchronize their activity to produce periodic hormonal pulses. Several studies with GnRH-producing cell lines supported this idea. The authors of the *in vitro* experiments found that the GnRH producing GT1-7 cells can synchronize their activity, which is associated with hormone secretion (24-26). However, the fact that cell bodies of real GnRH neurons are widely dispersed throughout the brain suggests that *in vivo* synchronization is unlikely to occur through gap junctions and/or humoral communication observed *in vitro*. Interactions between GnRH neurons in the brain seem to be far more complex. Despite experimental proof from acute brain slice electrophysiology and results of optogenetic studies indicate that GnRH neurons can synchronize their activity *in vivo*. However, there is no compelling evidence to indicate that synchronous activation of GnRH neurons would result in LH secretion (27, 28).

Interestingly, it also occurs that the communication or synchrony between GnRH cell bodies is not even an essential requirement for the pulsatile release of GnRH to occur at the ME. Acute hypothalamic tissue preparations lacking GnRH cell bodies can still exhibit pulsatile GnRH secretion for several hours (29). Therefore, other mechanisms are likely involved in coordinating pulsatile GnRH releases, such as synchronization between neurosecretory GnRH processes and/or interactions of these GnRH dendrons with other types of neurons or glial cells in the mediobasal hypothalamus (MBH) (30).

The extrinsic model proposes that GnRH neurons do not have direct interactions with each other. Instead, the synchronization of GnRH neuron activity is generated by a separate group of neurons upstream from the GnRH system. In other words, synchronization does not result from interactions between GnRH neurons, but from a separate population of neurons that generate a synchronized pattern of activity. This synchronized signal is thought to activate enough GnRH neurons to generate a pulse of

GnRH. The extrinsic pulse generator is likely located in the ARC and acts on the distal dendrons of GnRH neurons, at least in rodents (1).

1.2.2. The preovulatory GnRH/LH surge

When the frequency of GnRH secretory pulses and the amount of GnRH released per unit of time increase, a GnRH surge occurs. At the same time, gonadotrope cells in the adenohypophysis increase their GnRH receptor expression and become more responsive to GnRH. The surge of GnRH caused by the rising E2 levels induces a corresponding surge of LH in the pituitary. LH reaches the ovary through systemic circulation and initiates ovulation (8, 23, 31). Additional hormonal interactions and mechanisms acting at different levels of the reproductive axis are complex and involve many other players. To understand the underlying mechanism of the pulsatile secretion and the GnRH/LH surge, we have to direct our focus to estrogens which are crucial hormones in the neuroendocrine regulation of reproduction.

1.3. Estrogens

1.3.1. Sources of estrogen hormones

Estrogen biosynthesis from cholesterol occurs through well-described and characterized enzymatic steps. The last step is the conversion of androgens to estrogens by aromatase. In the female body, the main sites of estrogen production are the ovarian follicles, the corpus luteum (following ovulation) and the placenta (during pregnancy). The major form of estrogens is E2. In men, estrogen production mainly takes place in the testes. Smaller amounts of estrogen are also produced in the liver, the adrenal glands, and the brain (32). It is interesting to note that testosterone can be converted to E2 in males. Hence, many of the known biological effects of male sex steroids can also be exerted via estrogen receptor-mediated signaling (33).

1.3.2. Estrogen receptors

Estrogen receptors belong to the nuclear hormone receptor superfamily. These classical estrogen receptors are ligand-dependent transcription factors (TFs), located intracellularly partly in the cytoplasm and partly in the cell nucleus (34). Members of the nuclear hormone receptor superfamily have a characteristic multidomain structure, with individual domains responsible for functions that are essential for hormone response.

Estrogen receptors have six domains out of which the ligand-binding domain (LBD) and the DNA-binding domain (DBD) play key roles in high-affinity binding of E2 and the estrogen-response element (ERE) of target genes, respectively (35). While the consensus ERE consists of a 13-base pair inverted repeat sequence (GGTCAnnnTGACC), most ERE sequences deviate from this consensus by containing one or more variations (36).

The major types of estrogen receptor signaling include genomic, tethered, non-genomic, and ligand-independent mechanisms. The genomic process, following estrogen binding ER undergoes conformational changes, translocates to the nucleus, dimerizes, and binds to ERE -containing regions of the DNA to regulate the transcription of target genes (37) (38). Pioneer factors such as FOXA1 are required to open the chromatin structure and allow the interactions of ER with ERE. ERs attract coregulators (coactivators and corepressors), which facilitate the interaction between ERs and the transcriptional machinery ERs recruit coregulators such as members of the p160 family or the TRAP220 complex. Previous studies have shown that p160 and TRAP220 complexes are cycle through exchange in a process of chromatin remodeling and transcription initiation. The RNA helicase activity of the coactivator p68, which interacts with the AF-1 region of ERα, is associated with SRA, an RNA molecule with coactivator activity (39-41). As a result, ERs can activate or inhibit transcription of target genes (42).

The tethered response is associated with indirect DNA interactions by "tethering" the ER to a response motif via other transcription factors, including AP-1 Fos/Jun dimers. (43). The tethered mode of ER response, involving indirect DNA interactions, has been studied primarily in vitro (44). However, studies in mutant ER mouse models suggest that tethering alone does not mediate key physiological or transcriptional reactions of the ER (38).

In the 1970s, it was observed that E2 could also induce rapid non-genomic changes in neurons and non-neuronal cells. This rapid signaling is mediated by membrane-associated estrogen receptors. Non-genomic actions of estrogens account for the rapid increase in cyclic adenosine monophosphate (cAMP) levels in the uterus (45), the altered firing pattern of hypothalamic neurons observed within a few seconds (46), and the rapid induction of neuropeptide release (47). The molecular identity of the membrane-associated steroid receptors mediating these effects remained unknown for a long time

(48, 49). Finally, in 1990, membrane-localized ERα was detected in pituitary cells and in the hippocampal cornu ammonis cell line (50, 51). Razandi et al. (52) also described nuclear and membrane-associated receptors that were encoded by the known ER genes, but linked to the G protein-coupled signaling cascade (53-55). In addition, several groups have also identified membrane estrogen receptors (mER) that were not encoded by the two nuclear receptor genes. This receptor has been named GPR30/GPER1 (56, 57). These authors have reported a non-genomic signaling mechanism that activates ion channels through membrane-associated (or cytoplasmic) estrogen receptors. In many cases, membrane-associated rapid signaling can be clearly distinguished from the classical nuclear receptor signaling pathway (58).

Within the membrane-bound receptor signaling cascade, the complex pathway whereby estrogens activate the Gβγ subunit, which, in turn, promotes the release and activation of the epidermal growth factor (EGF) precursor, pro-heparin-binding EGF (HB-EGF), is not yet fully understood (57, 59, 60). Activated HB-EGF binds to the EGF receptor, promotes receptor dimerization, and activates Mitogen-activated protein kinase (MAPK). Several studies have shown that GPR30 is involved in the short, rapid estrogenic response in migrating GnRH neurons from the monkey olfactory placode. Thus, E2 can rapidly alter neuronal excitability via ERα, ERβ, and GPR30 (61-65).

1.3.3. Physiological effects of estrogens

In the ovary, granulosa cells of the maturing follicles secrete estrogens in response to the adenohypophysial FSH stimulation. Estrogens, in turn, promote follicular maturation (folliculogenesis), increase gonadotropin receptor expression and steroid hormone synthesis, and inhibit granulosa cell apoptosis. Growing follicles produce increasing amounts of estrogens as the follicular phase progresses, reaching their maximum level before ovulation. Estrogens have a variety of other target cells in both sexes. The best-known effects are on the reproductive system, as estrogens regulate the development, maturation, and function of the female reproductive system (66, 67). E2, also plays a role in regeneration, the proliferation of endometrial epithelial cells, uterine blood volume, fluid replacement, recruitment of inflammatory leukocytes, and endometrial progesterone sensing (68). After ovulation, the corpus luteum produces estrogens along with progesterone. The combined secretion of these hormones is a marker of the luteal phase.

It indicates that the uterine lining is ready to receive the fertilized egg (69). In the vagina, E2 promotes cyclic epithelial cell proliferation, stratification, and keratinization. Estrogens also play a role in the pubertal growth of the mammary gland by promoting proliferation of the ductal epithelial cells (70).

Estrogens also play an essential role in male reproduction. In a 1975 study (71), McLachlan and colleagues treated pregnant mice with diethylstilbestrol. When male offsprings were subsequently born, they developed cryptorchidism or epididymal cysts. Subsequent studies have described that rodent and human testes also express aromatase, which catalyzes the formation of E2 from testosterone (72-74). In addition, in estrogen receptor (ERα and ERβ) gene knockout mouse models, males are also infertile, providing evidence for the role of estrogens in male reproduction (75, 76). The role of estrogens extends beyond the regulation of female and male reproduction. Several well-known non-reproductive effects include the maintenance of cardiovascular health and metabolism, cognition and memory, bone density, healthy adipose tissue, lipid and glucose homeostasis and E2 also exerts beneficial effects on wound healing (77-81).

1.3.4. Negative sex steroid feedback by estrogens

Hypothalamic and hypophysial feedback actions of E2 play an essential role in the central regulation of the HPG axis. In males and females during most of the estrous cycle, episodic secretion of GnRH is inhibited in the presence of high levels of gonadal steroid hormones (E2, progesterone). This inhibitory effect is mediated to the GnRH neurons by estrogen-sensitive interneurons. Particularly important among these interneurons is the kisspeptin (KP) neuronal system with cell bodies located in the ARC of the MBH. In 2007, studies using multiple immunofluorescence labeling of ovine and rat hypothalami revealed that almost all KP[ARC] neurons co-express the tachykinin peptide neurokinin B (NKB) and the endogenous opioid peptide dynorphin (82-84). Based on the names of the three colocalizing peptides, the KP[ARC] cell cluster is commonly referred to as "KNDy" neurons (85). KNDy neurons play a prominent role both in pulsatile GnRH release (86, 87) and in mediating negative estrogen feedback to GnRH neurons (88). The importance of NKB in KP[ARC] neurons was also demonstrated in a 2009 study showing that mutations in the genes encoding NKB (*TAC3*), or its receptor (*TAC3R*) lead to hypogonadotropic hypogonadism in humans (89). In sheep, KP was found to be a substantial mediator of

progesterone negative feedback as well (85). In rodents and sheep, the expression of two stimulatory peptides, KP, and NKB, is increased in KNDy neurons after ovariectomy. In contrast, the production of these peptides is inhibited by negative feedback in the presence of high hormone levels (90-92). In humans, a similar increase in KP and NKB gene expression is observed in postmenopausal women in the infundibular nucleus of the hypothalamus, corresponding to the rodent ARC (91, 93, 94). This condition coincides with the robust hypertrophy of these cells due to the absence of E2 signaling (91, 94). At the same time, the level of dynorphin (the third peptide of KNDy neurons), which inhibits LH secretion, is reduced in KP[ARC] neurons of postmenopausal women. This decrease may be partly due to increased LH secretion (93). Similarly to the human, estrogen increases ARC dynorphin expression and the number of dynorphin-containing neurons in sheep (95), whereas E2 treatment negatively regulates dynorphin expression in the ARC of mice (96, 97). The opposite regulation of dynorphin in humans and rodents suggests a significant species difference in regulatory mechanisms. One obvious species difference in the regulation of reproduction is the absence of a luteal phase in rodents (98).

ERα plays a critical role in estrogen-negative feedback and is thus essential for fertility. (99-101). When the ERα gene is deleted in the mouse ARC, feedback regulation is impaired and fertility is lost (102). ERα is expressed in a high percentage of KNDy neurons (84, 92, 103-106). It has been reported that ERα-containing KP[ARC] neurons are susceptible to low prepubertal estrogen concentrations, resulting in low levels of KP[ARC] expression with low levels of GnRH and LH secretion (98).

1.3.5. The positive feedback effects of estrogens

At the end of the follicular phase, the estrogen level is elevated enough to switch negative into positive feedback. This mechanism triggers a preovulatory LH surge. KP[RP3V] neurons (rostral periventricular area of ventricle III) play a crucial role in this phenomenon. KP[RP3V] neurons express ERα and display a dramatic rise in *Kiss1* gene expression when faced with high levels of E2 (92, 107, 108). KP[RP3V] neurons respond with neuronal activation to E2, as evidenced by an increase in cFos mRNA or Fos protein during the LH surge in proestrus females or those who have received E2 supplementation after ovariectomy (109, 110).

On the other hand, these neurons did not display such activation in diestrous females or those with limited E2 levels after ovariectomy. Several studies have shown that when ERα protein is absent from the KP neurons of female mice, LH surge fails to occur in response to elevated E2 levels (92, 111). However, because ERα was eliminated from all KP cells in these studies, it was unclear whether or not this effect was due specifically to the absence of ERα in KP[RP3V] neurons (112). Partial adeno-associated virus-mediated silencing of ERα selectively in KP[RP3V] neurons in another study decreased the intensity of LH surges in proestrus and in E2-treated ovariectomized mice (113), providing stronger support for the involvement of the KP[RP3V] neuron population in the generation of LH surges. The fluctuation of estrogen levels throughout the estrous cycle results in heightened electrical activity and frequent action potentials firing of KP[RP3V] neurons during proestrus when estrogen levels are elevated (114). This activation is caused by the regulation of various ionic currents in these cells (115, 116). The critical role of KP[RP3V] neurons in the regulation of LH secretion has also gained important support from studies using optogenetics. Optical stimulation of these KP -expressing neurons, either continuously or in a burst-like manner, caused sustained activation of GnRH neurons and significantly increased LH secretion that closely mimicked the natural LH surge (117). Thus far, these findings suggest that estrogen positively impacts the function of KP[RP3V] neurons, boosting their activity and leading to increased secretion of KP and other co-transmitters, which, in turn, activate GnRH neurons to trigger the GnRH/LH surge.

GnRH neurons do not express ERα. While GnRH neurons contain ERβ receptors (118, 119), the primary mechanisms whereby estrogens influence the GnRH neurons are indirect and involve ERα containing interneurons (120). These interneurons, such as the KP[ARC] neuron, likely play a crucial role in mediating the effects of estrogen on GnRH neurons. Via ERα receptor, the KP[ARC] neuron can effectively integrate estrogen signaling and modulate the activity of GnRH neurons in response to changing estrogen levels (121).

1.4. Crucial importance of KP signaling in pubertal development and reproductive health

Human clinical cases of infertility provided the driving force for studies of the connection between *KISS1*, and *KISS1R* genes, puberty, and fertility. Individuals with mutations in either one of these two genes have a condition known as idiopathic hypothalamic

hypogonadism, which is characterized by absent/delayed puberty and a reduced frequency/lack of LH pulses (122, 123). These disease characteristic can be replicated mice with deleted genes for either *Kiss1* or *Kiss1r (122, 124)*. Current research suggests that KP acts as a gatekeeper in the HPG axis by facilitating GnRH secretion and showing an association with pulsatile LH secretion. The idea that KP^{ARC} neurons serve as the pulse generator for GnRH has become widely accepted by now. KP is also a critical regulator of puberty onset, follicular development, oocyte maturation, ovulation, and reproductive behaviors. Because of these critical reproductive aspects, KP receptor is an excellent candidate for pharmacological targeting and clinical applications (125).

1.4.1. The structure of the KP gene and peptide

The first two out of the four exons of the *kiss1* gene do not encode amino acids, whereas the remaining two partly translate into a 145-amino acid precursor peptide, including a 19-amino-acid signal peptide (126). Cleavage products of the precursor include four biologically active peptides, KP-54, KP-13, KP-14 and KP-10, from which KP-54 represents the most common molecular form in humans. KP-s belong to the RF-amide peptide family and share a conserved Arg-Phe-NH2 motif in their C-terminal region which is involved in KP receptor (KISS1R) binding (127, 128).

1.4.2. KP receptor and signaling pathway

The discovery of KISS1R, initially identified as G-protein coupled receptor 54 (GPR54), was made in 1999 in the brain of rats. At the time of its discovery, it was recognized as an orphan receptor (129, 130). Structurally, KISS1R is a seven-transmembrane domain G protein-coupled receptor which acts through interaction with Gq/11 proteins (131, 132). In the mouse brain, KP receptor can be found in various regions, including the POA, the hypothalamus ARC and the hippocampus (128, 131, 133). Importantly, most GnRH neurons in both juvenile and mature mice exhibit *kiss1r* mRNA expression (134). KP binding to KISS1R activates the G protein-coupled receptor and triggers the release of Gαq/11-GTP and Gβγ (135). This activation causes phospholipases C beta to hydrolyze phosphatidylinositol 4,5-bisphosphate to inositol trisphosphate and diacylglycerol (DAG), leading to intracellular Ca^{2+} mobilization. (136, 137). This process can lead to hormone secretion and regulation of cell proliferation. Activation also triggers MAPKs such as ERK1/2 and p38. Interestingly, when DAG is released, it simultaneously opens a

non-specific cation channel (138). Furthermore, it closes an inward rectifying potassium channel, leading to a persistent depolarization of GnRH neurons and GnRH secretion (139).

1.4.3. Anatomical distribution
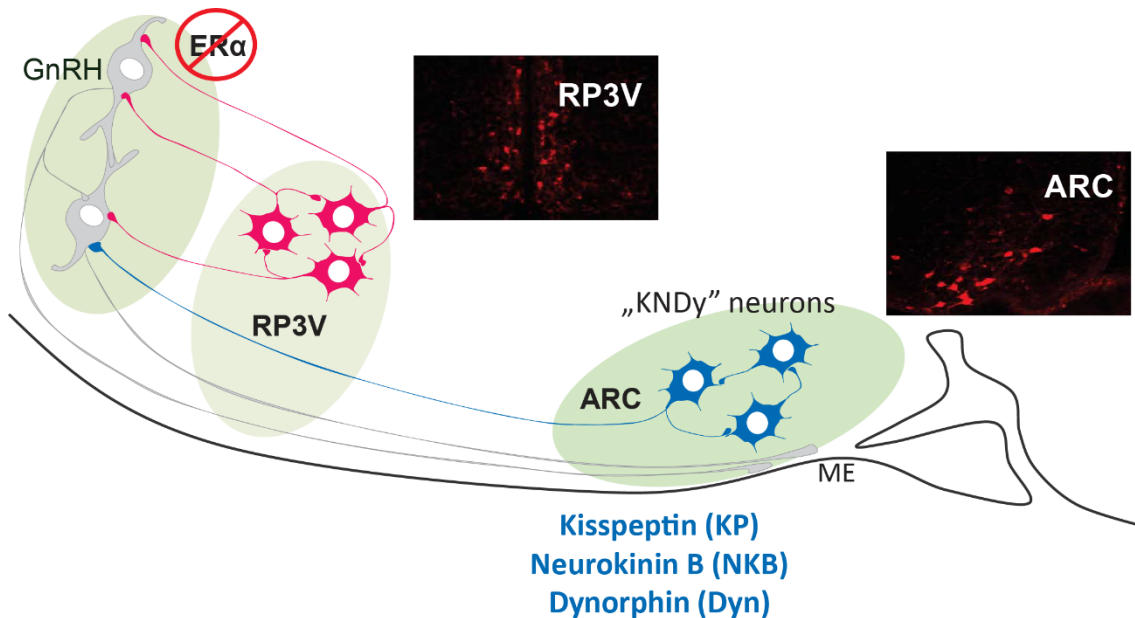
Figure 2. The anatomical distribution of the KP neurons in mice.

GnRH neurons cannot directly receive the dominant estrogen signal since they lack the classical α-type estrogen receptor. The estrogen-sensitive interneurons, especially KP neurons, mediate estrogen's action on GnRH neurons. In mammals, two main groups of KP neurons exist, one in the ARC of the MBH and the other one in the RP3V. The former group primarily regulates negative estrogen feedback, whereas the latter population mediates positive estrogen feedback before ovulation and exhibits robust sexual dimorphism in rodents, with 10-times higher cell numbers in females vs. males. Modified from Kalló et al. (140).

KP is expressed in various organs, such as the pancreas, the brain, the gonads, the pituitary, and the colon (131, 141). Neurons that express KP can be found primarily in two distinct anatomical localizations in the rodent hypothalamus. One is the RP3V region, whereas the other one, containing a much higher number of neurons, is the ARC (142). As already discussed above, the core group of KP^{RP3V} neurons is involved in positive feedback, whereas the KP^{ARC} neurons are responsible for negative feedback. Estrogen

20

increases the level of *Kiss1* mRNA in neurons located in the RP3V region, whereas it decreases the level of *Kiss1* mRNA in the ARC. This difference reflects the different regulatory roles of the two neuronal populations in positive and negative steroid feedback, respectively (92). In addition to this interesting inverse regulation of the *Kiss1* gene in these cell populations, very little is known about the transcripts and molecular mechanisms underlying the estrogenic regulation of the functionally distinct two KP cell types.

1.5. Development of a high-throughput RNA-Seq method for spatial transcriptomic analysis of estrogen-regulated genes in transgenic

The molecular mechanisms that drive negative and positive E2 feedback remain largely unknown. One major hindrance to understanding these mechanisms is the lack of efficient methods to identify estrogen-responsive transcripts of KP neurons. To address transcriptomic changes of the two KP neuron populations in response to E2, we needed to develop a versatile RNA-seq method for fluorescently tagged neuronal populations.

To develop this new strategy, we first studied the stability of fluorescent proteins expressed in transgenic mice. Harvesting fluorescent neurons with laser capture microdissection (LCM) for downstream RNA applications, such as RT-qPCR, microarray and RNA-Seq, requires stabilization of the fluorescent signals with the cross-linking fixative formaldehyde (143-145). To optimize our new approach, fluorescently labeled cholinergic neurons of choline acetyltransferase (ChAT)-tdTomato and ChAT-ZsGreen transgenic mice were used. As the first step toward an optimized LCM-Seq strategy, we compared the fluorescence stability and signal intensity of formaldehyde-fixed ZsGreen and tdTomato proteins expressed selectively in cholinergic systems (**Figure 3**). We perfused the vasculature of ChAT-tdTomato and ChAT-ZsGreen transgenic mice (N=3/group) transcardially with either 0.5%, 2% or 4% formaldehyde, followed by 20% sucrose. Forebrain sections were mounted on microscope slides and analyzed with fluorescence microscopy. We found that tdTomato fluorescence was extremely weak using 0.5% formaldehyde, with very little improvement using 2% or 4% fixative. In contrast, all three formaldehyde concentrations preserved the bright ZsGreen signal in cholinergic neurons for subsequent isolation with LCM (**Figure 3a**).
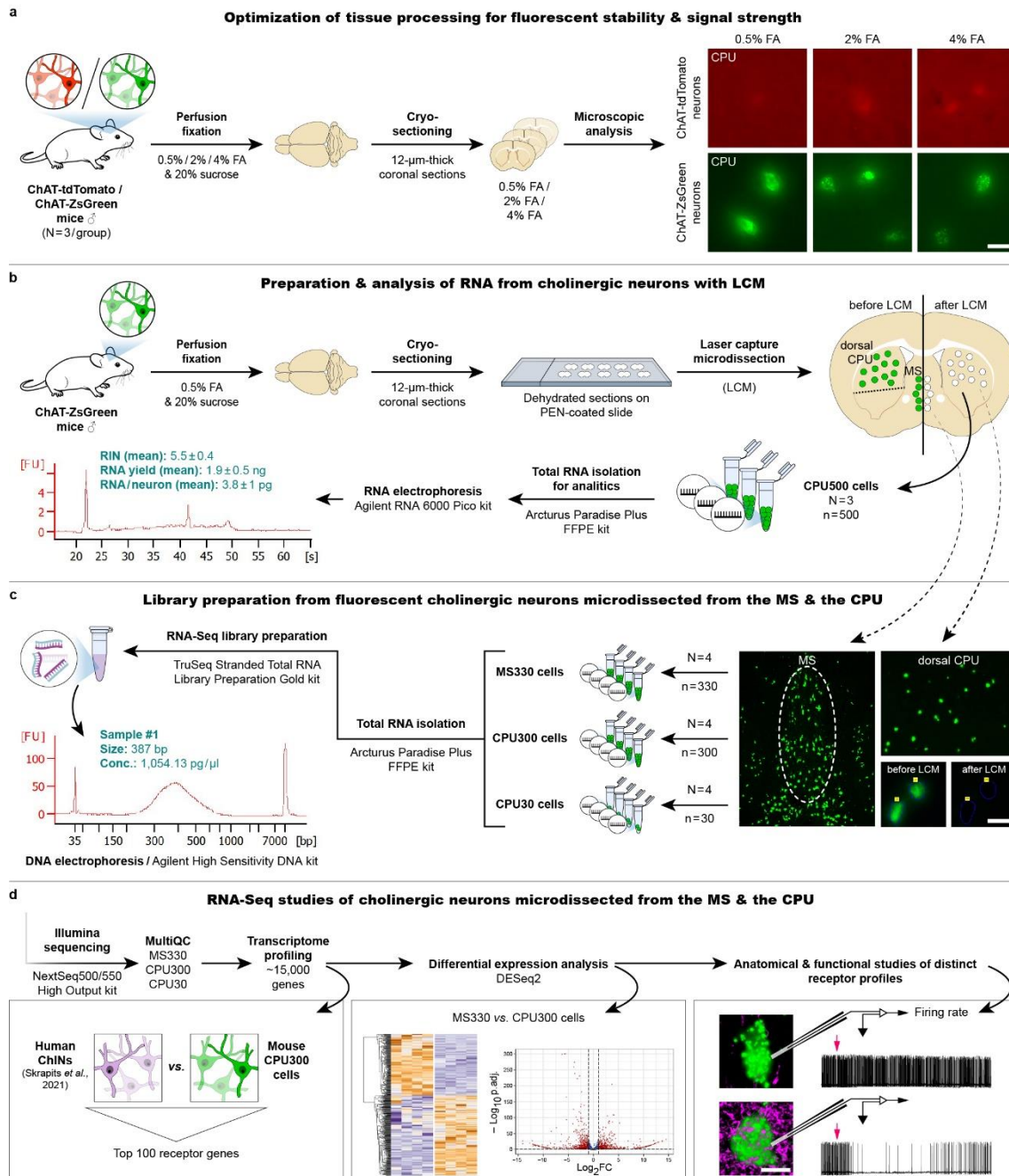
Figure 3. LCM-Seq protocol developed for whole transcriptome profiling of spatially resolved cholinergic neuron populations. *a: Effect of fixation on marker protein fluorescence. Microscopic analysis of sections obtained from the CPU of ChAT-tdTomato and ChAT-ZsGreen transgenic mice provides evidence for superior signal intensity of formaldehyde-fixed ZsGreen over tdTomato, irrespective of fixative concentration. b: Bioanalyzer measurements on RNA isolated from 500 pooled ChINs. c: Random primer-based RNA-Seq library preparation from 330 MS cholinergic neurons*

(MS330) and 300 CPU ChINs (CPU300) occupying equal section areas. Additional libraries from 30 ChINs (CPU30) are prepared to investigate how limited RNA input affects sequencing quality. d: Illumina sequencing and bioinformatic analysis of two spatially distinguished cholinergic neuron populations. Quality control, transcriptome profiling and differential expression analysis are followed by neuroanatomical and functional confirmation of unique receptorial mechanisms revealed in the two distinct cell types. Scale bar: 25 µm (a and high-power images in c), 200 µm (low-power images in c), 10 µm.

To minimize fixation-related RNA damages (146), we optimized further the LCM-Seq protocol using ChAT-ZsGreen brains fixed only lightly with 0.5% formaldehyde. Twelve-µm-thick coronal sections of three mice were mounted on PEN membrane slides. Fluorescent ChINs were microdissected individually and collected from the dorsal caudate-putamen (CPU) with LCM (**Figure 3b**). Results of Bioanalyzer measurements on RNA isolated from these cells indicated that RNA integrity was slightly compromised ("RIN" value: ~ 5.5) and RNA quantity was around 3.8 pg/neuron. Orthodox RNA-Seq library preparation protocols rely on the reverse transcription of mRNA with oligo(dT) primers which becomes inefficient using low-quality and low-quantity input RNA (147). Available commercial kits optimized for low amounts and fragmented RNA require inventive hybridization-based removal of ribosomal RNA (rRNA) or cDNA sequences with highly efficient random primer-based reverse transcription of RNA transcripts (147, 148). From a variety of approaches available, we chose to prepare cDNA libraries from cholinergic neurons with the TruSeq Stranded Total RNA Library Preparation Gold kit (Illumina, San Diego, CA, USA) which has recently enabled us to bulk sequence 300-400 formaldehyde-fixed neuronal cells from both mice (143) and humans (149) (**Figure 3c**). To exceed safely the cDNA sample requirements of Illumina sequencing, we increased the number of amplification cycles from 15 to 16 while preparing libraries from 330 LCM-isolated basal forebrain cholinergic cells of the medial septum (MS; MS330; N=4) and 300 microdissected ChINs of the dorsal CPU (CPU300; N=4). Use of 30 CPU neurons only (CPU30; N=4) in a pilot experiment was found to provide unacceptable sensitivity and accuracy. Sequencing of twelve RNA-Seq libraries generated 516.5 M raw reads (27.3 M-48.6 M per sample). LCM-Seq studies of the 300-330 pooled cholinergic neurons allowed us to detect 14,926±422 different transcripts in MS330 and 15,353±231

transcripts in CPU300 samples (cutoff: 5 reads/sample), confirming high detection sensitivity of the LCM-Seq method. In addition, differential expression analysis identified 2,891 transcripts that were expressed at significantly different levels between the two cholinergic cell types in the CPU and the MS, respectively. This observation showed that the new LCM-Seq method is not only sensitive but also compatible with differential expression analysis.

This versatile LCM-Seq method we developed using cholinergic neurons as a test system provided a powerful tool for us to investigate the molecular changes that take place in spatially defined KP neuron populations in response to estrogen treatment.

2. Objectives

As discussed in Introduction, sex steroid feedback mechanisms in rodents involve two major hypothalamic sites: the ARC and the RP3V. Both regions contain KP neurons which play particularly important roles in mediating the effects of estrogen in the hypothalamus and specifically, on KISS1R positive GnRH neurons, but not the classical estrogen receptor-α implicated in estrogen feedback (150). Although strong evidence from multiple laboratories exists for the crucial importance of the ARC in negative sex steroid feedback and the RP3V in positive estrogen feedback, the molecular changes underlying these phenomena are poorly understood. In my PhD work, I first used RNA-Seq to investigate the transcriptional changes induced by E2 in the ARC region. In a subsequent set of experiments, I focused on KP^{ARC} neurons using an LCM-Seq strategy we developed for gene expression profiling of fluorescently-tagged neuron populations isolated and pooled with LCM. Finally, I made use of this latter strategy to identify estrogen–responsive genes of the KP^{RP3V} neuron population involved in positive estrogen feedback. The results of these studies also allowed me to compare transcriptional responses of the two anatomically and functionally distinct KP neuron populations to the very same estrogen treatment. The three specific aims of my studies were as follows:

2.1. Identification of estrogen-regulated genes and pathways in the mouse ARC region

The ovaries of mice were removed surgically to eliminate endogenous estrogens. Nine days later, a single silastic capsules filled with E2 (100µg/ml; OVX+E2 group) or its carrier (sunflower oil; OVX+Veh group) was implanted under the skin of the animals. The E2 treatment produced high physiological serum E2 levels, whereas endogenous E2 was undetectable in the OVX+Veh group. On day four after capsule implantation, the mice were perfused transcardially with a 10% RNA-Later solution. The brains were frozen and sectioned in the coronal plane with a cryostat. The ARC area was isolated with LCM. After RNA isolation, RNA quality was determined with RNA Pico Chip on a Bioanalyzer instrument. RNA-Seq cDNA libraries were generated and used for RNA-Seq. Bioinformatic programs were used to identify estrogen-responsive genes and pathways of the ARC.

2.2. Characterization of the estrogen-dependent regulation of KNDy neurons

By crossing Kiss-Cre mice with a ZsGreen indicator mouse strain, we generate an animal model in which KP^{ARC} neurons exhibited an intense green fluorescence under blue to ultraviolet illumination. Animal models with low (OVX+Veh group) and high E2 levels (OVX+E2 group) were generated using surgeries as described in aim 2.1. To preserve the fluorescent signal of the indicator protein, the animals were fixed with a 0.5% formaldehyde solution, followed by sterile 20% sucrose for cryoprotection. The sections of the ARC were collected with a cryostat. For transcriptomic studies, 300-300 fluorescent KP^{ARC} neurons were collected from each animal. Isolation of RNA (Arcturus Paradise kit) was followed by RNA-Seq cDNA library preparation and sequencing using the Illumina NextSeq500/550 High output kit with 75 bp reads per strand. The sequencing was done in collaboration with the University of Debrecen. For bioinformatic analysis, we used the R software package.

2.3. Uncovering estrogen-dependent mechanisms in KP^{RP3V} neurons

In order to gain insight into the E2-induced molecular changes of KP^{RP3V} neurons implicated in positive feedback, we utilized the same methods and animal models as described above (2.2.), except that RP3V sections were used as sources of the 300 KP^{RP3V} neurons from each animal. The estrogen regulated transcriptomes of KP neurons from the ARC and the RP3V were compared to identify overlapping and inverse regulatory mechanisms induced by the same estrogen treatment in the two cell types.

3. Methods

3.1. Animals

Animal experiments were carried out in accordance with the Institutional Ethical Codex, Hungarian Act of Animal Care and Experimentation (1998, XXVIII, section 243/1998) and the European Union guidelines (directive 2010/63/EU) and approved by the Institutional Animal Care and Use Committee. All efforts were made to minimize potential pain or suffering and to reduce the number of animals used. Young adult (day 60-80) female mice (N=50) were housed under standard conditions (lights on between 0600 and 1800 h, temperature 22 ± 1 °C, chow and water ad libitum) in the animal facility of the Institute of Experimental Medicine. E2-regulated transcripts of the ARC region were studied in C57Bl/6J mice. The E2-dependent transcripts of KP neurons were identified in KP-Cre/ZsGreen mice generated by crossing Kiss-Cre (151). males with females of the Ai6 (RCL-ZsGreen) indicator strain (The Jackson Laboratory, JAX No. 007906). When Kiss-Cre mice were crossed with a tdTomato reporter line, the ratio of tdTomato expressing KP neurons in OVX female mice was 85-91%, suggesting that around 10% of fluorescent neurons in this model cease to express KP protein during development (151).

3.2. Surgical treatments to generate mouse models with low and high E2 levels

To remove endogenous estrogens, all mice were first anesthetized with a cocktail of ketamine (25 mg/kg), xylazine (5 mg/kg), and promethazine (2.5 mg/kg) in saline and ovariectomized (OVX) bilaterally. To prevent infections, Augmentin (GlaxoSmithKline plc, Brentford, UK; 30 µg/10 g bw in saline) was injected into the peritoneal cavity during the surgery and Baneocin ointment (Sandoz Gmbh, Kundl, Austria) was applied to the wound before the skin was clipped. On postovariectomy day 9, animals were re-anesthetized and implanted subcutaneously with a single silastic capsule (Sanitech, Havant, UK; l=10 mm; id=1.57 mm; od=3.18 mm) containing either 100 µg/ml E2 (Sigma Chemical Co., St Louis, MO) in sunflower oil (OVX+E2 group) or oil vehicle (OVX+Veh group) (152). Four days later, mice were anesthetized and sacrificed between 0900-1100h. Additional animals were used to study serum E2 levels (N=8) and uterine weight (N=12) in the two animal models. The efficacy of estrogen treatment was confirmed by the increased uterine weight (136.5 ± 11.8 mg in OVX+E2 vs. 18.0 ± 0.4 mg

in OVX+Veh animals), mimicking the maximal uterotropic effect observed in the proestrus phase of 2-month-old normal cycling female mice (168.4±20.4 mg; N=7) and exceeding the uterus weight found in mixed-stage (85±7.3 mg; N=15) or metestrus-stage (71.4±4.0 mg; N=6) mice.

To determine serum E2 levels in response to these treatments, the CalBiotech Kit ES180S-100 was used. This kit showed the best E2 parallelism to the standard curve and accuracy in previous studies comparing nine commercial mouse E2 kits (153).

3.3. Transcriptomic studies

3.3.1. Perfusion fixation

For all experiments, reagents were of molecular biology grade. Buffers were pretreated overnight with diethylpyrocarbonate (DEPC; Sigma-Aldrich; 1 ml/L) and autoclaved or prepared using DEPC-treated and autoclaved water as diluent. The working area was cleaned with RNaseZAP (Sigma-Aldrich). For RNA-Seq studies of the ARC region, OVX+Veh (N=5) and OVX+E2 (N=6) C57Bl/6J mice were perfused with ice-cold 10% RNAlater (Thermo Fisher Scientific, Waltham, MA, USA) solution in 0.1 M phosphate buffered saline (PBS; pH 7.4). To study the E2-regulated transcripts of KP neurons, OVX+Veh (N=3) and OVX+E2 (N=3) KP-Cre/ZsGreen mice were perfused transcardially with 80 ml of 0.5% formaldehyde in PBS, followed by 20% sucrose in PBS.

3.3.2. Section preparation and laser capture microdissection

For transcriptomic analysis of the whole ARC region, the brains were snap-frozen in isopentane precooled to -40 °C with a mixture of dry ice and ethanol, and tissue blocks containing the MBH were dissected. Then, 20-µm-thick coronal sections corresponding to Atlas plates 43-47 of Paxinos (between Bregma levels -1.46 and -1.94 mm) (154) were cut from the ARC with a Leica CM1860 UV cryostat (Leica Biosystems, Wetzlar, Germany), collected onto PEN membrane glass slides (Membrane Slide 1.0 PEN, Carl Zeiss, Göttingen, Germany) and air-dried in the cryostat chamber. Sections were stained with cresyl violet as follows: 50% ethyl alcohol (EtOH), 30 sec; 70% EtOH, 30 sec; 0.5% cresyl violet in 70% EtOH, 60 sec; 70% EtOH, 30 sec; 96% EtOH, 30 sec; 100% EtOH, 30 sec. For transcriptomic analysis of the KP^{ARC} cells, formaldehyde-fixed sections

containing fluorescent KP neurons were pretreated for LCM as described elsewhere (144). In brief, the 12-μm-thick-sections were air-dried and then, treated sequentially with 50% EtOH (20 sec), n-butanol:EtOH (25:1; 90 sec) and xylene substitution:n-butanol (25:1; 60 sec). The slides were stored at -80 °C in clean slide mailers containing silica gel desiccants, unless processed immediately for LCM. In studies of the whole ARC, the nucleus was microdissected from every 4th cresyl violet-stained section between bregma levels -1.43 mm and -1.91 mm (154) using the PALM Microbeam system with the PALM RoboSoftware (Carl Zeiss). For KP neuron-specific transcriptomics, 300 KP-Cre/ZsGreen neurons were microdissected from ARC and RP3V sections of each mouse. Microdissected samples were pressure-catapulted into 0.5 ml tube caps (Adhesive Cap 200, Carl Zeiss) with a single laser pulse using a 40x objective lens. The LCM caps were stored at -80 °C until RNA extraction.

3.3.3. RNA extraction, RNA-seq library preparation and sequencing

Total RNA from the ARC and from KP neurons were prepared with the Arcturus Pico Pure RNA and the Arcturus Paradise Plus RNA Extraction and Isolation Kits, respectively (Applied Biosystems, Waltham, MA, USA). RNA integrity numbers (RINs) were determined with the Agilent 2100 Bioanalyzer system using the Eukaryotic Total RNA Pico Chips and the 2100 Expert software (Agilent, Santa Clara, CA, USA). RIN values were 7.1-8.2 for ARC samples and 4.8-6.9 for the formaldehyde-fixed test sections obtained from KP-Cre/ZsGreen mice. Total RNA from the ARC and from KP neurons were converted into cDNA libraries with the NEBNext Ultra II RNA Library Preparation Kit (New England Biolabs, Ipswich, MA, USA) and the TrueSeq Stranded Total RNA Library Preparation Gold kit (Illumina, San Diego, CA, USA), respectively. Although the latter kit has been optimized for 10-100 ng input RNA, a recent study found that it can generate reliable libraries from RNA amounts as little as 1-2 ng (148). For DNA fragment enrichment, our protocol used 16, instead of 15 cycles recommended by the manufacturer. Sequencing was performed on Illumina NextSeq500 instrument using the NextSeq500/550 High Output Kit v2.5 (75 cycles). Recent use of the same RNA isolation, library preparation and sequencing protocols allowed the successful characterization of size-selected and LCM-isolated cholinergic interneurons and medium spiny projection neurons from the human putamen (149).

3.3.4. Bioinformatics

Following FastQC quality control, sequencing reads with low quality bases were removed using Trimmomatic 0.39 (settings: LEADING:3, TRAILING:3, SLIDINGWINDOW:4:30, MINLEN:50). Sequencing reads from ARC samples were mapped to the mm100 mouse reference genome using STAR (v 2.7.3a) (155) which resulted in an average overall alignment rate of 86.8±5.2%. Read summarization and gene level quantification were performed by featureCounts (Subread v 2.0.0) (156). 89.1±0.3% of mapped reads were assigned to genes. Mapping of sequencing reads from KP cells to the mm100 reference genome yielded an average overall alignment rate of 74.9±3.5%. After read summarization, 38.6±0.9% of mapped reads were assigned to genes.

Based on the raw read counts for each gene the count per million (CPM) was calculated by the edgeR (157) R-package. The differential expression analysis gene by gene was performed by DESeq2 (158) R-package. Changes in mRNA expression were quantified by log2 fold change (log2FC). P values were corrected by the method of Benjamini and Hochberg (159) to take multiple testing into account. Functional annotation was based on the PANTHER database (v. 15.0) (160). Genes were assigned to Kyoto Encyclopedia of Genes and Genomes (KEGG) (161) signaling pathways by the R package KEGGREST (Dan Tenenbaum (2019): KEGGREST: Client-side REST access to KEGG., R package version 1.26.1). Using these gene sets, over-representation analysis (ORA) (162) and Signaling Pathway Impact Analysis (SPIA) (163) were performed by the clusterProfiler (164) and ToPASeq (165) R packages. All program packages for differential expression analysis and pathway analysis were run in the R environment (R2020).

3.3.5. Classification of regulated transcripts

Functional classification of estrogen-regulated transcripts (at p.adj.<0.05) was carried out using multiple online databases and methods, including the Ensembl gene description and its Biomart data mining tool (166) and neuropeptide (167) TF (168) and Gene Ontology databases (169).

3.4. Immunofluorescence experiments

3.4.1. Perfusion-fixation

To study neuronal inputs to KP cells, OVX+Veh (N=5) and OVX+E2 (N=5) KP-Cre/ZsGreen mice were used. The mice were anesthetized and sacrificed by transcardiac perfusion with 40 ml 4% formaldehyde in 0.1 M PBS (pH 7.4). The brains were removed, postfixed for 1 h, infiltrated with 20% sucrose overnight, and then, snap-frozen on dry ice.

3.4.2. Section preparation

20-µm-thick coronal sections containing KP^{ARC} neurons were prepared with a Leica SM 2000R freezing microtome (Leica Microsystems) and stored at -20 °C in 24-well tissue culture plates containing antifreeze solution (30% ethylene glycol, 25% glycerol, 0.05 M phosphate buffer (pH 7.4).

3.4.3. Fluorescent visualization of KP^{ARC} neurons and their afferents

Floating sections were pretreated with 1% H_2O_2 and 0.5% Triton X-100 and then, incubated in the primary antibodies (48 h, 4 °C). KP cells were detected based on their ZsGreen fluorescence. Serotonergic inputs to KP^{ARC} neurons were visualized with a rabbit anti serotonin transporter (SERT) antiserum (#24330; Immunostar Inc, Hudson, WI; 1:2,000) [170], orexinergic inputs with a goat orexin-B antibody (sc-8071, Santa Cruz Biotechnology Inc, Santa Cruz, CA, USA; 1:1,000) [171, 172], somatostatin fibers with a guinea pig antiserum (IS-7/51; 1:1,000) [173, 174] and NPY inputs with a sheep antiserum (FJL 14/3A; 1: 1,000) [174, 175]. The primary antibodies were reacted with Cy3-conjugated secondary antibodies (Jackson ImmunoResearch; 1:1,000; 2 h). The labeled sections were mounted on microscope slides, coverslipped with the aqueous mounting medium Mowiol and analyzed with confocal microscopy.

3.4.4. Confocal microscopy

Fluorescent signals were studied with a Zeiss LSM780 confocal microscope. High-resolution images were captured using a 20×/0.8 NA objective, a 0.6–1× optical zoom and the Zen software (CarlZeiss). ZsGreen was detected with the 488 nm and Cy3 with the 561 nm laser line. Emission filters were 493–556 nm for ZsGreen and 570–624 nm

for Cy3. Emission crosstalk between the fluorophores was prevented using 'smart setup' function. To illustrate the results, confocal Z-stacks (Z-steps: 0.85-1 μm, pixel dwell time: 0.79-1.58 μs, resolution: 1024×1024 pixels, pinhole size: set at 1 Airy unit) were merged using maximum intensity Z-projection (ImageJ). Appositions were defined as contacts with no gap between the juxtaposed profiles in confocal slices and illustrated in orthogonal side-views of z-stacks created by the Zen software (CarlZeiss). The final figures obtained from OVX+Veh mice were adjusted in Adobe Photoshop using the magenta-green color combination and saved as TIF files.

3.4.5. Immunoelectron microscopic studies of somatostatin inputs to KP^ARC neurons

KP-Cre/tdTomato mice (N=3) were generated by crossing Kiss-Cre (151) males with females of the Gt(ROSA)26Sor_CAG/LSL_tdTomato (Ai9) indicator strain (The Jackson Laboratory, JAX No. 007905). Surgeries were carried out as described above for OVX+Veh mice. 4 days after the implantation of the silastic capsule containing oil Veh, the mice were anesthetized and sacrificed by transcardiac perfusion with 50 ml 4% acrolein (Merck KGaA, Darmstadt, Germany) and 2% formaldehyde in 0.1 M PBS (pH 7.4). The brains were removed and postfixed overnight in 2% formaldehyde at 4 °C. Then, serial 30-μm-thick coronal sections were prepared through the ARC with a Compresstome VF-300-0Z vibrating microtome (Precisionary Instruments Inc., Greenville, US). The sections were stored in antifreeze solution at -20 °C. Before labeling, they were rinsed copiously with PBS, treated with 1% sodium borohydride (30 min in PBS) and with 0.5% H2O2 (15 min in PBS) and then, with 2% normal horse serum tissue blocker (10 min in PBS). The sections were cryoprotected in 15% sucrose in PBS for 30 min at room temperature and in 30% sucrose in PBS overnight at 4 °C and then permeabilized with liquid nitrogen using repeated freeze-thaw cycles (176). Somatostatinergic inputs to KP^ARC neurons were visualized with a guinea pig somatostatin antibody (IS-7/51; 1:5,000) (173, 174) and a sheep polyclonal tdTomato antibody (1:80,000) (177). The sections were incubated in serum diluent for 4 days at 4 °C. Following overnight incubation in biotinylated anti guinea pig IgG (Jackson ImmunoResearch Laboratories; 1:500) at 4 °C, the sections were placed for 2 h in donkey anti sheep IgG conjugated with 0.8 nm colloidal gold (Aurion Immuno Gold Reagents & Accessories, Wageningen, The Netherlands) diluted at 1:100 in 0.01 M PBS containing

0.1% cold water fish gelatin and 1% bovine serum albumin. The sections were fixed in 1.25% glutaraldehyde in 0.1 M phosphate buffer (PB; pH 7.4) for 10 min at room temperature and then washed with Aurion ECS buffer (Aurion; 1:10 in distilled water) for 2 x 10 min. Silver intensification of the gold particles was performed with the Aurion R-Gent SE-LM Kit. The sections were washed again in Aurion ECS buffer for 2 x 10 min and in PBS for 2 x 10 min followed by incubation in avidin-biotin complex (ABC Elite, PK-6100, Vector Laboratories Ltd., Peterborough, UK; 1:1,000). The signal was visualized with nickel-diaminobenzidine chromogen in 50 mM Tris buffer (pH 7.6). The dual-labeled sections were osmicated (0.5% osmium tetroxide in 0.1 M PB) for 30 min on ice, dehydrated with an ascending series of ethanol and acetonitrile (Sigma Aldrich), including a 30-min contrasting step with 1% uranyl acetate in 70% ethanol. Dehydrated sections were flat-embedded in Durcupan ACM epoxy resin (Fluka) on liquid release agent (Electron Microscopy Sciences, Fort Washington, PA, USA) –coated microscope slides at 56 °C. After polymerization, 60-nm-thick ultrathin sections were cut from a resin block with a Leica UCT ultramicrotome (Leica Microsystems, Wetzlar, Germany). The sections were collected onto Formvar-coated, single-slot grids, treated with 2% lead citrate (Biomarker) and examined with a Jeol-100C transmission electron microscope (JEOL, Tokyo, Japan).

3.5. Slice electrophysiology

3.5.1. Brain slice preparation

Adult OVX+Veh (N=27) and OVX+E2 (N=15) KP-Cre/ZsGreen mice were decapitated in deep isoflurane anesthesia. The brain was immersed in ice-cold low-Na cutting solution bubbled with carbogen (mixture of 95% O_2 and 5% CO_2). The cutting solution contained the following (in mM): saccharose 205, KCl 2.5, NaHCO3 26, MgCl2 5, NaH2PO4 1.25, CaCl2 1, glucose 10. Hypothalamic blocks including the ARC were dissected. 220-μm-thick coronal slices were prepared with a VT-1000S vibratome (Leica Microsystems) and transferred into oxygenated artificial cerebrospinal fluid (aCSF; 33 °C) containing (in mM): NaCl 130, KCl 3.5, NaHCO3 26, MgSO4 1.2, NaH2PO4 1.25, CaCl2 2.5, glucose 10. The solution was then allowed to equilibrate to room temperature for 1 hour.

3.5.2. Whole-cell patch clamp experiments

Recordings were carried out in oxygenated aCSF at 33 °C using Axopatch-200B patch-clamp amplifier, Digidata-1322A data acquisition system, and pClamp 10.4 software (Molecular Devices Co., Silicon Valley, CA, USA). Neurons were visualized with a BX51WI IR-DIC microscope (Olympus Co., Tokyo, Japan). KP-ZsGreen neurons showing green fluorescence were identified by a brief illumination at 470 nm using an epifluorescent filter set. The patch electrodes (OD=1.5 mm, thin wall; WPI, Worcester, MA, USA) were pulled with a Flaming-Brown P-97 puller (Sutter Instrument Co., Novato, CA, USA).

Firing activity of KP-ZsGreen neurons was recorded in whole-cell current clamp mode. A holding current of +10 pA was used to evoke action potentials in silent neurons. Measurements started with a control recording (3 min). The effective concentrations range of serotonergic agents was estimated based on previous literature (178) and pilot experiments. First, we determined the lowest doses of serotonergic drugs eliciting a response from KP^{ARC} neurons using a single bolus of 5-HT between 100 nM-1 μM (Tocris, UK) or the selective 5-HT4R agonist Cisapride at 1-100 μM (Tocris). The 100 nM 5-HT and 1 μM Cisapride concentrations we identified were lower by one order of magnitude than the doses used in similar slice electrophysiology experiments by others (178). The agonist drugs were pipetted into the aCSF-filled measurement chamber and the recording continued for 5 min. In some experiments, the aCSF was supplemented with the 5-HT4R selective antagonist SB204070 (178) (13 μM, Tocris), the broad-spectrum glutamate-receptor inhibitor kynurenic acid (KYN, 2 mM, Sigma) (179) and the γ-aminobutyric acid A-receptor (GABA) inhibitor picrotoxin (PIC, 100 μM, Sigma) (179) 7 min before the recording started. In studies using the membrane impermeable G-protein inhibitor Guanosine 50-[β;-thio] diphosphate (GDP-β-S; 2 mM) in the intracellular pipette solution (180), the intracellular milieu was allowed to reach equilibrium for 15 min after the whole-cell patch clamp configuration was achieved and before recording started. Each neuron served as its own control when drug effects were evaluated. Input resistance and series resistance were monitored at the beginning and at the end of each experiment from the membrane current response to a 20 ms, 5 mV hyperpolarizing voltage step to monitor recording quality. Baseline voltage was monitored throughout each measurement. Using the criteria established for KP^{ARC} neurons (181), all recordings

with input resistances (Rin) < 0.5 GΩ, and series resistances (Rs) > 20 MΩ, or unstable baseline voltage were rejected.

3.5.3. Statistical analysis

Recordings were stored and analyzed off-line. Event detection was performed using the Clampfit module of the pClamp 10.4 software (Molecular Devices Co., Silicon Valley, CA, USA).

Mean firing rates were calculated from the number of action potentials (APs) over the 3-min control and 5-min treatment periods. All the recordings were self-controlled in each neuron and the effects were expressed as percentage changes relative to the control periods.

Treatment group data were expressed as mean ± SEM. Statistical significance was determined with two-tailed Student's t-tests using the Prism3.0 software (GraphPad Inc., CA). Similarly, two-tailed Student's t-tests were used to compare responses of OVX+E2 and OVX+Veh animals to the same concentrations of each drug. Group data were compared by ANOVA followed by Dunnett's post-hoc test. Differences were considered significant at $p < 0.05$.

3.6. Gene-based burden analysis

From the 2329 transcripts that were regulated by E2 in KP^{ARC} neurons at False Discovery Rate (FDR) <0.05, 565 showed at least a 3-fold enrichment (in mean CPM) in KP^{ARC} neurons vs. the ARC region (using always the animal model which showed the higher expression level). This list was reduced further to 193 by only keeping the transcripts with 100 CPM in average and above (considering always the higher expression level in either the OVX+Veh or the OVX+E2 models). From these 193 transcripts, only 134 were up- or downregulated in KP^{ARC} neurons at least twice. Finally, after the omission of regulatory RNA transcripts (and triplicates for Kiss1), the remaining 125 transcripts (85 upregulated and 40 downregulated) were used for burden analysis.

3.6.1. Subjects

Our study included 337 unrelated Congenital hypogonadotropic hypogonadism (CHH) probands (252 males and 85 females) affected by normosmic CHH (nCHH, 152) or

35

Kallmann syndrome (KS, 185), 70% of which were of European descent. Diagnosis of nCHH and KS were made as previously described (182). All subjects provided written informed consent, and the study was approved by the institutional ethics committee at the University of Lausanne.

3.6.2. DNA Sequencing and Bioinformatic Analysis

Genomic DNA extraction from peripheral blood (or saliva), Whole Exome Sequencing (WES), and bioinformatics analysis were performed as previously described (182, 183). All variants were annotated with minor-allele frequencies (MAFs) from gnomAD v2.1.1 and with pathogenicity score from ClinVar database in order to search for rare non-benign variants. WES data from CHH cohort and gnomAD control database were used to select nonsense variants (including stop gain, frameshift, and acceptor-donor splice sites ± 2 bp from the exon), missense, and inframe indels. After removing variants failing QC, all remaining were filtered for frequency (MAF $\leq 0.01\%$), and for pathogenicity (not Benign nor Likely Benign in Clinvar). Then a gene-based burden analysis was run on candidate genes with a one tailed Fisher's Exact test comparing the frequency of selected variants in CHH probands versus controls (gnomAD). FDR was used to correct for multiple testing.

4. Results

4.1. Identification of estrogen-regulated genes and pathways in the mouse ARC region

4.1.1. E2 treatment of OVX mice results in high physiological serum E2 levels and robust uterine hypertrophy

Estrogen-regulated transcripts were investigated in surgically OVX mice receiving a 4-day E2 substitution (OVX+E2) from a subcutaneous capsule implant (**Figure 4A**).
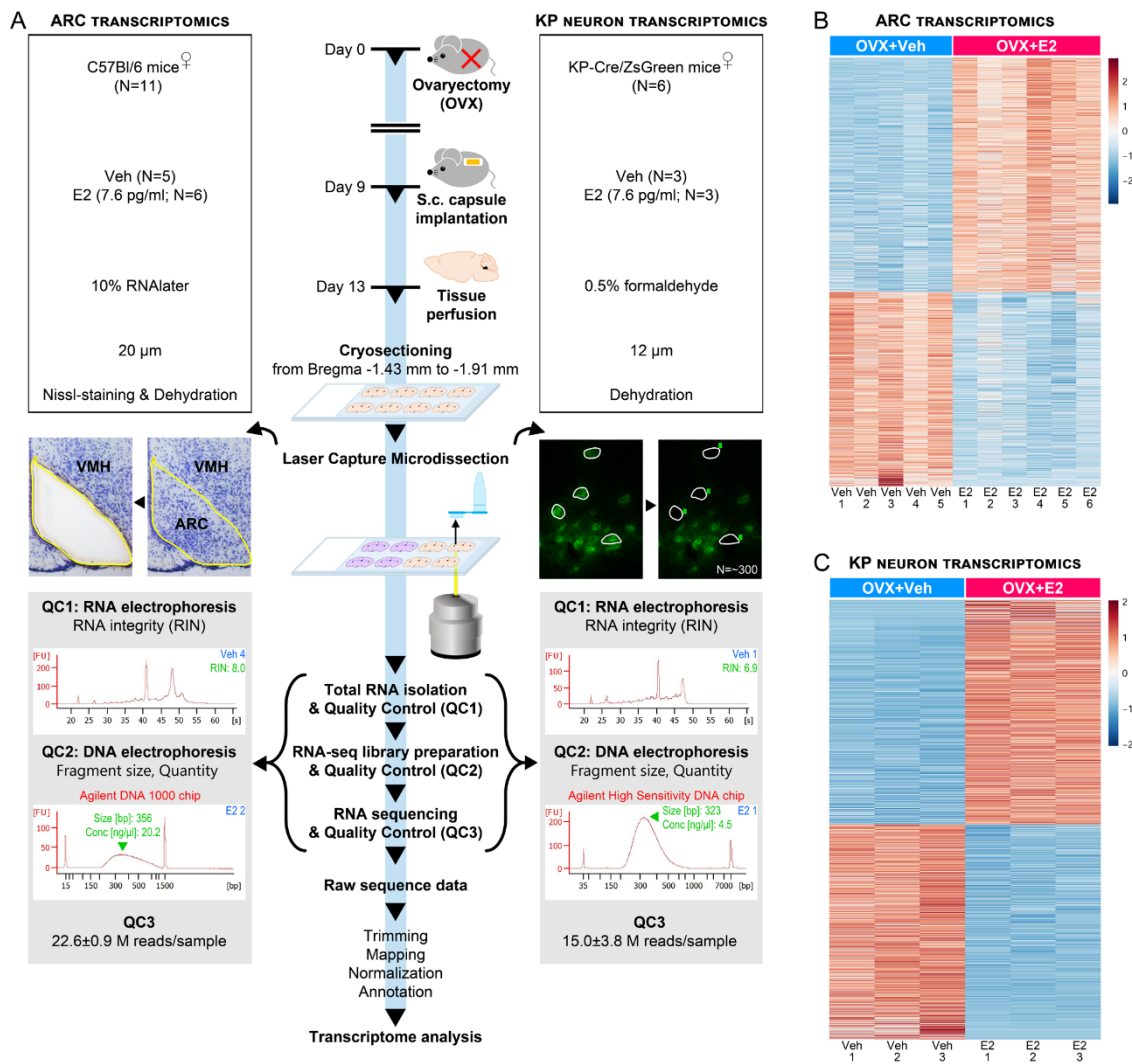
Figure 4. Protocols developed for deep transcriptome profiling of the laser capture microdissected ARC region and KP^{ARC} neurons reveal thousands of genes regulated by E2 replacement to OVX mice. *A: Flowchart outlining the protocols used for differential expression analysis of tissue samples from E2-treated OVX mice (OVX+E2) and vehicle-treated controls (OVX+Veh). To generate mice with low vs. high serum E2, surgical ovariectomy (OVX) is followed by subcutaneous implantation of a single silastic capsule containing sunflower oil vehicle (OVX+Veh) or E2 (OVX+E2). The animals are sacrificed 96 hours later. OVX+E2 mice show a clear uterotropic effect (~7.6-fold weight increase) and a high physiological serum E2 level (7.59±0.7 pg/ml). Two optimized methods are developed for RNA harvesting and RNA-Seq library preparation from the rostro-caudal extent of the ARC of unfixed and Nissl-stained tissues (shown under 'ARC transcriptomics') and from fluorescently-tagged KP^{ARC} neurons identified in*

formaldehyde-fixed ARC sections (shown under 'KP^ARC neuron transcriptomics'), respectively. B: Heat maps reveal conspicuous group homogeneity of the 5 OVX+Veh and 6 OVX+E2 transcriptomes, with clear color separation of 1157 upregulated (red) and 960 downregulated (blue) transcripts in the OVX+E2 model. C: In studies of microdissected and pooled individual KP^ARC neurons (~300/ARC), 1190 and 1139 transcripts show up- and downregulation, respectively, in OVX+E2 (N=3) mice, vs. the OVX+Veh (N=3) controls. VMH, ventromedial hypothalamic nucleus.

This treatment produced a 7.59±0.7 pg/ml (Mean±SEM) serum E2 concentration in test animals (N=4) which falls within the physiological range in cycling female mice (~6pg/ml in diestrus and ~8pg/ml in proestrus) (184) and exerts strong negative feedback on the neuroendocrine hypothalamus. The biological response of the OVX mice to the 4-day E2 treatment was confirmed by a robust increase in uterine weight (136.5±11.8 mg of OVX+E2 animals; N=6 *vs.* 18.0±0.4 mg of OVX+Veh controls; N=6; p=6.3E-07).

4.1.2. The laser-capture microdissected ARC provides high-quality RNA for deep transcriptome profiling

An optimized protocol developed for deep transcriptome profiling of the ARC is shown in **Figure 4A**. This hypothalamic nucleus was readily recognized in Nissl-stained coronal sections. Laser-microdissected tissues collected and pooled proportionally from the rostral, middle and caudal ARC of OVX+E2 (N=6) and OVX+Veh (N=5) mice provided sources for well-preserved RNA (RIN: 7.1<RIN<8.2). Sequencing of cDNA libraries with the Illumina NextSeq 500/550 High Output (v2.5) kit generated 22.6 M reads as an average from the 11 cDNA libraries. Reads were mapped to the mouse reference genome with a mean overall alignment rate of 86.8%. Gene level quantification of read counts was performed by featureCounts and 89.1% of mapped reads were assigned to genes.

4.1.3. Bioinformatic analysis identifies 1157 upregulated and 960 downregulated transcripts in the ARC of E2-treated OVX mice

The 2117 estrogen-regulated transcripts (p.adj.<0.05) showed conspicuous sample homogeneity among animals of the same treatment group. The ARC of OVX+E2 mice contained 1157 upregulated (fold change; FC>1) and 960 downregulated (FC<1) transcripts (**Figure 4B**).

235 transcripts exhibited a |$\log_2$FC| above 1.0. Top changes in each direction are shown in **Figure 5A.** Categorized transcripts were related to autophagy (N=115), ubiquitination (N=37) and encoded neuropeptides or neuropeptide-associated proteins (N=20), miscellaneous ion channels (N=42), transporters (N=83), classical receptors (N=30), other receptors (N=136), ribosomal proteins (N=21), TFs (N=104), lncRNAs (N=40) and microRNAs (miRNAs; N=9).
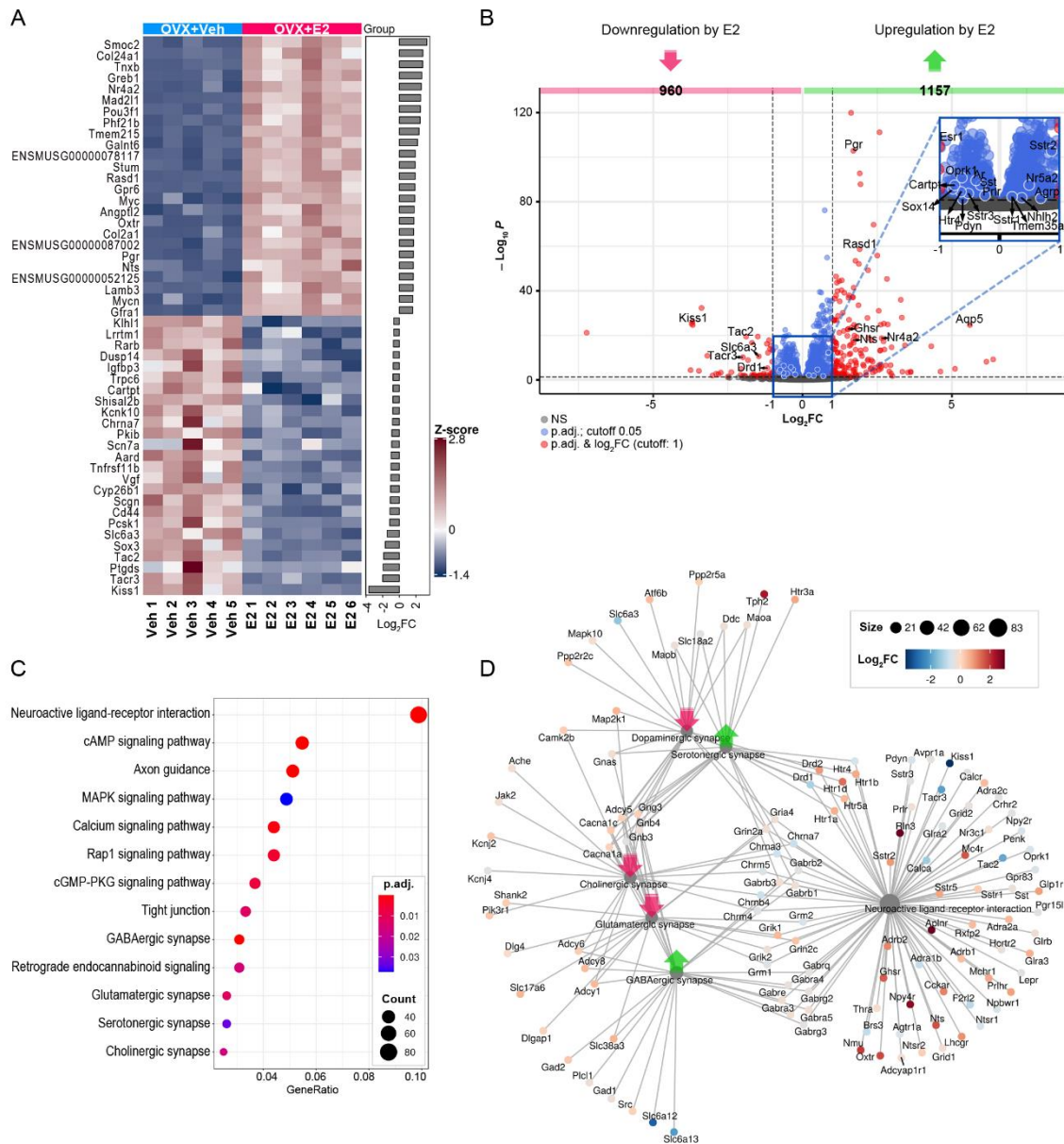
Figure 5. E2 treatment of OVX mice fundamentally changes the gene expression profile of the ARC. *A: Heat map of the most downregulated (lower half) and most*

upregulated (upper half) 25 genes (arranged by size of fold change /FC/ shown in the gray bar chart) includes known markers of KP^ARC neurons (Kiss1, Tac2, Nr4a2, Tacr3), transcripts expressed in non- KP neurons (Slc6a3, Cartpt, Nts) and in multiple (Pgr, Vgf) or unknown (Smoc2, Col24a1, Tnxb, Greb1, Cyp26b1, Tnfrsf11b) cell types. B: Volcano plot illustrates additional E2-induced changes many of which happen to genes known to be enriched in KP^ARC neurons (e.g.: Esr1, Nhlh2, Pdyn, Prlr, Nr5a2, Tmem35a, Rasd1, Sox14). While significant E2 responses are most often moderate (blue dots), the |log2FC| exceeds 1.0 in case of 235 transcripts (red dots). C: Dot plot illustrates the results of ORA, with the most relevant 13 KEGG pathways affected by estrogen treatment. D: Altered neuropeptides, neuropeptide receptors and classic neurotransmitter receptors illustrated graphically provide evidence for profound E2-induced changes in ARC neurotransmission. Arrows suggest overall activation or inhibition of the different classic synapse pathways by Signaling Pathway Impact Analysis (SPIA) (163).

The list also included predicted protein coding genes (N=17) and other predicted genes (N=83) with unknown functions. Genes regulated by E2 in the ARC were known to be expressed in multiple cell types (e.g.: *Esr1*, *Ar*, *Pgr*, *Ghsr*…), unknown cell types (e.g.: *Aqp5*, *Drd1*, *Sstr1-3*, *Htr4*…), non- KP neurons (e.g.: *Agrp*, *Sst*, *Cartpt*, *Slc6a3*, *Nts*…), in addition to a large set found enriched in KP^ARC neurons in earlier Drop-seq analyses (e.g.: *Tac2*, *Nhlh2*, *dyn*, *Prlr*, *Nr5a2*, *Tmem35a*, *Rasd1*, *Nr4a2*, *Tacr3*, *Sox14*, *Oprk1*, *Kiss1*) (**Figure 5B**) (185, 186).

4.1.4. ORA detects 47 functional pathways altered by E2 treatment in the ARC

ORA identified 47 functional (KEGG) pathways that were altered significantly in response to E2. The highest number of E2-regulated transcripts (N=56) occurred in the Neuroactive ligand-receptor interaction KEGG pathway, with changes related to both classic and peptidergic (orexin, neuropeptide Y, somatostatin, etc.) neurotransmission (**Figures 5C, D**). Given that ORA does not consider the functional connectivity of regulated transcripts, SPIA was used additionally to predict net changes in selected neurotransmitter functions. Results of SPIA indicated the overall activation of the GABAergic and serotonergic pathways and inhibition of the glutamatergic, cholinergic and dopaminergic synapse pathways (**Figure 5D**).

41

4.2. Characterization of the estrogen-dependent regulation of mouse KNDy neurons

4.2.1. RNA-Seq studies of laser-capture-microdissected fluorescent neurons provide insight into the estrogen-dependent KP neuron transcriptome

Although the ARC hosts some estrogen-receptive cell types (185, 186), a large number of genes critical for pubertal development, GnRH/LH pulsatility and estrogen negative feedback are expressed in KP^{ARC} neurons of this region (e.g.: *Kiss1*, *Tac2*, *Tacr3* and *Esr1*). To shed light specifically on the estrogenic regulation of KP^{ARC} cells, in a second RNA-Seq experiment we compared the transcriptomes of these neurons from OVX+Veh (N=3) and OVX+E2 (N=3) mice. Collection and pooling of 300 fluorescently-tagged KP^{ARC} neurons of each mouse was performed with laser capture from sections of formaldehyde-fixed brains. Total RNA samples were isolated (RIN 4.8–6.9) and RNA-Seq libraries were prepared with the TruSeq Stranded Total RNA Library Prep Gold kit, as recommended for partly degraded RNA falling into the ng range (148). RNA sequencing generated 20.5 M reads/sample, as an average. Reads were mapped to the mouse reference genome using STAR (v 2.7.3a) with an average overall alignment rate of 74.9% (s.d. = 3.5%). Gene level quantification of read counts based on mouse genome with Ensembl (release 100) annotation was performed by featureCounts (subread v 2.0.0) with a 38.6% mean of mapped reads assigned to genes (s.d.=0.9%). The optimized protocol (**Figure 4A**) resulted in highly homogeneous blocks within the heat map, with significant (p.adj.<0.05) effects of the E2 treatment (**Figure 4C**).

4.2.2. Bioinformatic analysis identifies 1190 upregulated and 1139 downregulated KP^{ARC} neuron transcripts in OVX mice substituted with E2

The number of KP^{ARC} neuron transcripts that changed significantly (p.adj.<0.05) in response to the 4-day E2 treatment was 2329. Genes with the highest |log$_2$FC| values shown in **Figure 6A** included many low-to-medium abundance transcripts which were undetected in earlier Drop-seq studies of hypothalamic cell types (185, 186). 1442 changes (774 up- and 668 downregulations) within KP^{ARC} cells exceeded |log$_2$FC| 1.0 (**Figure 6B**), unlike during the analysis of the whole ARC where the magnitude of most changes was much smaller (**Figure 5B**).
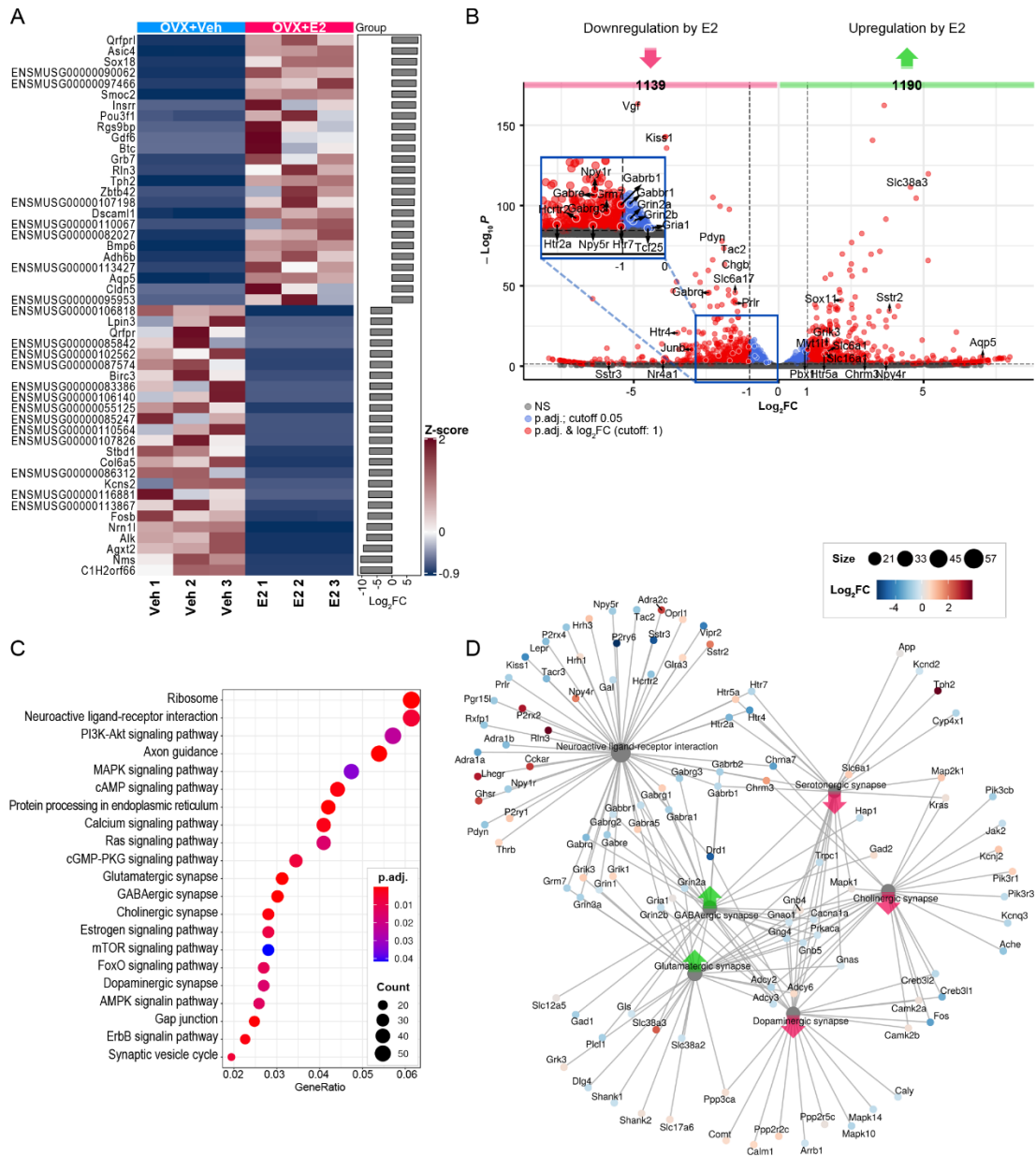
Figure 6. E2 treatment of OVX mice causes profound transcriptomic changes within KP^ARC neurons. *A: Heat map of the most downregulated (lower half) and most upregulated (upper half) 25 genes (arranged by fold change shown in the gray bar chart) mostly includes transcripts that were previously unreported in KP^ARC neurons. B: Volcano plot reveals a large number of regulatory changes (1442) that exceed |log2FC| 1.0 (red dots), in contrast with the mostly small E2-induced changes typical for the entire ARC region (Figure 5). C: ORA detects 83 significantly altered functional (KEGG) pathways from which the most relevant 21 are shown in dot plot. Significant changes happen to the Neuroactive ligand-receptor interaction, GABAergic, glutamatergic,*

cholinergic and dopaminergic synapse pathways, among others. D: The altered neurotransmitter and transmitter receptor profiles of KP^{ARC} cells reveal the involvement of multiple neurotransmitters in the estrogen-dependent control of KP^{ARC} neuron functions. SPIA suggest overall activation of the GABAergic and glutamatergic synapse pathways and inhibition of the cholinergic, dopaminergic and serotonergic synapse pathways.

4.2.3. ORA detects 83 estrogen-regulated functional pathways in KP^{ARC} neurons

ORA identified 83 significantly altered KEGG pathways, with the highest numbers of changing genes in the Ribosome (N=57) and the Neuroactive ligand-receptor interaction (N=57) functional pathways (**Figures 6C, D**). Use of SPIA indicated overall activation of the GABAergic and glutamatergic synapse pathways and overall inhibition of the cholinergic, dopaminergic and serotonergic synapse pathways in response to the E2 treatment. Changes in neurotransmitter and neurotransmitter receptor transcripts are presented graphically in **Figure 6D**.

4.2.4. Estrogen-responsive transcripts of KP^{ARC} neurons fall into various functional categories.

As in case of the ARC transcriptome, we used several online databases for the functional classification of estrogen-regulated transcripts. Many E2-regulated genes were related to autophagy (N=156) or ubiquitination (N=45). Others encoded neuropeptides (N=15), miscellaneous ion channels (N=46), transporters (N=72), classical neurotransmitter receptors (N=26), other receptor types (N=110), ribosomal (N=60) and mitochondrial (N=37) proteins, TFs (N=109), lncRNAs (N=60) and microRNAs (miRNAs; N=5). They included predicted protein coding genes (N=31) and a large number of other predicted genes (N=192), in addition to transcripts left uncategorized. Members of selected gene categories are listed in **Figure 7**.

Classical Transmitter Receptors

Gene	CPM	Gene	CPM	Gene	CPM
Chrm3	25	Gabrg2	149	Grin2b	505
Drd1	74	Gabrg3	80	Grin3a	58
Gabbr1	670	Gabrq	359	Grip1	58
Gabra1	69	Gria1	556	Grm7	135
*Gabra5	49	Grik1	139	Htr2a	22
Gabrb1	331	Grik3	130	Htr4	88
Gabrb2	54	Grin1	263	Htr5a	122
Gabre	236	Grin1os	125	Htr7	52
Gabrg1	139	Grin2a	239		

Transporters

Gene	CPM	Gene	CPM	Gene	CPM
Abca3	182	Slc20a1	115	Slc41a2	111
Abca5	161	Slc20a2	59	Slc44a5	31
Abca8b	51	Slc2a13	160	Slc45a1	77
Aqp5	105	Slc33a1	81	Slc6a1	147
Slc12a3	5	Slc37a1	64	Slc6a17	753
Slc12a5	672	Slc38a2	169	Slc7a5	43
Slc12a7	30	Slc38a3	400	Slc7a8	40
Slc16a1	82	Slc38a9	64	Slco1a4	24
Slc16a5	5	*Slc39a7	137	Slco2a1	53

lncRNAs

Gene	CPM	Gene	CPM
1110038B12Rik	33	Gm29374	29
2610203C20Rik	73	Gm32014	50
4632427E13Rik	165	Gm32849	31
4930570G19Rik	39	Gm3294	33
5930430L01Rik	28	Gm45159	121
9330118I20Rik	14	Gm45847	58
9530059O14Rik	23	Gm47456	10
AC137871.4	10	Jpx	45
AC162938.1	14	Lncpint	211
C230004F18Rik	487	Miat	189
D430020J02Rik	11	Mir670hg	49
Dubr	12	Mir9-3hg	13
ENSMUSG00000117869	66	*Mirg	376
F730043M19Rik	115	Pvt1	28
Gas5	236	RF01962	157
Gm14827	19	Snhg1	55
Gm15834	18	Snhg12	50
Gm19619	11	Snhg5	24
Gm26953	261	Xist	2220

...
(For full list, see **Table S2**)

miRNAs

Gene	CPM
Gm23134	57
Gm26377	320
Mir6402	6
Mir6901	7
Mir8091	4

Neuropeptides/Granins

Gene	CPM	Gene	CPM
Chga	152	Nxph3	40
Chgb	1004	Pdyn	1626
Gal	69	Prok2	7
Kiss1	534	Rln3	12
Nampt	267	Scg3	302
Nms	56	Tac2	2745
Nucb2	68	Vgf	1566
*Nxph1	66		

Other Receptors

Gene	CPM	Gene	CPM	Gene	CPM	Gene	CPM	Gene	CPM
Ackr3	8	Glra3	98	Lhcgr	4	P2rx4	57	Sorcs3	170
Adgrb2	142	Gosr2	112	*Lingo2	79	Paqr3	30	Sorl1	237
Adgrl3	386	Gpr139	48	Lrp1	1216	Pdgfrb	13	Sstr2	112
Adgrl4	17	Gpr162	101	Lrp5	9	Pgr15l	30	Sstr3	42
Adra1a	43	Gpr171	26	Lrpap1	426	Pnrc2	75	Tacr3	555
Adra1b	32	Gpr26	174	Mertk	8	Prlr	726	Tgfbr3	47
Adra2c	21	Gpr6	82	Mmd	53	Procr	6	Tnfrsf11b	40
AF529169	91	Gprc5b	33	Mrap2	95	Ptgdr2	8	Tnfrsf21	96
Alk	14	Grb7	12	Ncoa6	93	Ptpn13	40	Trip11	205
Atp6ap2	160	Grk3	257	Ncor2	330	Ptprg	471	Trpc1	46
C130060K24Rik	25	Grk5	32	Npcd	244	Ptprj	75	Trpc3	54
Cckar	6	Hcrtr2	47	Npr2	197	Ptprn	1742	Trpc5	131
Cd93	23	Hrh1	99	Npr3	407	Ptprs	629	Trpc6	41
Cxadr	113	Hrh3	25	Nptxr	1077	Ptprt	265	Trpm4	14
Csf1r	24	Il13ra1	41	Npy1r	238	Ptpru	217	Trpv2	65
Epha5	58	Il1rap	88	Npy4r	34	Qrfpr	6	Tyk2	37
Epha7	29	Il1rapl2	27	Npy5r	58	Rack1	229	Tyro3	36
Eps8	84	Insrr	15	Nrbp2	74	Reep5	362	Unc5c	329
Eps8l3	44	Irs4	224	Nrip1	178	Robo1	64	Vipr2	11
*Fgfr1	137	Kdelr2	68	Nrip3	124	Rxfp1	110	Vldlr	276
Gfra1	373	Lepr	157	Olfr1417	7	Ryr3	86	Vmn2r-ps3	3
Ghsr	314	Lgr4	60	Oprl1	156	Sorcs1	169		

Transcription Factors

Gene	CPM	Gene	CPM	Gene	CPM	Gene	CPM	Gene	CPM
Adnp	240	Foxn2	40	Mterf4	121	Relb	15	Trps1	50
Ar	290	Gabpa	64	Myt1	148	Rora	194	Zbtb10	97
Arhgap35	417	Gatad2a	66	Myt1l	327	Scml4	100	Zbtb20	299
Baz2a	136	Glis1	32	Nfat5	247	Sgsm2	134	Zbtb38	107
Cebpb	16	Grhl1	25	Nfatc2	127	Ski	69	Zbtb42	11
Cic	160	Gtf2i	339	Nfe2l1	254	Skil	171	Zfhx2	117
Creb3l1	61	Hif1a	303	Nhlh2	207	Smyd3	57	Zfhx4	183
Creb3l2	110	Hivep1	276	Npas4	35	Son	608	Zfp219	66
Crem	65	Hivep2	307	Nr1d2	178	Sox11	613	Zfp266	130
Csrnp3	480	Hivep3	82	Nr2c2	192	Sox14	58	Zfp317	58
Dbp	47	Ikzf3	27	Nr4a1	78	Sox18	19	Zfp318	149
Dot1l	140	Jazf1	43	Nr4a2	427	Sox3	90	Zfp334	128
Egr1	55	Jdp2	40	Nr4a3	36	Sox4	26	Zfp503	14
Egr3	10	Junb	55	Nr5a2	481	Sox5	38	Zfp516	85
Egr4	41	Jund	108	Pbx1	254	Srebf1	61	Zfp607a	16
Esr1	759	Klf4	12	Peg3	3202	Srebf2	82	Zfp667	78
Ets2	225	Klf6	57	Pgr	737	Stat3	183	Zfp804a	73
Etv5	42	L3mbtl4	8	Pknox1	21	Stat5a	54	Zfp846	64
Etv6	20	Lcorl	122	Pknox2	49	Stat5b	160	Zfp92	96
Fos	37	Mbd6	64	Plagl1	249	Tef	202	Zkscan1	161
Fosb	36	Mef2a	159	Preb	119	Tet2	116	Zzz3	126
Fosl2	304	Mef2c	73	Purb	638	Thrb	64		

Mitochondrial Transcripts

Gene	CPM	Gene	CPM	Gene	CPM	Gene	CPM	Gene	CPM
Abcb6	4 / 63	Glrx2	58	Mrpl37	45	Nudt9	55	Slc25a25	94
Acot9	34	Gls	396	Mrps11	78	Oat	51	Star	59
Acss1	24	Glud1	186	*Mrps28	19	Opa1	199	Stard7	138
Agxt2	31	Gpd2	159	Mrps34	60	Pdk1	77	Timm8b	67
Atp5d	74	Guf1	103	Mtch1	273	Pdk3	25	Trnt1	88
Bcs1l	23	Me3	189	Mterf4	121	Pgs1	86		
Chchd10	36	Micu1	88	Mtfr2	3	Prdx5	93		
*Ckmt1	66	Mmadhc	43	Mtus1	64	Sdha	287		

Ribosomal Proteins

Gene	CPM	Gene	CPM	Gene	CPM	Gene	CPM	Gene	CPM
Nop56	199	Rpl14	176	Rpl6	198	Rps14	190	Rps8	203
Rpl10	190	Rpl17	190	Rpl7	220	Rps3	333	Rps9	167
Rpl12	192	Rpl3	572	Rpl8	437	Rps4x	194	Rpsa	170
Rpl13a	293	Rpl4	529	Rpl9	287	Rps5	192	Xpo1	169

...

Numeric values in CPM

- mean cpm in **OVX+Veh** group (blue)
- mean cpm in **OVX+E2** group (pink)

Gene: similarly changed in the ARC
*Gene: inversely changed in the ARC

Figure 7. Estrogen-regulated KP^ARC neuron transcripts fall into diverse functional categories. *E2-regulated transcripts of KP^ARC neurons were categorized based on function using online databases. Many of these transcripts are related to autophagy*

45

(N=156) and ubiquitination (N=45). They encode neuropeptides (N=15), miscellaneous ion channels (N=46), transporters (N=72), classical neurotransmitter receptors (N=26), other receptor types (N=110), ribosomal (N=60) and mitochondrial (N=37) proteins, TFs (N=109), lncRNAs (N=60), microRNAs (miRNAs; N=5). They include predicted protein coding genes (N=31) and a large number of other predicted genes (N=192). Genes that also show significant E2-dependent regulation in the ARC are underlined. Asterisks indicate inverse regulatory changes in the ARC region and in KP^{ARC} neurons, whereas all other genes changed significantly p.adj.<0.05) only in KP^{ARC} neurons. Numbers in dots reflect transcript abundances in CPM units. Dot areas change in proportion to transcriptional responses, the larger dot representing 100%.

The large number of regulated TFs (N=109) likely contributed to secondary transcriptional changes. E2 suppressed mRNA expression of nuclear hormone receptors (*Ar*, *Esr1*), AP-1 TFs (*Fos*, *Fosb*, *Junb*, *Jund*), early growth response proteins (*Egr1, 3, 4*), the neuronal activity dependent TF (*Npas4*), orphan nuclear receptors (*Nr4a1*, *Nr4a3*), steroidogenesis regulators (*Crem*) and many zinc finger proteins. Estrogen inhibited the prohormone convertase PC1/3 transcriptional regulator *Creb3l1*, and the enzyme (*Pcsk1*) as well. Furthermore, E2 activated mRNA expression of some hormone receptors (*Pgr*, *Thrb*), transcriptional mediator of progesterone synthesis (*Cebpb*), and TFs SOX (*Sox11*, *Sox18*) and STAT (*Stat5a*, *Stat5b*).

4.2.5. Estrogen regulates postsynaptic receptors for classic and neuropeptide neurotransmitters innervating KP^{ARC} neurons

A number of neurotransmitter receptors responded to the 4-day E2 treatment. These included the *Htr2a*, *Htr4*, *Htr5a* and *Htr7* serotonin receptors, the *Npy1r*, *Npy4r* and *Npy5r* neuropeptide Y (NPY) receptors, the *Sstr2* and *Sstr3* somatostatin receptors and the *Orx2* orexin receptor, among others (**Figures 6D, 7**). These changes suggested that the receptor ligands can exert estrogen-dependent afferent control on KP^{ARC} neurons. To provide anatomical support to this notion, a series of dual-immunofluorescence experiments was carried out on ARC sections of OVX+Veh and OVX+E2 KP-Cre/ZsGreen mice. Confocal microscopic analysis demonstrated the presence of the 5-HT marker serotonin transporter (SERT; **Figure 8A**), orexin B (OX B; **Figure 8B**), NPY (**Figure 8C**) and somatostatin (**Figure 8D**) in axosomatic and axodendritic afferents to

KP^{ARC} neurons, thus suggesting the potential contribution of these transmitters to the estrogen-dependent neuronal control of KP^{ARC} cells.
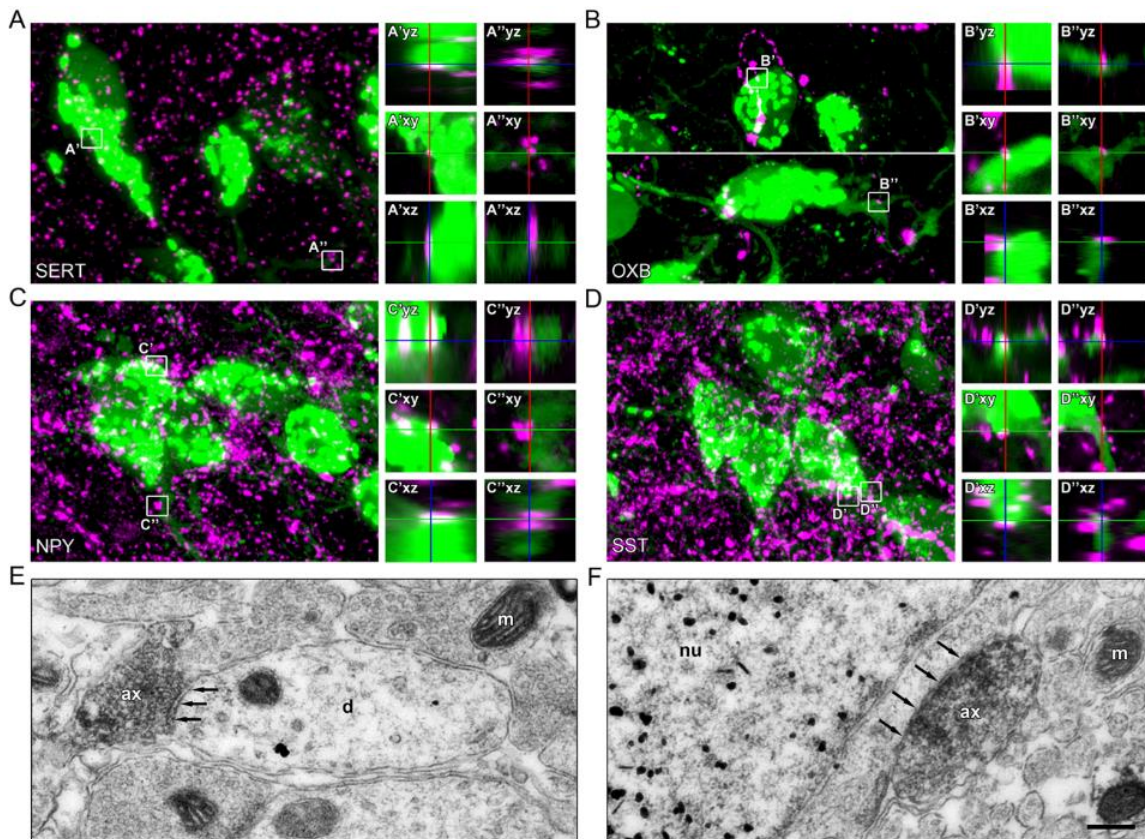

Figure 8. Confocal- and electron microscopic studies reveal the ligands of various estrogen-regulated neurotransmitter receptors in neuronal afferents to KP^{ARC} neurons. *A-D: Results of immunofluorescence studies on hypothalamic sections of OVX+Veh KP-Cre/ZsGreen mice confirm presence of the serotonergic marker serotonin transporter (SERT; A) and the neuropeptides orexin B (OX B; B), neuropeptide Y (NPY; C) and somatostatin (SST; D) in axosomatic and/or axodendritic afferents (magenta) to MBH KP^{ARC} neurons (natural green color of ZsGreen-tagged cells). Low-power images represent confocal z-stacks. Orthogonal views (z axis) of the neuronal contacts shown in high-power insets illustrate the absence of gaps between the juxtaposed profiles in single optical slices. Regulation of receptor transcripts for serotonin, OX B, NPY and SST supports the concept that all of these transmitters contribute to the estrogen-dependent afferent control of KP^{ARC} neuron functions. E, F: Electronmicroscopic studies confirm the presence of synaptic specializations (arrows) between SST-immunoreactive axons (ax) labeled with nickel-diaminobenzidine and tdTomato-immunoreactive KP^{ARC} neurons*

47

(silver-intensified gold nanoparticles) of transgenic mice. Synapses are present both on the dendrites (d; E) and the cell bodies (F) of KP^{ARC} neurons. Note in F that tdTomato fills the nucleus (nu) of the labeled KP^{ARC} neuron. m, mitochondrion. Scale bar: 10 µm in A-D, 4 µm in insets and 270 nm in electron micrographs.

As clear differences in innervation patterns were not noticed between the two animal models, the number of contacts was not analyzed quantitatively. To confirm that somatostatinergic fibers provide synaptic input to KP^{ARC} neurons, dual-label immuno-electronmicroscopy was used. This study established that somatostatin-immunoreactive fibers establish synaptic contacts on KP^{ARC} dendrites (**Figure 8E**) and cell bodies (**Figure 8F**). Similar ultrastructural evidence for serotonin, NPY and orexin containing synapses onto KP^{ARC} cells is currently unavailable.

4.2.6. Estrogenic regulation of serotonergic receptors correlates with reduced excitatory responses of KP^{ARC} neurons to low doses of 5-HT and the 5-HT4R agonist Cisapride

The serotonergic system has emerged as an important mediator of leptin (187) and estrogen (188) effects on reproduction. Four distinct serotonin receptors showed robust estrogenic regulation within KP^{ARC} neurons; the inhibitory *Htr5a* was upregulated and the excitatory *Htr2a*, *Htr4* and *Htr7* isoforms were all downregulated in E2-treated mice (**Figure 9A**). We hypothesized that these changes cause reduced KP^{ARC} neuron responsiveness to 5-HT stimulation in OVX+E2 mice. Whole-cell patch-clamp electrophysiology was carried out in KP^{ARC} neurons from brain slices of OVX+Veh and OVX+E2 KP-Cre/ZsGreen mice (**Figure 9B**). A holding current of +10 pA was used to evoke action potentials in KP^{ARC} neurons most of which (~94%) are silent in OVX mice (189). 1000 nM 5-HT increased the mean firing rate of KP^{ARC} neurons similarly in the OVX+E2 (266.1 ± 14.06% of ctrl) and the OVX+Veh (267.9 ± 12.69% of ctrl) models.
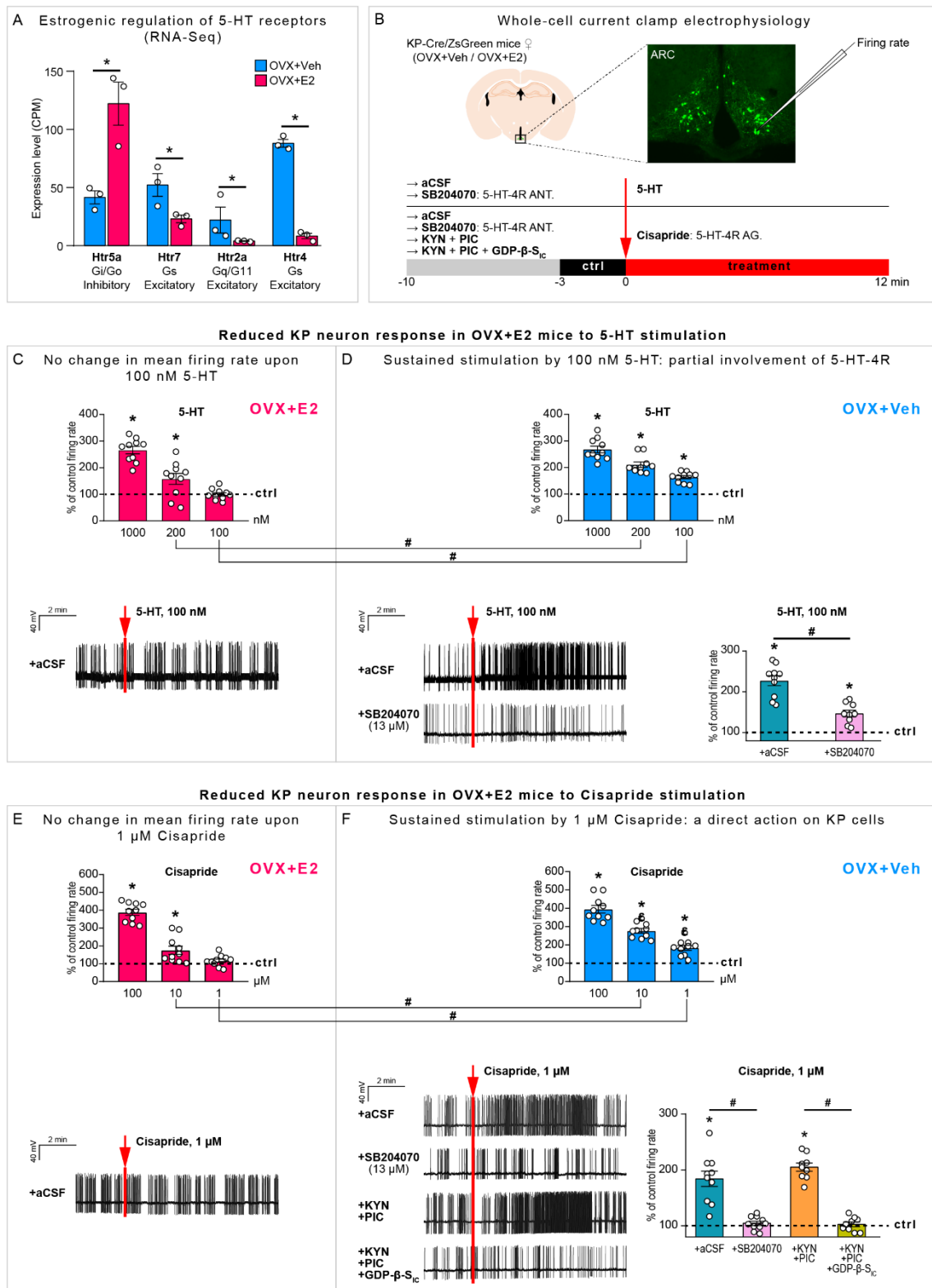
Figure 9. Transcriptional changes of serotonin receptor isoforms cause reduced excitatory serotonergic neurotransmission to KP^ARC neurons in E2-treated OVX mice. *A: The 4-day E2 treatment of OVX mice (OVX+E2) causes upregulation of the*
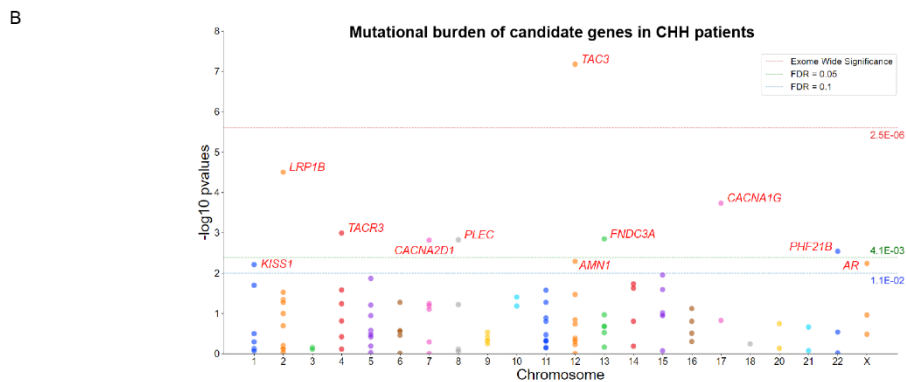
inhibitory Htr5a and downregulation of the excitatory Htr2a, Htr4 and Htr7 serotonin (5-HT) receptor isoforms in KP^{ARC} neurons, leading to a prediction that 5-HT might stimulate KP^{ARC} neurons more efficiently in the OVX+Veh model. B: Electrophysiological studies address the differential responsiveness of KP^{ARC} neurons from OVX+E2 vs. OVX+Veh mice to decreasing doses of 5-HT or the selective 5-HT4R agonist (AG) Cisapride. C-F: The highest doses of 5-HT (1000 nM) and Cisapride (100 µM) elicite similar increases in the mean firing frequency of KP^{ARC} neurons in OVX+E2 and OVX+Veh mice. In contrast, the OVX+Veh mouse model responds more to the medium and low doses (D vs. C; F vs. E). p<0.05 in OVX+Veh vs. OVX+E2 model with ANOVA. C, D: 100 nM 5-HT, which has no effect in the OVX+E2 model (C), increases the mean firing frequency of KP^{ARC} cells in OVX+Veh mice to 163.6±6.10 of the ctrl rate (D). Preincubation of slices with the selective 5-HT4R receptor antagonist (ANT) SB204070 (13 µM) blunts this response (D), indicating the contribution of 5-HT4R isoform to the effect of 5-HT. E, F: The 1 µm dose of the selective 5-HT4R AG Cisapride has no significant effect on the mean firing rate of KP^{ARC} neurons in OVX+E2 mice (E; 116.6±10.06% of ctrl; p=0.13) but efficiently stimulates KP^{ARC} neuron firing in the OVX+Veh model (F; 184.1±13.64% of ctrl; p=0.0002). Cisapride acts selectively on 5-HT4R and, therefore, is ineffective in the presence of 13 µM SB204070 (second trace in F). The effect on KP^{ARC} neurons is direct because it is preserved in the presence of the ionotropic glutamate and GABAA receptor inhibitors KYN (2 mM) and PIC (100 µM), respectively (third trace in F). Further, Cisapride is ineffective if the intracellular solution is supplemented with the G-protein inhibitor GDP-β-S (2 mM; fourth trace in F). Scatter dot plots summarize the results obtained with different blockers.

A medium 5-HT dose we used (200 nM) produced significantly higher response in OVX+Veh mice ($210.4 \pm 10.34\%$ of ctrl) than in OVX+E2 mice ($157.9 \pm 20.76\%$ of ctrl), whereas the lowest applied dose (100 nM) increased the mean firing frequency in OVX+Veh ($163.6 \pm 6.10\%$ of ctrl) but not in OVX+E2 ($99.5 \pm 6.60\%$ of ctrl) animals (**Figures 9C, D**). Preincubation of slices with the selective 5-HT4R antagonist SB204070 (13 µM) blunted this response ($123.4 \pm 4.14\%$ of OVX+Veh ctrl), indicating that the 5-HT4R receptor isoform has a major contribution to the effect of 5-HT (**Figure 9D**). The highest 100 µM dose of the selective 5-HT4R agonist Cisapride stimulated KP^{ARC} neurons equally in the OVX+E2 ($388.6 \pm 17.12\%$ of ctrl) and OVX+Veh ($394.7 \pm 20.64\%$

of ctrl) models. The magnitude of response to a medium dose (10 μM) was significantly higher in OVX+Veh (277.2 ± 13.18% of ctrl) than in OVX+E2 (175.6 ± 22.95% of ctrl) mice, whereas 1 μM Cisapride (the lowest dose having an effect in pilot studies) raised the mean firing frequency of KP^{ARC} cells in the OVX+Veh (184.1 ± 13.64% of ctrl) but not in the OVX+E2 (116.6 ± 10.06% of ctrl) model (**Figures 9E, F**). Cisapride acted selectively on 5-HT4R because its effect was entirely eliminated in the presence of 13 μM SB204070 (**Figure 9F**). The action was direct because i) it was maintained in the presence of the ionotropic glutamate and receptor GABAA inhibitors KYN (2 mM) and PIC (100 μM), respectively, and ii) it was absent if the intracellular solution was supplemented with the membrane impermeable G-protein inhibitor Guanosine 50-[β;-thio] diphosphate (GDP-β-S; 2mM) (**Figure 9F**). The higher responsiveness of the OVX+Veh model to low doses of 5-HT and Cisapride supported the notion that estrogenic regulation of the 5-HT receptor isoforms reduces the sensitivity of KP^{ARC} cells to the stimulatory serotonergic input in OVX+E2 mice.

4.2.7. The estrogen-regulated transcriptome of KP^{ARC} neurons may shed new light onto the pathomechanisms of fertility disorders and designates new disease gene candidates

We hypothesized that similarly to *Kiss1*, *Tac2* and *Tacr3*, other transcripts heavily involved in reproductive regulation and disorders are i) enriched in KP^{ARC} neurons *vs.* their ARC environment, ii) expressed abundantly in KP^{ARC} cells (high CPM) and iii) regulated robustly (high $|\log_2 FC|$) by E2. Searches of mouse (190) and human (191) disease phenotype databases revealed that 7.1% (N=166) and 1.8% (N=42), respectively, of the 2329 E2-regulated KP neuron transcripts can be linked to pubertal and reproductive disorders, including CHH (**Figure 10A**).

A

Abhd16a, Acd, Ace, Ache, Adamts15, Adcy3, Adra1b, Akap12, Alk, Apc2, Arhgap1, Arsb, Asph, Atcay, Bbip1, Bbof1, Bcl2l1, Cacna1a, Cadm1, Cdkn1b, Cebpb, Chst10, Chsy3, Cldn11, Cntnap1, Comt, Cpe, Cpeb3, Crem, Ctnna2, Cux1, Ccs, Csf1r, Dcaf17, Dcx, Dkc1, Dmd, Eda, Egr1, Egr4, Ehd4, Elavl4, Emc10, Epb41l2, Esr1, Etv5, Fbxo7, Fkbp4, Fndc9, Gabbr1, Gabre, Gadd45g, Galnt3, Glb1, Gnao1, Golga3, Gorasp2, Gpd2, Grin1, Gtf2i, Hdac2, Hip1, Hspa4l, Hydin, Iqub, Irs4, Jade1, Jag2, Jund, Katnal1, Kif19a, Kl, Kmt2e, L1cam, Lgr4, Lpin1, Lsm14b, Mad2l2, Man2a2, Map1b, Marcksl1, Mfge8, Mgat2, Mkrn2, Msi2, Myo6, Nlh2, Npr2, Nr2c2, Nsun2, Nxph1, Osbp2, Pacsin1, Pcsk2, Pdgfb, Pgap1, Plekha1, Pomgnt1, Ppp2r5c, Prkce, Prkcq, Ptprj, Qk, Rad18, Rapgef6, Rdx, Relb, Reln, Rhobtb3, Sec23ip, Selenop, Shank1, Sik3, Smarca2, Sms, Snap25, Sox3, Spag9, Sulf2, Tdrd7, Tdrkh, Tekt4, Tgfbr3, Tns1, Tpst1, Trpc5, Vasn, Vgf, Vipr2, Zfp318

BCS1L, CHRM3, DNAH9, DUSP6, FGFR1, FMR1, GNAS, GUCY1A1, LAS1L, LMNB1, NDN, PROK2, RTN2, SEMA3A, SIL1, STAR, TBL1X, TTC12, TTC8, VWF, WNT4

Akap13, Amn1, Amotl1, Angptl2, Aqp5, Arvcf, Atp11a, Cacna1h, Cacna2d1, Cdh11, Cdh8, Cdkl5, Cers6, Cntnap5, Col24a1, Col2a1, Col4a2, Cxadr, Csmd3, Dip2b, Dscam, Dscaml1, Epb41l4a, Fam135b, Fgf14, Fosl2, Galnt6, Gdpd2, Ghsr, Glce, Gramd1b, Greb1, Grm7, Hcn1, Hivep1, Hmcn2, Hs3st5, Htr5a, Igdcc4, Igsf9b, Itgbl1, Kcna4, Kcnk10, Kcnt1, Kctd4, Lamb1, Lrp1b, Mad2l1, Mark1, Mcf2l, Mctp1, Me3, Med13l, Mterf4, Neil1, Nfatc2, Npy1r, Nr4a2, Nr5a2, Nup205, Osbpl3, Parp8, Pcdh11x, Pdyn, Phf21b, Phldb1, Plec, Plekha5, Ptchd1, Ptpru, Rai14, Rbms3, Sema5a, Serinc5, Shisa6, Slc38a3, Smoc2, Sned1, Sorcs1, Sox11, Spon1, Sv2c, Tgfb3, Thsd7a, Tmem131l, Tmem132b, Tmem25, Tmem266, Tmtc4, Tnxb, Tp53inp1, Ttn, Ugcg, Unc13b, Xylt1, Zc3h12c

B

Mutational burden of candidate genes in CHH patients

Causative genes and new putative CHH-candidate genes identified by gene-based burden analysis comparing CHH patients and controls

Ensembl transcript ID	HGNC symbol	Gene name	Gene MIM number	Human phenotype (Inheritance)	Phenotype MIM number	Enrichment p-value
ENST00000458521	TAC3	Neurokinin B	162330	Hypogonadotropic hypogonadism 10 with or without anosmia (AR)	614839	6.61E-08*
ENST00000389484	LRP1B	Low density lipoprotein receptor-related protein 1B	604065	-	-	3.14E-05*
ENST00000359106	CACNA1G	Calcium channel, voltage-dependent, T-type, alpha-1G subunit	608766	Spinocerebellar ataxia 42 (AD) Spinocerebellar ataxia 42, early-onset, severe, with neurodevelopmental deficits (AD)	616795, 618087	1.84E-04*
ENST00000304883	TACR3	Neurokinin B receptor	162332	Hypogonadotropic hypogonadism 11 with or without anosmia (AR)	614840	1.01E-03*
ENST00000492622	FNDC3A	Fibronectin type III domain-containing protein 3A	615794	-	-	1.41E-03*
ENST00000322810	PLEC	Plectin	601282	Epidermolysis bullosa simplex (AR)	616487	1.49E-03*
ENST00000356860	CACNA2D1	Calcium channel, voltage-dependent, alpha-2/delta subunit 1	114204	-	-	1.52E-03*
ENST00000313237	PHF21B	PHD finger protein 21B	616727	-	-	2.88E-03*
ENST00000281471	AMN1	Antagonistic of mitotic exit network 1 homolog	-	-	-	5.12E-03
ENST00000374690	AR	Androgen receptor	313700	Androgen insensitivity (XLR)	300068	5.74E-03
ENST00000367194	KISS1	Kiss1 metastasis suppressor	603286	Hypogonadotropic hypogonadism 13 with or without anosmia	614842	6.15E-03

Figure 10. The E2-regulated KP^ARC neuron transcriptome may serve as a resource to discover new genes causing fertility disorders. *A: The 2329 E2-regulated genes of KP^ARC neurons overlap with the lists of genes proposed to cause reproductive disturbances in mice and/or humans, according to the Jackson Mammalian Phenotype*

Ontology (green circle) and the Human Phenotype Ontology (blue circle) databases. 17 disease genes are shared between mice and humans in the Venn diagram. Information about the E2-dependent transcripts of KP^{ARC} neurons may serve as an important resource to identify new genetic causes of reproductive disturbances, including CHH. 125 out of the 2329 regulated transcripts (in yellow circle) are enriched at least 3-times in KP^{ARC} neurons vs. the ARC region, expressed abundantly in KP^{ARC} cells (mean CPM≥100) and respond to E2 at |log2FC|≥1.0. Gene names in red show overlaps with known mouse or human disease genes. B: Manhattan plot illustrates the results of gene-based burden analysis of the top 125 candidate genes in a cohort of CHH patients versus gnomAd controls. Dotted lines indicate the threshold for statistical significance after correction for multiple testing (red: exome wide Bonferroni correction N=20,000, p < 2.5E-06; green: 5% FDR threshold; blue: 10% FDR threshold). Table contains basic data of putative CHH-candidate genes. Asterisks indicate enrichment p-values below the 0.05% FDR threshold.

125 transcripts were expressed at mean CPM≥100, showed at least a 3-fold enrichment (in CPM) in KP^{ARC} neurons *vs.* the ARC region, and at least a two-fold up- or downregulation by E2. The incidences of mouse and human disease genes increased to 20% (N=25) and 8% (N=12), respectively, by applying the above stringent selection criteria (color symbols in **Figure 10A**). The list of the 125 candidate protein-coding genes was used for a gene-based burden analysis comparing the abundance of rare, likely pathogenic variants in a large cohort of CHH patients (N=337) versus gnomAD control database (**Figure 10B**). As expected, we observed an enrichment in known CHH genes such as *TAC3* (p=6.61E-08), *TACR3* (p=1.01E-03) and *KISS1* (p=6.15E-03). Moreover, this analysis highlighted novel putative CHH-candidate genes like the Low-Density Lipoprotein Receptor-Related Protein 1B (*LRP1B*, p=3.14E-05) and the Calcium Voltage-Gated Channel Subunit Alpha1 G (*CACNA1G*, p=1.84E-04), a gene previously associated with spinocerebellar ataxia. Interestingly, also the Calcium Voltage-Gated Channel Auxiliary Subunit Alpha2delta 1 (*CACNA2D1*, p=1.49E-03) was found among the enriched genes, suggesting an important role of L-type and T-type calcium channels in human reproduction. The emerging role of these novel candidate genes in KP^{ARC} neurons and CHH pathophysiology requires further clarification by basic research and clinical genetic studies.

4.3.   Uncovering estrogen-dependent mechanisms in mouse KP[RP3V] neurons

4.3.1.   RNA-Seq of KP[RP3V] neurons reveals 222 E2-dependent genes

To examine estrogenic regulation of KP[RP3V] neurons, we dissected and pooled fluorescent KP[RP3V] neurons by LCM from OVX mice substituted with either oil or E2. Illumina-based RNA-Seq was performed to determine the transcriptional landscape of KP[RP3V]. Initial DESeq2 analysis identified 203 E2-regulated genes in KP[RP3V] neurons with the p.adj<0.05 cutoff. p.adj values are highly sensitive to the number of comparisons which can severely compromise the detection power for true positives (192, 193). Noisy, low-expression genes were shown to have adverse impact on the power of statistics in RNA-Seq studies (193). Given that these genes likely have relatively minor effect on KP neuron biology, we improved the power of DeSeq2 analysis by filtering out low-expression genes. Using the basemean>20 and p.adj<0.05 cutoffs, we identified 10,623 transcripts, 247 of which were E2-dependent including 222 protein coding genes. The 222 genes contained 45 new changes that were not included in the list unfiltered to low basemean. The heat map of E2-regulated transcripts showed disparate expression in the two experimental groups (**Figure 11A**).
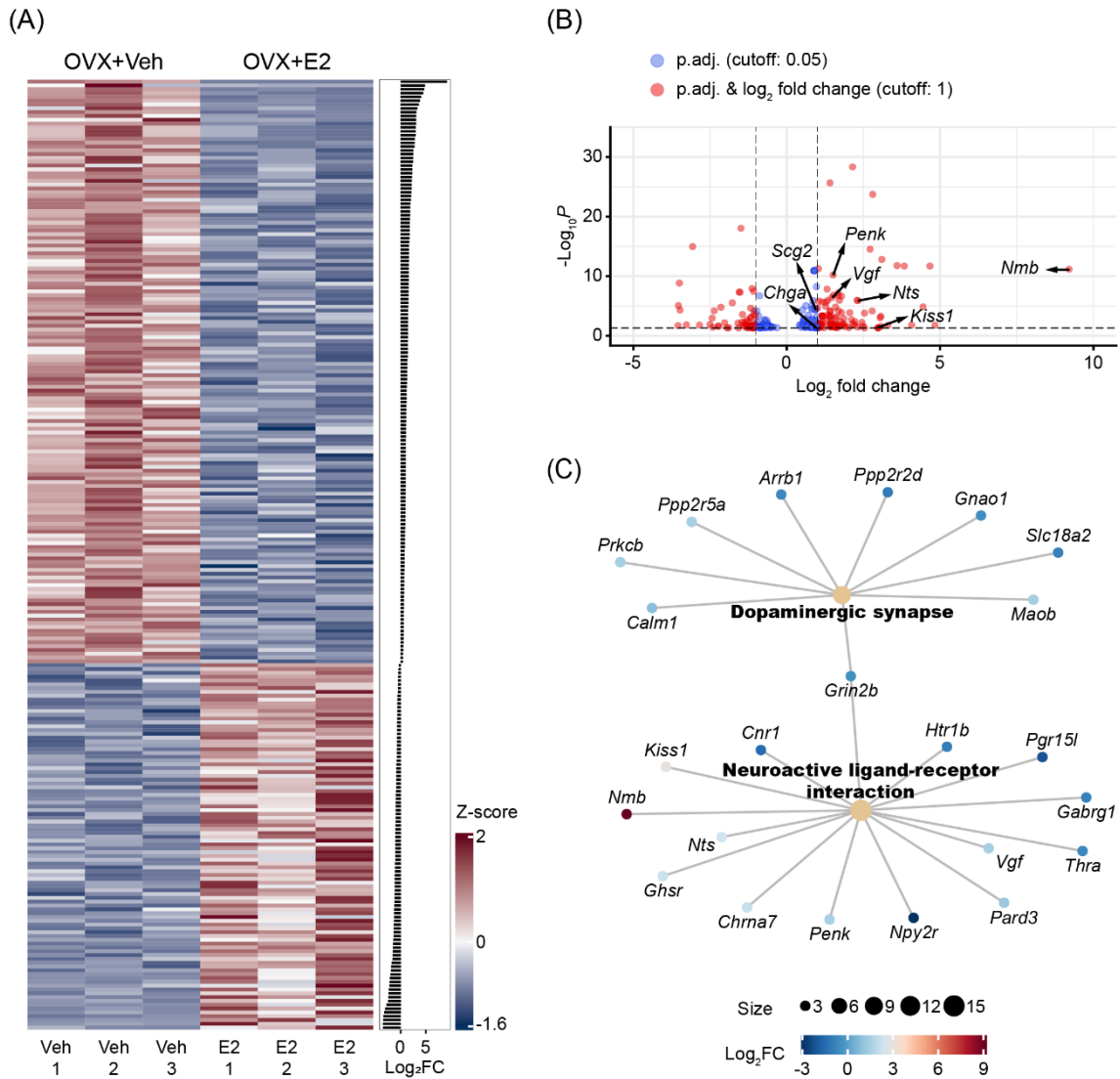
Figure 11. Estrogenic regulation of the KP^RP3V neuron transcriptome. *Heat map of all E2-dependent transcripts. Transcripts were arranged by size of fold change (FC). We used z-score values to illustrate the size of transcriptional changes, and the values are color coded. z-score is calculated from the CPM value, the mean CPM and the standard deviation of CPM values in a given experimental group (A). Volcano plot reveals 132 regulatory changes that exceed |log2FC| 1.0. Transcriptional changes of neuropeptides (Nmb, Kiss1, Nts, Penk) and granins (Chga, Scg2, Vgf) were marked (B). ORA of E2-dependent genes identified significant changes in the dopaminergic synapse and the neuroactive ligand-receptor interactions KEGG pathways. The number of genes in a given pathway is reflected in the size of the dot for the pathway. E2-induced changes of individual genes are color coded based on log2FC values (C).*

Among the 222 protein coding genes, 142 were up- and 80 were downregulated. The most robust upregulation was seen in the case of *Nmb* encoding neuromedin B (**Figure 11B**). Highly upregulated genes (log2FC>1) comprised additional neuropeptides (*Kiss1, Nts, Penk*) and a granin (*Vgf*), among others. *Cartpt* encoding neuropeptide CART was also highly upregulated, but the change did not reach statistical significance. ORA identified enrichment in changes of the dopaminergic synapse and neuroactive ligand-receptor interaction KEGG pathways (**Figure 11C**). Using gene ontology (GO) terms, ORA revealed significant enrichment of changes in the regulation of membrane potential (GO:0042391), synapse organization (GO:0050808), peptide transport (GO:0015833), hormone secretion (GO:0046879) GO categories, among others.

4.3.2. Comparative analysis unveils disparate E2-driven transcriptional responses

For consistency, RNA-Seq data of KP^{ARC} neurons were re-analyzed with the same filtering which resulted in 1583 medium-to-high abundance E2-regulated genes. While 470 low-expressed genes were excluded by this filtering, the enhanced statistical power resulted in the identification of 48 newly identified genes in KP^{ARC} neurons. Compared to KP^{RP3V} neurons, the KP^{ARC} neurons showed much higher number and more robust transcriptional responses to E2.
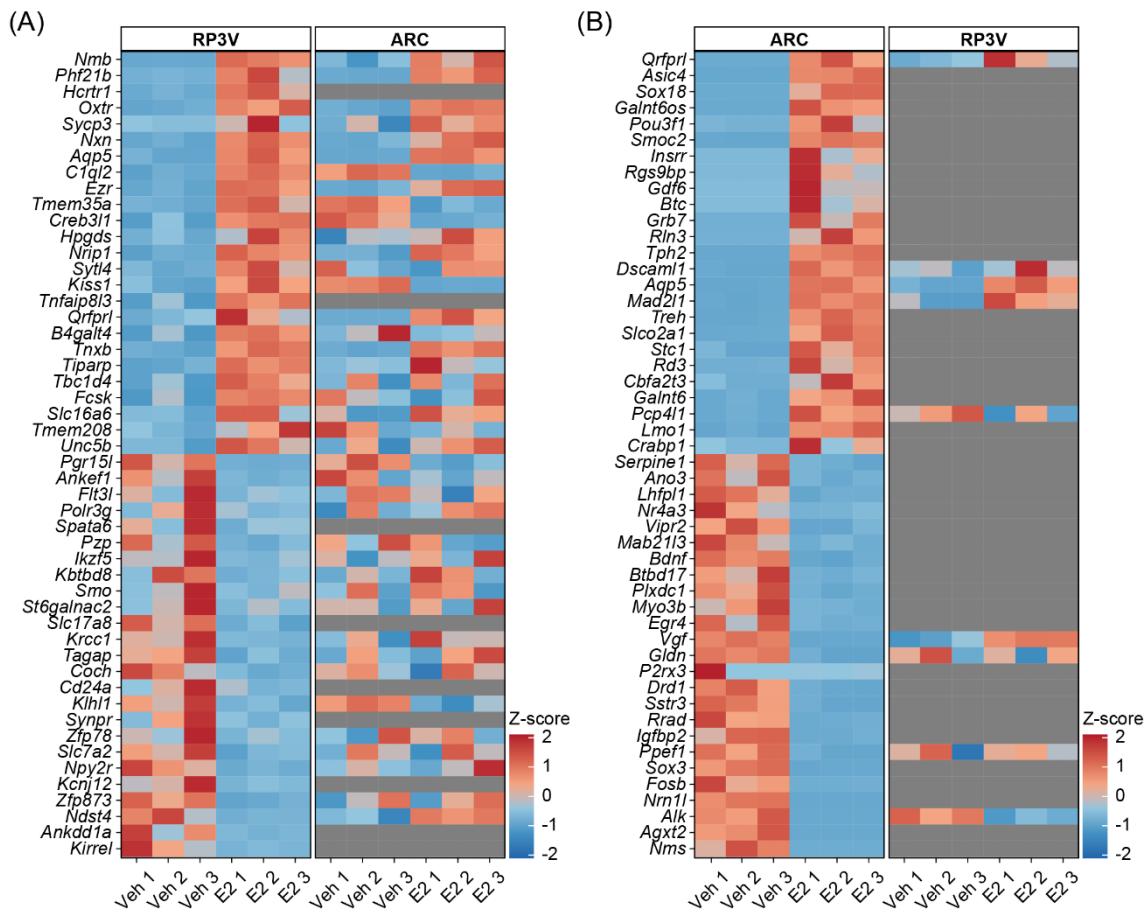
Figure 12. E2 differentially regulates the transcriptomes of KP^{RP3V} and KP^{ARC} neurons. *Heat map of the top 25 activated and top 25 inhibited genes in KP^{RP3V} neurons and behavior of the same genes in KP^{ARC} neurons (A). Heat map of the top 25 activated and top 25 inhibited genes in KP^{ARC} neurons and their behavior in KP^{RP3V} neurons (B).*

To display differences in estrogenic regulation of the two populations, we generated heat maps with the top 25 activated and top 25 suppressed genes in KP^{RP3V} neurons and illustrated in parallel expression of the same genes from KP^{ARC} neurons (**Figure 12A**). The top 25 activated and top 25 suppressed genes of KP^{ARC} neurons and their behavior in KP^{RP3V} neurons are shown similarly in **Figure 12B**. Markedly different responses of the two KP neuron populations to E2 prompted us to check the expression of major estrogen receptors. We detected abundant mRNA expression of *Esr1* encoding ERα in both KP^{RP3V} and KP^{ARC} neurons. However, we did not detect transcription of *Esr2* and Gper1 encoding ERβ and G-protein coupled estrogen receptor, respectively.

4.3.3. Despite disparate regulation there are ninety-six overlapping E2 target genes

Although the E2-driven transcriptional responses were different, we found ninety-six overlapping genes with sixty-two analogous and thirty-four opposite changes in KP^{RP3V} and KP^{ARC} neurons.
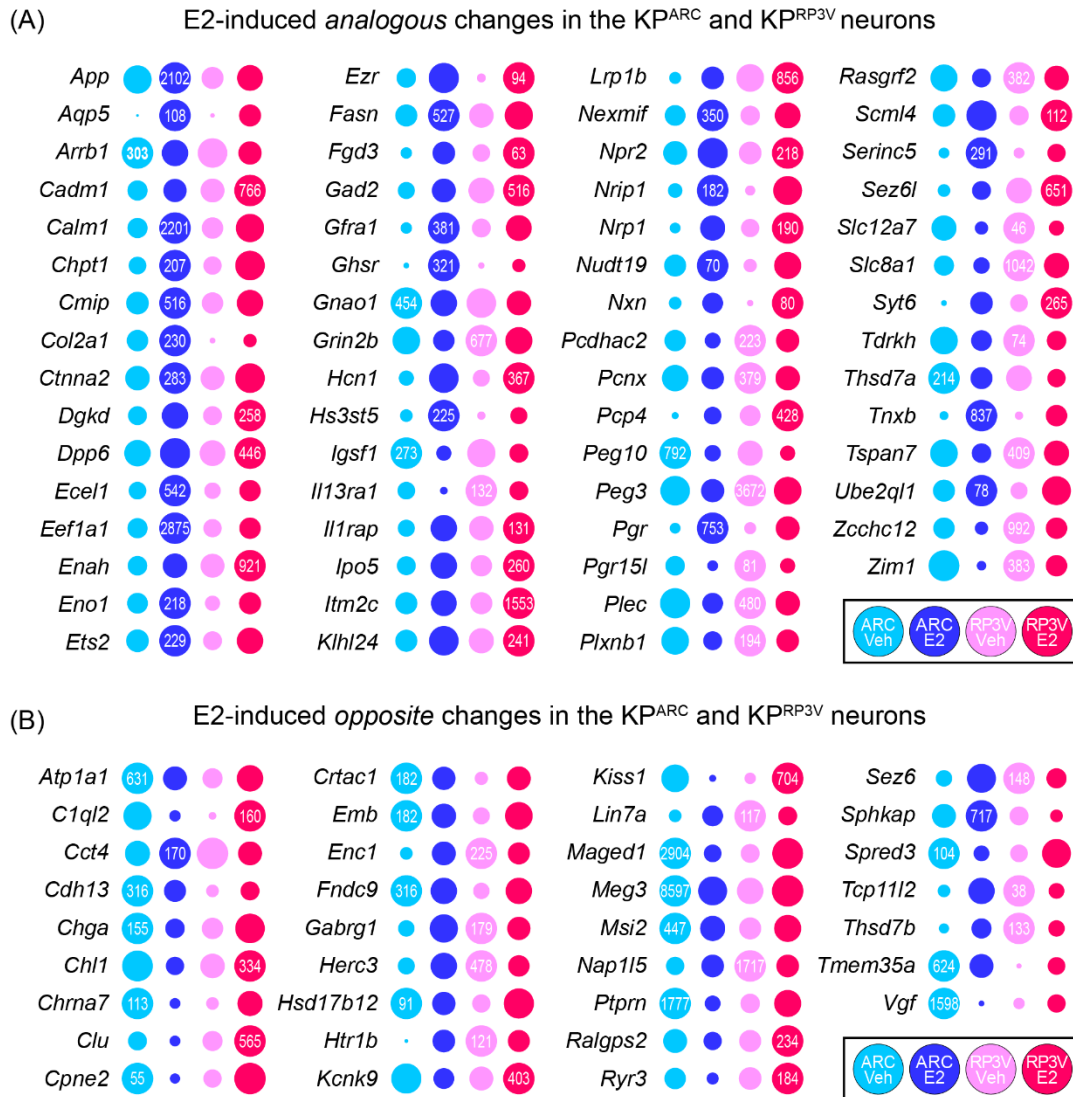
Figure 13. Overlapping E2 target genes in KP^{RP3V} and KP^{ARC} neurons. *E2 regulated 62 genes in the same (A, analogous changes), and 34 genes in opposite direction (B, opposite changes). Numbers in the dots reflect transcript abundance in CPM units.*

The sixty-two genes, which were regulated in the same direction consisted of TFs, synapse associated genes and calcium signaling molecules, among others (**Figure 13A**). There were 25 genes that displayed |log2FC| >1.0 changes in both populations

representing the highly responsive, common E2-dependent genes in KP neurons. Among highly expressed genes, E2 upregulated *App, Itm2c* (inhibits APP processing), *Calm1, Eef1a1*. E2 also increased expression of some synapse-associated genes including *Cadm1, Enah, Gad2, Syt6*, and decreased *Grin2b*. In addition, E2 enhanced mRNA expression of major calcium signaling molecules (*Pcp4, Calm1*) and pacemaker channel *Hcn1* in both cell populations. Thirty-four genes including *Kiss1* were oppositely regulated (**Figure 13B**), and several of them, regulated in a similar fashion as *Kiss1* (*Atp1a1, Chga, Vgf, Ptprn, Ralgps2*), were associated with neuropeptide secretion. Other oppositely regulated genes encoded proteins related to translational control (*Msi2*), calcium signaling (*Cpne2, Ryr3*), protein quality control (*Clu*), synaptic plasticity (*Cct4, Chl1*), cholinergic transmission (*Chrna7, Tmem35a*), among other functions.

4.3.4. E2 activates neuropeptide precursor and granin genes in KP[RP3V] neurons

In KP[RP3V] neurons, we identified seven E2-regulated neuropeptide and granin genes. Transcriptional activation of *Nmb, Kiss1, Nts* and *Penk* was significant (**Figure 14A**), and these neuropeptide genes were ranked first, eleventh, seventeenth and fiftieth in the list of E2-regulated genes. E2-induced increase of *Pnoc, Prok2* and *Cartpt* did not reach statistical significance. KP[RP3V] neurons highly expressed *Cartpt*, *Kiss1, Nmb, Nts* and *Penk*, while *Gal* was expressed moderately in OVX mice with E2 replacement. Neuropeptide precursor proteins are transported from the endoplasmic reticulum to the trans-Golgi network, where they are sorted and packed into dense-core vesicles (DCV). We showed upregulation of three granin genes, namely *Chga*, *Scg2, Vgf* and another gene of the secretory pathway, *Ptprn* (**Figure 14A**). Maturation of neuropeptides requires peptide bond cleavages in precursor molecules. E2 stimulated transcription of *Cpe Pam* and *Pcsk2* prohormone processing enzymes, but the changes did not reach statistical significance (p.adj<0.05). Genes related to DCV translocation, transport and fusion were not regulated.
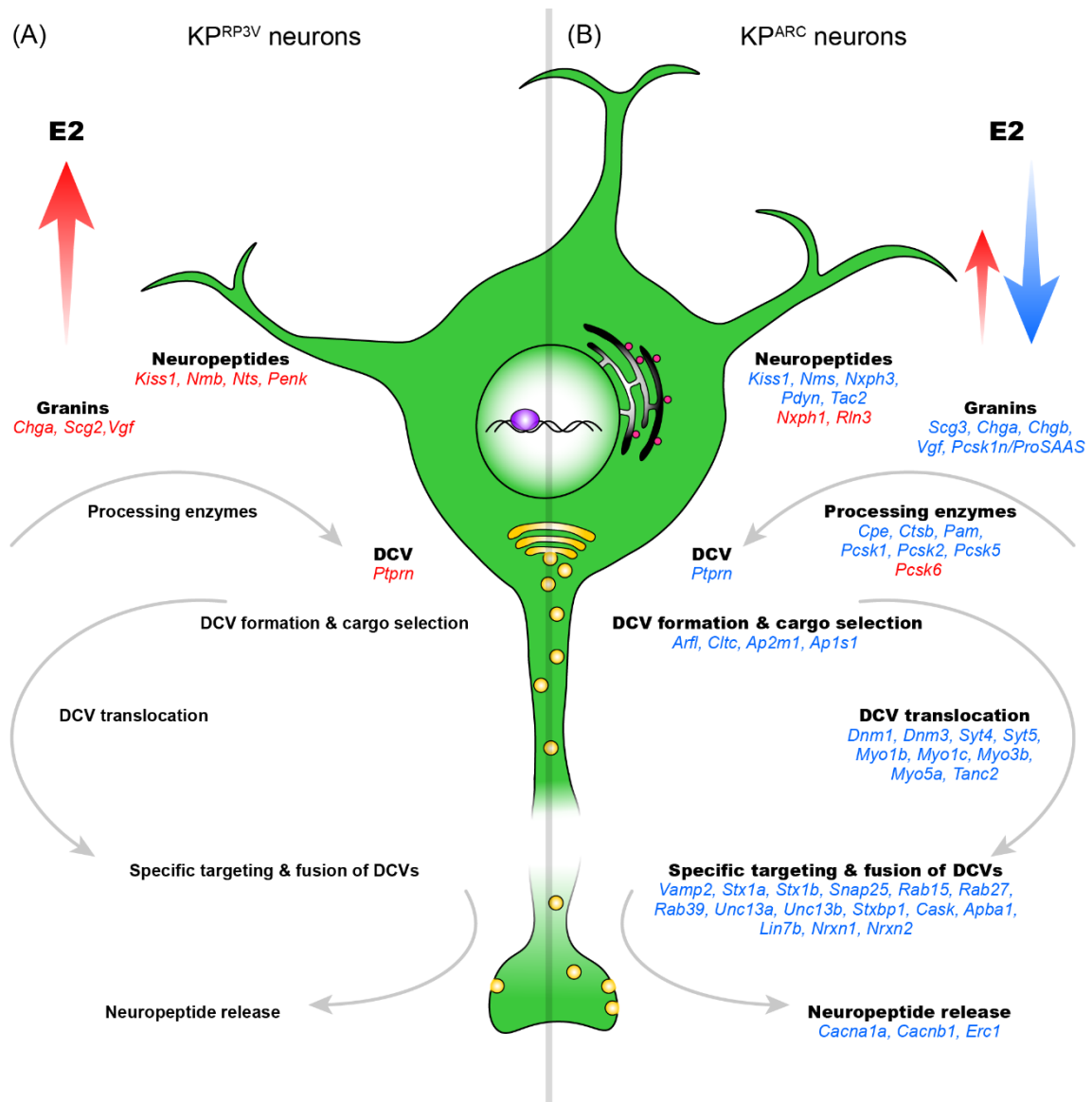
Figure 14. **E2-dependent elements of the regulated secretory pathway in KP^{RP3V} and KP^{ARC} neurons.** *E2-regulated genes involved in neuropeptide secretion are shown in KP^{RP3V} (A) and KP^{ARC} neurons (B). Genes in red and blue are up- and downregulated, respectively. DCV, dense-core vesicle.*

4.3.5. E2 inhibits neuropeptide precursors, granins, processing enzymes and multiple secretory pathway genes in KP^{ARC} neurons

In KP^{ARC} neurons, we found transcriptional inhibition of five co-expressed neuropeptide precursor genes including *Kiss1, Nms, Nxph3, Pdyn* and *Tac2* (**Figure 14B**). We showed downregulation of five members of the granin family including *Scg3, Chga, Chgb, Vgf, Pcsk1n/ProSAAS* and another gene, *Ptprn* (**Figure 14B**). Neuropeptide maturation takes

place in DCVs. E2 decreased mRNA expression of six processing enzymes including *Cpe, Ctsb, Pam, Pcsk1, Pcsk2* and *Pcsk5*, whereas the protease, *Pcsk6*, showed increased expression (**Figure 14B**). DCV formation and cargo selection depend on ADP-ribosylation factor 1 (*Arf1*) and components of the coat machinery. In KP^{ARC} neurons, E2 decreased transcription of *Arf1, Cltc, Ap2m1* and *Ap1s1*. From the trans-Golgi network, DCVs move towards the plasma membrane to release their content. Translocation relies upon dynamins, syntaxins, scaffolding and myosin motor proteins. In KP^{ARC} neurons, E2 downregulated mRNA expression of a large number of genes encoding dynamins (*Dnm1, Dnm3*), synaptotagmins (*Syt4, Syt5*) myosin (*Myo1b, Myo1c, Myo3b, Myo5a*) and scaffolding (*Tanc2*) proteins (**Figure 14B**). The SNARE complex and accessory factors are required for specific targeting and fusion of DCVs with the plasma membrane. E2 suppressed transcription of genes encoding components of the SNARE complex (*Vamp2, Stx1a, Stx1b, Snap25*) and accessory factors (*Rab15, Rab27, Rab39, Unc13a, Unc13b*). The DCV fusion machinery is linked to the *Munc18-1/CASK/Mint1/Lin7b* organizer complex, which binds to synaptic adhesion molecules neurexins. E2 downregulated constituents of the organizer complex (*Stxbp1* (coding *Munc18-1*), *Cask, Apba1* (coding *Mint1*), *Lin7b*) and neurexins (*Nrxn1, Nrxn2*) (**Figure 14B**). Cav2.1 and Cav2.2 channels orchestrate synchronous release of neuropeptides and neurotransmitters in most synapses. E2 downregulated *Cacna1a* (Cav2.1) and auxiliary Cav subunit *Cacnb1*, among others. Rab3-interacting proteins (RIMs), chief organizers of the active zone, are linked to Cav2.1 via RIM-binding protein encoded by *Erc1*, which was also suppressed by E2.

4.3.6. TFs show markedly different estrogenic regulation

Strikingly different transcriptional responses to E2 in KP^{RP3V} and KP^{ARC} neurons prompted us to determine the number of E2-dependent TFs. In KP^{RP3V} neurons, E2 regulated ten TFs. Based on the result of a recent publication (194), none of them interacted with ERα. In accord, STRING predicted no protein-protein interaction among them (**Figure 15A**). Neither transcriptional regulators, nor lncRNAs displayed E2-dependent expression in KP^{RP3V} neurons.
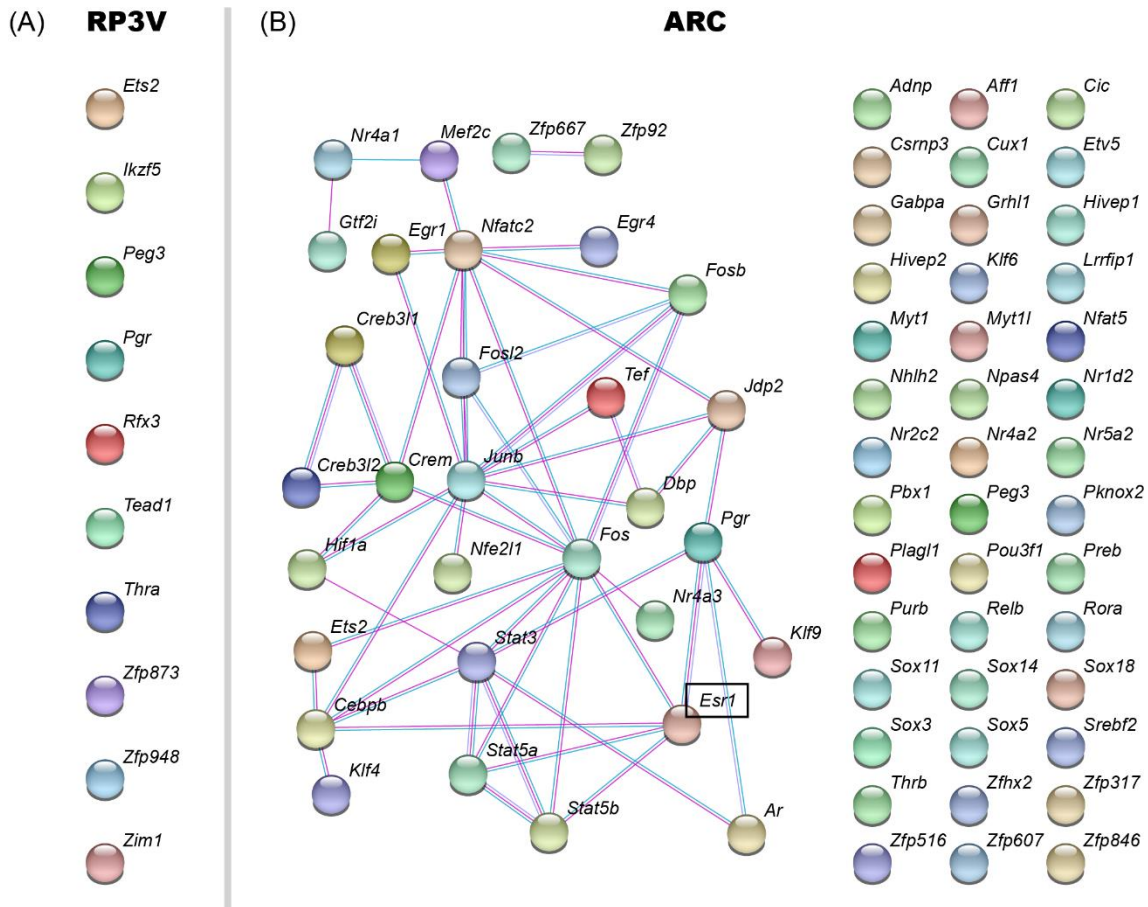
Figure 15. Protein interaction map of E2-dependent TFs in KP[RP3V] and KP[ARC] neurons. *Based on the STRING database, protein interaction map of E2-regulated TFs was built using stringent settings (interaction source: experiment and databases, minimum required interaction score: medium confidence). STRING identified no potential interactions in KP[RP3V] neurons (A). In contrast, STRING found potential interactions between 31 E2-dependent TFs in KP[ARC] neurons (B). Genes in bold are regulated in both cell types. Esr1, which encodes ERα is in bold and framed.*

In KP[ARC] neurons, E2 regulated mRNA expression of seventy TFs. E2-dependent TFs included nuclear hormone receptors (*Pgr, Rora, Thrb, Nr1d2, Nr2c2, Nr4a2, Nr5a2, Ar, Esr1, Nr4a1, Nr4a3*), homeobox proteins (*Adnp, Cux1, Pbx1, Pknox2, Zfhx2*), subunits of the AP-1 complex (*Fos, Junb, Jdp2*) and zinc finger proteins (*Hivep1, Zfp317*), among others. Of note, eight TFs including *Cebpb, Cic, Cux1, Fosl2, Gtf2i, Hivep1, Hivep2, Junb* were able to interact with ERα according to recently published data (194). To build a protein interaction map of E2-dependent TFs including putative interactions with ERα, we used the STRING database (195). Using strict settings (interaction source: experiment

and databases, minimum required interaction score: medium confidence), STRING predicted thirty-four protein-protein interactions between thirty-one TFs (**Figure 15B**). According to STRING, five TFs can interact with ERα. The STRING protein interaction map predicted hubs in the network including ERα, Fos, Junb and Nfatc2.

In addition, E2 also modulated mRNA expression of genes encoding transcriptional regulators, chromatin modifiers and regulatory lncRNAs in KP^ARC neurons. E2 upregulated components of the SWI/SNF (*Smarca2, Smarca4, Smarcd3, Bicral*) and ATRX:DAXX (*Atrx, Daxx*) chromatin remodelling complexes, histone methyltransferases (*Kmt2e, Wdr82*) and deacetylases (*Hdac11*). E2 downregulated some transcriptional repressors (*Gatad2a, Trps1, Zfp219*), DNA methyltransferases (*Dnmt3a*) and histone deacetylases (*Hdac3, Hdac9*). Among them, one transcriptional coregulator (*Ncoa6*) and several repressors/activators (*Atrx, Gatad2a, Nrip1, Smarca2, Smarca4, Trim24, Trps1*) may interact with ERα. E2 also modified expression of numerous regulatory lncRNAs in KP^ARC neurons.

5. Discussion

5.1. Differential Transcriptional Responses in Two Populations of KP Neurons Elicited by E2 Stimulation

Studies underlying this thesis were aimed at investigating the transcriptome profile regulated by estrogen in the ARC and in two distinct populations of KP neurons found in the ARC and the RP3V of mice. Revealing estrogen-dependent transcripts and biological processes in these systems contributed to our understanding of the intricate molecular mechanisms that may underlie negative feedback regulated by ARC neurons including KP^{ARC} (KNDy) neurons and positive feedback accounted for by KP^{RP3V} neurons.

To achieve our goal, we used female mouse models; a silicone capsule containing E2 or sunflower oil was implanted after OVX to obtain OVX+E2 and OVX+Veh models, respectively. After tissue fixation, coronal sections were prepared, and the entire ARC or more specifically, 300 KP^{ARC} or KP^{RP3V} neurons were harvested by laser microdissection. After RNA isolation, RNA sequencing was performed on these samples. The results were then evaluated using bioinformatic methods.

In KP^{ARC} neurons from female animals, many significant gene changes were detected in response to E2 (p.adj.<0.05, upregulated: 1190, downregulated: 1139). Changes in several TFs, neuropeptides, ribosomal and mitochondrial proteins, ion channels, transporters, receptors, and regulatory RNAs were identified. Alterations in the stimulatory serotonin receptor-4 transcript (*Htr4*) reduced the sensitivity of KP^{ARC} neurons to serotoninergic stimulation. In addition, several estrogen-regulated transcripts have been associated with pubertal/fertility abnormalities. By studying a cohort of patients with CHH (N=337), we were able to detect the enrichment of rare variants of known and novel putative CHH candidate genes (*LRP1B, CACNA1G, FNDC3A*).

Bioinformatics identified 222 E2-dependent genes in KP^{RP3V} neurons. Expression of four genes encoding neuropeptide precursors (*Nmb, Kiss1, Nts, Penk*) changed robustly, and changes of *Cartpt* (encoding for cocaine- and amphetamine regulated transcript) was sub-significant. These changes suggest the putative contribution of multiple neuropeptides to estrogen feedback mechanisms. When comparing the two KP neuronal populations, we found that in addition to different regulatory responses, KP^{RP3V} and KP^{ARC} neurons shared

sixty-two common alterations in genes encoding, among others, three hormone receptors (*Ghsr, Pgr, Npr2*), GAD-65 (*Gad2*), calmodulin and its regulator (*Calm1, Pcp4*). Intriguingly, thirty-four genes (*Kiss1, Vgf, Chrna7, Tmem35a*) regulated in opposite direction were also identified.

5.2. Critical assessment of the animal models utilized in our research

We chose to use non-physiological animal models for several reasons. First, it would have been challenging to identify significant transcriptional effects of physiological E2 fluctuations throughout the estrous cycle. Second, transcriptomic snapshots from normally cycling animals would be difficult to interpret due to the variable expression dynamics of E2-dependent transcripts. In addition, ovarian progesterone dynamics would further complicate the interpretation of estrogen effects based on the gene expression profile of intact females. Finally, we used OVX and subsequent treatment of OVX mice with exogenous E2 or vehicle to generate two easily reproducible groups of animals with low biological variation and high group homogeneity. Young mixed cycle female mice have a serum E2 concentration of 2.7 pg/mL (Diestrus: ~6 pg/ml; Proestrus: ~8pg/ml; Estrus: <0.3 pg/ml; Metestrus: ~0.5 pg/ml), as determined by GC-MS/MS) (184), while the OVX+E2 test mice have a serum E2 concentration of 7.59±0.74 pg/mL, within the physiological range. However, the natural serum E2 concentration in this OVX+E2 model may be slightly lower due to the previously noted serum matrix effect we detected. Based on the findings of this study, it can be reasonably assumed that the transcriptomes of ARC and KP^{ARC} neurons are influenced by estrogen and may exhibit fluctuations in intact female mice in response to cyclic changes in E2 negative feedback.

Nevertheless, the expression level of individual transcripts in our OVX+E2 model may not necessarily reflect the transcriptional landscape of intact diestrus/proestrus animals. Therefore, we propose that the prolonged 4-day E2 treatment of OVX mice may be clinically relevant to chronic estrogen exposure with relative progesterone deficiency, a common perimenopausal pathology. Furthermore, the transcriptomes of the OVX+Veh model may mimic the gene expression status of the ARC and its KP^{ARC} neurons following estrogen loss in postmenopausal women. Despite technical issues, we found that the CalBiotech ES180S-100 kit is the only one currently available that shows good E2 parallelism to the standard curve and accuracy compared to the gold standard GC-MS/MS

technique (153), based on a systematic comparison of nine commercial enzyme immunoassay kits.

5.3. Comparison of RNA-sequencing results from the ARC with earlier research findings

Although the ARC transcriptome's estrogen responsiveness has been previously investigated using RNA-Seq experiments, that study employed OVX wild-type mice, ERα-knockout mice, and mice with ERα containing a mutated DNA binding domain to differentiate between ERα-mediated, ERE-dependent, and ERα-independent E2 signaling, respectively (196). The number of significant transcript changes (at $p<0.05$ and $FC>1.5$) was 132, 35, and 22, respectively. Our study, which utilized OVX+E2 mice, found that several transcriptional changes were replicated in the ARC, but not all. Moreover, we identified additional significant changes in the ARC transcriptome that previous investigators did not report. We observed 4039 transcripts at $p<0.05$ and 2117 at $p.adj.<0.05$ that were differentially expressed between the two treatment groups. Of these, 844 and 483 changed more than 1.5 times at $p<0.05$ and $p.adj.<0.05$, respectively. The high number of regulated transcripts in our study may have been due to different methods, including unique LCM-based tissue collection, which allowed us to delineate precisely the structure of interest. Additionally, differences in estrogen treatment of OVX mice may have contributed to the differing transcriptional responses and gene regulation dynamics. While our focus was on KNDy neuron regulation, future studies may benefit from comparing the E2-dependent ARC and KP[ARC] neuron transcriptome databases to identify specific transcripts regulated within KP[ARC] neurons. Newly discovered peptide co-transmitters of KNDy neurons include *Vgf* and *Nms*, and regulated receptors expressed more highly in KP[ARC] neurons than in the ARC include *Npy4r, Ghsr, Lepr,* and *Prlr*, among others. Notably, KP[ARC] neurons are not the only estrogen-dependent cell type in the ARC, as evidenced by the altered expression of several transcripts such as *Nts, Sst, Agrp, Pnoc, Penk,* and *Cartpt* in the ARC of our OVX+E2 model. These E2-dependent transcripts contribute to our understanding of the estrogenic control of non-KP neurons, which may include presently undiscovered ARC neuron populations.

5.4. Investigating the molecular mechanisms involved in estrogen-induced transcriptional alterations

Our study found that multiple mechanisms contribute to the changes in gene expression profile in OVX mice treated with estrogen. We observed that many changes in our study could be consequences of indirect estrogen actions on other cell types communicating with the ARC and KP^{ARC} neurons. We found that the effects of estrogens are mediated solely by ERα in both KP^{ARC} and KP^{RP3V} neurons. We detected abundant expression of *Esr1*, which encodes ERα. Neither *Esr2* nor *Gper1* encoding ERβ and G-protein coupled estrogen receptors, respectively, showed expression in KP^{RP3V} and KP^{ARC} neurons. Multiple ERα-driven mechanisms that operate in hypothalamic KP neurons were inseparable in our study. ERα can bind in cis (chromatin association via direct DNA binding at ERE) or in trans (chromatin association via binding to other TFs) at enhancers. Enhancer activation requires the cooperative recruitment of multiple TFs and their cofactors.

We found approximately 2-300 TFs expressed in each cell type. Expression of ten TFs was E2-dependent in KP^{RP3V} neurons, while expression of seventy was E2-dependent in KP^{ARC} neurons, eight of which interacted with ERα. Specifically, the transcription of *Ar, Egr1, Fos, Fosb, Junb, Nr4a1,* and *Sox3* was suppressed by E2, while the well-known estrogen target *Pgr* showed a solid stimulatory response. This notion suggests that the transcriptional regulation of TFs may contribute significantly to secondary changes in the expression profile and functions of both KP cells. The STRING database predicted an intricate network of estrogen-regulated TFs in KP^{ARC} neurons. Additionally, E2 regulated several transcriptional regulators, chromatin modifiers, and regulatory lncRNAs, adding another layer of complexity to the ERα-mediated transcriptional mechanism in KP^{ARC} neurons.

Overall, our results suggests that the complex, multi-layered transcriptional regulatory mechanism allows KP^{ARC} neurons to respond and integrate various inputs that influence reproduction, including metabolic, circadian, and stress-related cues. In contrast, the less complex estrogen-dependent mechanisms revealed in KP^{RP3V} neurons suggest a less integrative role of this population in our model.

5.5. Impacts of E2 administration on neurotransmitter signaling towards KP^{ARC} neurons

The ORA analyzed the changes in KEGG pathways in response to E2 treatment. The results showed significant changes in 83 pathways, including several signaling pathways such as mitogen-activated protein kinase, PI3K-Akt, calcium, cyclic guanosine monophosphate-dependent protein kinase, and cAMP-dependent protein kinase. These pathways are known to play critical roles in various cellular functions, including proliferation, differentiation, and survival. The alterations observed in these pathways could have significant implications for the overall functioning of cells. However, the functional consequences of these changes require further investigation, which is beyond the scope of this thesis.

We found that E2 treatment profoundly altered neuropeptidergic, GABAergic, glutamatergic, dopaminergic, cholinergic, and serotonergic signaling to KP^{ARC} neurons. Therefore, we focused on the neuroactive ligand-receptor interaction pathway, which showed 57 E2-regulated transcripts. The neuroactive ligand-receptor interaction pathway is involved in several neurological functions, including mood regulation, learning, and memory. It also plays a critical role in the control of reproductive behavior.

Using neuroanatomical approaches, we confirmed that neuropeptide receptor ligands such as OXB, SST, NPY, and serotonin are present in neuronal afferents to KP^{ARC} neurons. However, some of the changes we observed in this study are difficult to interpret. For example, it would not be easy to speculate on the physiological consequences of the opposite regulation of *Sstr2* and *Sstr3* by E2, both of which encode receptors that inhibit adenylyl cyclases. Similarly, changes in *Npyr* transcripts, which encode receptors for NPY/PYY/PP, were challenging to interpret.

In contrast, the changes observed in all four regulated serotonin receptors (H*tr2a, Htr5a, Htr7,* and *Htr4*) allowed us to hypothesize reduced serotonergic stimulation of KP^{ARC} neurons in the OVX+E2 model. This concept follows the reduced function of the serotonergic synaptic pathway predicted by SPIA. We used slice electrophysiology experiments to confirm this hypothesis, showing that serotonin exerts a reduced excitatory effect on KP^{ARC} neurons in the OVX+E2 mouse model, partly due to reduced excitatory signaling at serotonin receptor 4. The electrophysiology results suggest the

involvement of serotonergic mechanisms in the estrogen-dependent control of the pulsatile and surge modes of LH release.

Numerous studies have provided evidence that serotonergic mechanisms play a vital role in the estrogen-dependent regulation of LH release, both in the pulsatile and surge modes (188). In OVX rats, serotonin has been shown to inhibit the high rate of LH release, whereas, in rats pre-treated with E2, it stimulates LH secretion. Interestingly, our electrophysiological studies found that KP^{ARC} neurons in slices of OVX+Veh mice had higher responses to serotonin, indicating that some multiple hypothalamic sites and mechanisms contribute to serotonin in vivo reproductive actions. Additionally, it has been reported that OVX female rats exhibit a morning/afternoon oscillatory pattern in serotonin metabolism in several brain areas involved in controlling LH secretion (188). These findings suggest that the relationship between serotonergic mechanisms and estrogen-dependent regulation of LH release is complex and requires further investigation to understand the underlying mechanisms fully.

In addition, KP^{ARC} neurons are known to contribute to the reproductive effects of serotonin, as research indicates that intracerebroventricular serotonin injection in male rats increases hypothalamic Kiss1 expression (197). Moreover, dysregulation of NKB secretion from KP^{ARC} neurons has been implicated as an essential factor in developing postmenopausal hot flushes (198). Interestingly, selective serotonin reuptake inhibitors have emerged as one of the most effective non-hormonal treatment options for this condition (199), suggesting a close relationship between serotonin activity and the physiological mechanisms that underlie hot flushes. Our results may have important implications for developing new treatments for postmenopausal symptoms, including hot flashes.

5.6. Investigating estrogen-induced alteration of neuropeptide activity in KP^{RP3V} neurons

In addition, neuropeptides play a central role in the function of KP^{RP3V} neurons. We found that four co-expressed neuropeptides (*Kiss1, Nmb, Nts,* and *Penk*) were upregulated, with statistical significance (p.adj<0.05). In comparison, the highly increased expression of three additional neuropeptides (*Pnoc, Prok2,* and *Cartpt*) did not reach statistical significance (p.adj>0.05). Furthermore, a set of neuropeptides was found to be

transcriptionally activated in response to E2 in KP^{RP3V} neurons. Of these E2-dependent genes, *Nmb* showed the most robust response to E2 in our study.

Our study revealed that *Nmb* was the most responsive E2-dependent gene among those we analyzed. Neuromedin B has been shown to stimulate GnRH release from hypothalamic extracts and increase plasma LH levels when administered intracerebroventricularly (200). Moreover, neuromedin B has been implicated in the estrogen feedback loop, given that GnRH neurons express receptors for this neuropeptide (201). The robust upregulation of *Nmb* in response to E2 supports the idea that neuromedin B may be a key regulator of positive estrogen feedback, acting in conjunction with KPs and other upregulated neuropeptides. These findings highlight the potential importance of neuromedin B in regulating the hypothalamic-pituitary-gonadal axis and provide a foundation for future investigations into the precise mechanisms through which this neuropeptide contributes to estrogen-dependent regulation of reproductive function.

We also found that E2 increased *Nts* expression in KP^{RP3V} neurons. This idea aligns with previous research demonstrating that E2 upregulates Nts expression in the anteroventral periventricular nucleus of the hypothalamus (AVPV) and that blocking neurotensin signaling reduces the LH surge (202). Although *Ntsr2* is expressed in GnRH neurons, central administration of neurotensin does not stimulate an LH surge. Additionally, no co-expression of *Kiss1* and *Nts* has been detected using double-label ISH (202). Nonetheless, our results indicate the presence of neurotensin receptors (*Ntsr1, Ntsr2*) in KP^{RP3V} neurons, suggesting that neurotensin signaling is involved in the communication between KP^{RP3V} neurons, as well as signaling towards GnRH neurons.

Finally, we found that E2 enhanced *Penk* expression. Co-expression of KP and met-enkephalin has been observed in the AVPV (203), and it is tempting to speculate that increased transcription of a set of neuropeptide genes, including *Kiss1, Nmb, Nts*, and *Penk*, in KP^{RP3V} neurons might act in synergy to trigger the LH surge during positive feedback.

After synthesis, neuropeptide precursors undergo processing and transport prior to secretion. Granins, significant constituents of the DCV intravesicular matrix, bind Ca2+ and aggregate at acidic pH (204), which is considered the driving force of DCV

biogenesis. We provide evidence that estrogens activate the transcription of *Chga, Scg2,* and *Vgf*. The insulinoma-associated (Ia-2) protein is involved in the transcriptional control of DCV biogenesis (205). E2 activates *Ptprn*, encoding Ia-2 protein, which may result in elevated DCV biogenesis.

A newly released research article investigated the estrogenic regulation of KP^{RP3V} neurons' active translatome (206), identifying 683 differentially expressed transcripts using a p-value threshold of less than 0.05. Our study yielded 52 common genes with the Stephens and Kauffman study, with 13 being both E2-regulated and statistically significant (p.adj<0.05) in both studies. Furthermore, while our study found statistical significance for an additional 39 genes, they were not statistically significant in the Stephens and Kauffman study. In the Stephens and Kauffman study, several genes, such as *C1ql2*, *Nmb*, *Sytl4*, and 36 others, were differentially expressed but did not reach statistical significance. Interestingly, the four neuropeptides found to be upregulated in our study, namely Kiss1, *Nmb*, *Nts*, and *Penk*, were among the genes that overlapped between the two studies. Despite using different methodologies and targeting different RNA populations for sequencing, our study and the Stephens and Kauffman study shared more than fifty genes that had almost identical estrogenic regulation in KP^{RP3V} neurons.

5.7. Investigating estrogen-responsive genes as possible contributors to human fertility disorders

The role of estrogen in the regulation of reproduction is well established, and its effects on gene expression in the ARC are of particular interest due to its critical role in the control of fertility. Recently, several E2-regulated transcripts enriched in KNDy neurons have been identified that are known to play a role in the control of reproduction, including *Kiss1*, *Tac2*, *Tacr3*, and *Esr1*, among others. In addition, mutations in these genes may underlie currently unexplained cases of CHH, a rare disorder characterized by delayed puberty and infertility.

To facilitate future genetic screening of patient databases and identify putative disease genes, we generated a list of genes using stringent selection criteria, including at least threefold enrichment in KP^{ARC} neurons versus the ARC region, at least twofold change ($|log2FC|\geq1.0$) in response to E2, and mean CPM $\geq$ 100 within KP^{ARC} neurons. We found

that this strategy increased the incidence of known mouse disease genes in the list from 7.1% to 20.0% and the incidence of known human disease genes from 1.8% to 8.0%.

In addition, a gene-based burden analysis of the top 125 candidate genes from the expression study, comparing a large cohort of CHH patients with gnomAD controls, revealed enrichments for rare transcript variants of several known CHH genes, such as *TAC3*, *TACR3*, and *KISS1*, as well as putative CHH candidate genes, including two members of the voltage-gated calcium channel family. While the results of this preliminary analysis do not necessarily indicate a causal relationship between the rare variants and CHH, they suggest that the list of highly estrogen-dependent KP^{ARC} neuron transcripts may become an essential resource for discovering novel genes responsible for human reproductive phenotypes.

In conclusion, identifying E2-regulated transcripts enriched in KP^{ARC} neurons has provided valuable insights into the molecular mechanisms underlying fertility regulation. Furthermore, the list of putative disease genes generated using stringent selection criteria may serve as an essential resource for future genetic screening of patient databases and the discovery of new genes responsible for human reproductive phenotypes, including CHH.

6. Conclusion

According to conventional understanding, KNDy neurons play a crucial role in regulating pulsatile GnRH secretion by influencing negative feedback effects of E2, through KP/KP receptor signaling on the preterminal segments of hypophysiotropic GnRH processes. However, the molecular mechanisms responsible for this feedback are not well understood. This study has identified changes in neuropeptide genes enriched in non-KP cells, such as *Agrp*, *Nts*, and *Sst*, which may have a transsynaptic effect on KP^{ARC} neurons which express *Mc3r*, *Ntsr2* and *Sstr2/Sstr3* receptors. Additionally, E2 may indirectly affect the gene expression profile of KP^{ARC} neurons through transsynaptic effects outside of the ARC. However, our RNA-Seq studies found no evidence for glial/endothelial involvement in these indirect E2 effects on KP^{ARC} cells.

E2 produces different transcriptional responses in KP^{ARC} and KP^{RP3V} neurons, with 96 overlapping genes between the two KP neuronal populations. Among the upregulated genes in KP^{RP3V} neurons are four neuropeptide precursor genes: *Kiss1, Nmb*, *Nts*, and *Penk.* In contrast, several neuropeptide encoding genes, including *Kiss1*, *Nms*, *Nxph3*, *Pdyn*, and *Tac2,* were downregulated in KP^{ARC} neurons. Our models in this comparison suggest that the estrogenic regulation of gene expression is more complex in the KP^{ARC} population than in the population of KP^{RP3V} neurons.

In addition to changing the expression of neuropeptide transmitter genes, E2 significantly alters the expression of various nuclear hormone receptors, ion channels, and influences a large variety of biological processes, including transcription, mitochondrial and ribosomal function, and synaptic plasticity. We found a surprisingly large number of E2-regulated lncRNAs. The estrogenic regulation of these regulatory RNAs opens a new avenue in sex steroid research. Finally, our findings on the estrogen-dependent KP neuron transcriptome in mice have important clinical implications for the estrogenic regulation of the human hypothalamus during the menstrual cycle and for the putative molecular consequences of postmenopausal estrogen deficiency.

Major achievements:

1. We have determined 2117 estrogen-regulated genes and several functional pathways in the mouse ARC

2. We have detected 2329 estrogen-regulated genes falling into various functional categories and 83 functional pathways in ZsGreen-tagged KP^{ARC} neurons of estrogen treated mice.

3. We demonstrated that estrogen treatment also regulates the expression of multiple neurotransmitter receptors in KP^{ARC} neurons. The detection of the receptor ligands (somatostatin, serotonin) in neuronal afferents to KP^{ARC} neurons supports the idea that regulated receptor expression contributes to the estrogen-dependent neuronal control of KP^{ARC} neuronal functions.

4. We discovered a correlation between the estrogenic regulation of serotonergic receptors and a decrease in the excitatory responses of KP^{ARC} neurons to low doses of 5-HT, and the selective 5-HT4R agonist Cisapride. These data indicate that estrogen reduces the sensitivity of KP^{ARC} neurons to the excitatory actions of serotonin.

5. We described an overlap between the E2-regulated genes and patient databases, suggesting that the estrogen-regulated transcriptome of KP^{ARC} neurons has the potential to provide new insights into the complex pathomechanisms underlying fertility disorders and reveal novel candidate disease genes.

6. In studies of ZsGreen-tagged KP^{RP3V} neurons, we identified 222 significantly estrogen-regulated genes and a few functional pathways.

7. We established that E2 treatment elicits distinct transcriptional responses in KP^{RP3V} and KP^{ARC} neurons, with 96 overlapping genes consisting 62 similarly and 34 inversely regulated genes. We provided evidence that the regulation of gene expression by E2 is much more complex and involves many more genes and mechanisms in KP^{ARC} than in KP^{RP3V} neurons.

7. Summary

The KP neuronal system, with cell bodies located in the RP3V and the ARC, plays a crucial role in mediating positive and negative estrogen feedback, respectively, to the GnRH neuron system. The molecular background of feedback mechanisms is still poorly understood. To obtain better understanding of molecular changes accompanying sex steroid feedback, we used high throughput RNA sequencing technologies on tissues and KP neurons isolated from the hypothalamus of ovariectomized mice treated with E2 or vehicle. Differential expression analysis of transcriptomic data identified a large number of transcriptional changes (p.adj.<0.05; 1190 upregulated and 1139 downregulated transcripts) in KP^{ARC} neurons in response to E2. E2 decreased transcription of known neuropeptides including *Kiss1*, *Tac2*, *Pdyn*, and novel ones such as *Nms* and *Nxph3*. Changes in several TFs, ion channels, transporters, receptors, and regulatory RNAs were identified. In addition, we demonstrated that the estrogenic downregulation of the stimulatory serotonin receptor-4 transcript (*Htr4*) reduced the sensitivity of kisspeptin neurons to serotoninergic stimulation. Several estrogen-regulated transcripts have previously been associated with inborn errors of puberty/fertility. By studying a cohort of patients with CHH (N=337), we detected enrichment of rare variants of known and novel putative CHH candidate genes (*LRP1B, CACNA1G, FNDC3A*).

In studies of KP^{RP3V} neurons, 222 E2-dependent genes were identified by bioinformatic analysis. The expression of four genes encoding neuropeptide precursors (*Nmb, Kiss1, Nts, Penk*) was robustly upregulated, and *Cartpt* was sub-significantly upregulated. These observations suggest a combined contribution of several neuropeptides to the positive estrogen feedback mechanism. Comparing the two KP neuron populations, we found that in addition to distinct regulatory responses, KP^{RP3V} and KP^{ARC} neurons shared sixty-two common alterations, with genes encoding three hormone receptors (*Ghsr, Pgr, Npr2*), GAD-65 (*Gad2*), calmodulin and its regulator (*Calm1, Pcp4*). We also identified thirty-four inversely regulated genes (*Kiss1, Vgf, Chrna7, Tmem35a*) in the two KP cell populations. Our results shed new light on the molecular background of estrogen-dependent regulatory mechanisms in the two functionally distinct KP neuron populations. They also raise the potential importance of hitherto poorly studied neuropeptide cotransmitters and regulatory processes.

8. Összefoglalás

A harmadik agykamra rostrális periventrikuláris területén, illetve az arcuatus idegmagban elhelyezkedő KP neuron populációk kiemelt szerepet játszanak az ösztrogén GnRH neuronokra gyakorolt pozitív és negatív visszacsatolásának közvetítésében. A két visszacsatolási mechanizmus molekuláris hátterének vizsgálatára nagy-áteresztőképességű RNS szekvenálási módszertanokat alkalmaztunk. Az ARC KP neuronjaiban 17β-ösztradiol hatására nagyszámú szignifikáns génváltozás következett be (p.adj.<0,05; 1190 upregulált és 1139 downregulált transzkriptum). Számos transzkripciós faktor, neuropeptid, riboszomális és mitokondriális fehérje, ioncsatorna, transzporter, receptor és szabályozó RNS változását azonosítottuk. A serkentő szerotonin receptor-4 transzkriptum (*Htr4*) változása csökkentette a KP neuronok érzékenységét a szerotoninerg stimulációra. Számos ösztrogén által szabályozott transzkriptumot korábban már kapcsolatba hoztak a pubertás/fertilitás veleszületett rendellenességeivel. CHH-ban szenvedő beteg kohorszot (N=337) vizsgálva, ki tudtuk mutatni már ismert, és új, feltételezett CHH-jelölt gének (*LRP1B, CACNA1G, FNDC3A*) ritka variánsainak feldúsulását az ösztrogén által erősen regulált transzkriptumok között.

Az KP^RP3V neuronjaiban a bioinformatikai elemzés 222 E2-függő gént azonosított. Négy neuropeptid-prekurzort kódoló gén (*Nmb, Kiss1, Nts, Penk*) expressziója robusztusan, a *Cartpt* pedig szubszignifikánsan emelkedett volt. A megfigyelés több neuropeptid transzmitter együttes hozzájárulását sugallja a pozitív ösztrogén-visszacsatolási mechanizmushoz. A két KP neuron populáció változásait elemezve, megállapítottuk, hogy az eltérő szabályozási válaszok mellett a KP^RP3V és KP^ARC neuronok hatvankét azonos irányú génválaszt is mutattak, többek között három hormonreceptort (*Ghsr, Pgr, Npr2*), a GAD-65-öt (*Gad2*), a kalmodulint és annak szabályozóját (*Calm1, Pcp4*) kódoló génekben. Harmincnégy ellentétesen szabályozott gént (*Kiss1, Vgf, Chrna7, Tmem35a*) is sikerült azonosítanunk.Eredményeink új megvilágításba helyezik a két funkcionálisan különböző kisspeptin neuronpopuláció ösztrogén-függő szabályozásának molekuláris hátterét, továbbá, felvetik egyéb neuropeptide átvivőanyagok és ezidáig kevéssé tanulmányozott szabályozási folyamatok jelentőségét is a visszacsatolási mechanizmusokban.

9. References

1. Herbison AE. (2018) The Gonadotropin-Releasing Hormone Pulse Generator. Endocrinology, 159: 3723-3736.

2. Herbison AE. (1998) Multimodal influence of estrogen upon gonadotropin-releasing hormone neurons. Endocr Rev, 19: 302-330.

3. Karsch FJ, Foster DL. (1975) Sexual differentiation of the mechanism controlling the preovulatory discharge of luteinizing hormone in sheep. Endocrinology, 97: 373-379.

4. Knobil E. (1980) The neuroendocrine control of the menstrual cycle. Recent Prog Horm Res, 36: 53-88.

5. Yoshida K, Tobet SA, Crandall JE, Jimenez TP, Schwarting GA. (1995) The migration of luteinizing hormone-releasing hormone neurons in the developing rat is associated with a transient, caudal projection of the vomeronasal nerve. J Neurosci, 15: 7769-7777.

6. Herbison AE. (2020) A simple model of estrous cycle negative and positive feedback regulation of GnRH secretion. Front Neuroendocrinol, 57: 100837.

7. Moenter SM, Caraty A, Karsch FJ. (1990) The estradiol-induced surge of gonadotropin-releasing hormone in the ewe. Endocrinology, 127: 1375-1384.

8. Sarkar DK, Chiappa SA, Fink G, Sherwood NM. (1976) Gonadotropin-releasing hormone surge in pro-oestrous rats. Nature, 264: 461-463.

9. Schwanzel-Fukuda M, Pfaff DW. (1989) Origin of luteinizing hormone-releasing hormone neurons. Nature, 338: 161-164.

10. Wierman ME, Kiseljak-Vassiliades K, Tobet S. (2011) Gonadotropin-releasing hormone (GnRH) neuron migration: initiation, maintenance and cessation as critical steps to ensure normal reproductive function. Front Neuroendocrinol, 32: 43-52.

11. Merchenthaler I, Kovacs G, Lavasz G, Setalo G. (1980) The preoptico-infundibular LH-RH tract of the rat. Brain Res, 198: 63-74.

12. Rance NE, Young WS, 3rd, McMullen NT. (1994) Topography of neurons expressing luteinizing hormone-releasing hormone gene transcripts in the human hypothalamus and basal forebrain. J Comp Neurol, 339: 573-586.

13. Schwanzel-Fukuda M, Pfaff DW. (1990) The migration of luteinizing hormone-releasing hormone (LHRH) neurons from the medial olfactory placode into the medial basal forebrain. Experientia, 46: 956-962.

14. Wray S, Grant P, Gainer H. (1989) Evidence that cells expressing luteinizing hormone-releasing hormone mRNA in the mouse are derived from progenitor cells in the olfactory placode. Proc Natl Acad Sci U S A, 86: 8132-8136.

15. Campbell RE, Han SK, Herbison AE. (2005) Biocytin filling of adult gonadotropin-releasing hormone neurons in situ reveals extensive, spiny, dendritic processes. Endocrinology, 146: 1163-1169.

16. Herde MK, Iremonger KJ, Constantin S, Herbison AE. (2013) GnRH neurons elaborate a long-range projection with shared axonal and dendritic functions. J Neurosci, 33: 12689-12697.

17. Iremonger KJ, Herbison AE. (2012) Initiation and propagation of action potentials in gonadotropin-releasing hormone neuron dendrites. J Neurosci, 32: 151-158.

18. Iremonger KJ, Herbison AE. (2015) Multitasking in Gonadotropin-Releasing Hormone Neuron Dendrites. Neuroendocrinology, 102: 1-7.

19. Plant TM. (2015) 60 YEARS OF NEUROENDOCRINOLOGY: The hypothalamo-pituitary-gonadal axis. J Endocrinol, 226: T41-54.

20. Caraty A, Orgeur P, Thiery JC. (1982) [Demonstration of the pulsatile secretion of LH-RH into hypophysial portal blood of ewes using an original technic for multiple samples]. C R Seances Acad Sci III, 295: 103-106.

21. Clarke IJ, Cummins JT. (1982) The temporal relationship between gonadotropin releasing hormone (GnRH) and luteinizing hormone (LH) secretion in ovariectomized ewes. Endocrinology, 111: 1737-1739.

22. Goodman RL, Parfitt DB, Evans NP, Dahl GE, Karsch FJ. (1995) Endogenous opioid peptides control the amplitude and shape of gonadotropin-releasing hormone pulses in the ewe. Endocrinology, 136: 2412-2420.

23. Moenter SM, Brand RM, Midgley AR, Karsch FJ. (1992) Dynamics of gonadotropin-releasing hormone release during a pulse. Endocrinology, 130: 503-510.

24. Weiner RI, Wetsel W, Goldsmith P, Martinez de la Escalera G, Windle J, Padula C, Choi A, Negro-Vilar A, Mellon P. (1992) Gonadotropin-releasing hormone neuronal cell lines. Front Neuroendocrinol, 13: 95-119.

25. Moore JP, Jr., Shang E, Wray S. (2002) In situ GABAergic modulation of synchronous gonadotropin releasing hormone-1 neuronal activity. J Neurosci, 22: 8932-8941.

26. Terasawa E, Keen KL, Mogi K, Claude P. (1999) Pulsatile release of luteinizing hormone-releasing hormone (LHRH) in cultured LHRH neurons derived from the embryonic olfactory placode of the rhesus monkey. Endocrinology, 140: 1432-1441.

27. Campos P, Herbison AE. (2014) Optogenetic activation of GnRH neurons reveals minimal requirements for pulsatile luteinizing hormone secretion. Proc Natl Acad Sci U S A, 111: 18387-18392.

28. Constantin S, Jasoni C, Romano N, Lee K, Herbison AE. (2012) Understanding calcium homeostasis in postnatal gonadotropin-releasing hormone neurons using cell-specific Pericam transgenics. Cell Calcium, 51: 267-276.

29. Purnelle G, Gerard A, Czajkowski V, Bourguignon JP. (1997) Pulsatile secretion of gonadotropin-releasing hormone by rat hypothalamic explants without cell bodies of GnRH neurons [corrected]. Neuroendocrinology, 66: 305-312.

30. Rasmussen DD. (1993) Episodic gonadotropin-releasing hormone release from the rat isolated median eminence in vitro. Neuroendocrinology, 58: 511-518.

31. Xia L, Van Vugt D, Alston EJ, Luckhaus J, Ferin M. (1992) A surge of gonadotropin-releasing hormone accompanies the estradiol-induced gonadotropin surge in the rhesus monkey. Endocrinology, 131: 2812-2820.

32. Morato T, Hayano M, Dorfman RI, Axelrod LR. (1961) The intermediate steps in the biosynthesis of estrogens from androgens. Biochem Biophys Res Commun, 6: 334-338.

33. Wu MV, Manoli DS, Fraser EJ, Coats JK, Tollkuhn J, Honda S, Harada N, Shah NM. (2009) Estrogen masculinizes neural pathways and sex-specific behaviors. Cell, 139: 61-72.

34. McEwan IJ. (2016) The Nuclear Receptor Superfamily at Thirty. Methods Mol Biol, 1443: 3-9.

35. Gibson DA, Saunders PT. (2012) Estrogen dependent signaling in reproductive tissues - a role for estrogen receptors and estrogen related receptors. Mol Cell Endocrinol, 348: 361-372.

36. Hewitt SC, Harrell JC, Korach KS. (2005) Lessons in estrogen biology from knockout and transgenic animals. Annu Rev Physiol, 67: 285-308.

37. Jensen EV, DeSombre ER. (1973) Estrogen-receptor interaction. Science, 182: 126-134.

38. Hewitt SC, Korach KS. (2018) Estrogen Receptors: New Directions in the New Millennium. Endocr Rev, 39: 664-675.

39. Hermanson O, Glass CK, Rosenfeld MG. (2002) Nuclear receptor coregulators: multiple modes of modification. Trends Endocrinol Metab, 13: 55-60.

40. Glass CK, Rosenfeld MG. (2000) The coregulator exchange in transcriptional functions of nuclear receptors. Genes Dev, 14: 121-141.

41. Smith CL, O'Malley BW. (2004) Coregulator function: a key to understanding tissue specificity of selective receptor modulators. Endocr Rev, 25: 45-71.

42. Hah N, Kraus WL. (2014) Hormone-regulated transcriptomes: lessons learned from estrogen signaling pathways in breast cancer cells. Mol Cell Endocrinol, 382: 652-664.

43. Kushner PJ, Agard DA, Greene GL, Scanlan TS, Shiau AK, Uht RM, Webb P. (2000) Estrogen receptor pathways to AP-1. J Steroid Biochem Mol Biol, 74: 311-317.

44. Kushner PJ, Webb P, Uht RM, Liu M-M, Price RH. (2003) Estrogen receptor action through target genes with classical and alternative response elements. Pure and Applied Chemistry, 75: 1757-1769.

45. Szego CM, Davis JS. (1967) Adenosine 3',5'-monophosphate in rat uterus: acute elevation by estrogen. Proc Natl Acad Sci U S A, 58: 1711-1718.

46. Kelly MJ, Moss RL, Dudley CA. (1976) Differential sensitivity of preoptic-septal neurons to microelectrophoresed estrogen during the estrous cycle. Brain Res, 114: 152-157.

47. Sarkar DK, Fink G. (1980) Luteinizing hormone releasing factor in pituitary stalk plasma from long-term ovariectomized rats: effects of steroids. J Endocrinol, 86: 511-524.

48.   Lagrange AH, Ronnekleiv OK, Kelly MJ. (1997) Modulation of G protein-coupled receptors by an estrogen receptor that activates protein kinase A. Mol Pharmacol, 51: 605-612.

49.   Mermelstein PG, Becker JB, Surmeier DJ. (1996) Estradiol reduces calcium currents in rat neostriatal neurons via a membrane receptor. J Neurosci, 16: 595-604.

50.   Clarke CH, Norfleet AM, Clarke MS, Watson CS, Cunningham KA, Thomas ML. (2000) Perimembrane localization of the estrogen receptor alpha protein in neuronal processes of cultured hippocampal neurons. Neuroendocrinology, 71: 34-42.

51.   Pappas TC, Gametchu B, Watson CS. (1995) Membrane estrogen receptor-enriched GH(3)/B6 cells have an enhanced non-genomic response to estrogen. Endocrine, 3: 743-749.

52.   Razandi M, Pedram A, Greene GL, Levin ER. (1999) Cell membrane and nuclear estrogen receptors (ERs) originate from a single transcript: studies of ERalpha and ERbeta expressed in Chinese hamster ovary cells. Mol Endocrinol, 13: 307-319.

53.   Qiu J, Bosch MA, Tobias SC, Grandy DK, Scanlan TS, Ronnekleiv OK, Kelly MJ. (2003) Rapid signaling of estrogen in hypothalamic neurons involves a novel G-protein-coupled estrogen receptor that activates protein kinase C. J Neurosci, 23: 9529-9540.

54.   Qiu J, Bosch MA, Tobias SC, Krust A, Graham SM, Murphy SJ, Korach KS, Chambon P, Scanlan TS, Ronnekleiv OK, Kelly MJ. (2006) A G-protein-coupled estrogen receptor is involved in hypothalamic control of energy homeostasis. J Neurosci, 26: 5649-5655.

55.   Toran-Allerand CD, Guan X, MacLusky NJ, Horvath TL, Diano S, Singh M, Connolly ES, Jr., Nethrapalli IS, Tinnikov AA. (2002) ER-X: a novel, plasma membrane-associated, putative estrogen receptor that is regulated during development and after ischemic brain injury. J Neurosci, 22: 8391-8401.

56.   Revankar CM, Cimino DF, Sklar LA, Arterburn JB, Prossnitz ER. (2005) A transmembrane intracellular estrogen receptor mediates rapid cell signaling. Science, 307: 1625-1630.

57. Filardo EJ, Quinn JA, Bland KI, Frackelton AR, Jr. (2000) Estrogen-induced activation of Erk-1 and Erk-2 requires the G protein-coupled receptor homolog, GPR30, and occurs via trans-activation of the epidermal growth factor receptor through release of HB-EGF. Mol Endocrinol, 14: 1649-1660.

58. Wu GY, Deisseroth K, Tsien RW. (2001) Activity-dependent CREB phosphorylation: convergence of a fast, sensitive calmodulin kinase pathway and a slow, less sensitive mitogen-activated protein kinase pathway. Proc Natl Acad Sci U S A, 98: 2808-2813.

59. Filardo EJ. (2002) Epidermal growth factor receptor (EGFR) transactivation by estrogen via the G-protein-coupled receptor, GPR30: a novel signaling pathway with potential significance for breast cancer. J Steroid Biochem Mol Biol, 80: 231-238.

60. Filardo EJ, Quinn JA, Frackelton AR, Jr., Bland KI. (2002) Estrogen action via the G protein-coupled receptor, GPR30: stimulation of adenylyl cyclase and cAMP-mediated attenuation of the epidermal growth factor receptor-to-MAPK signaling axis. Mol Endocrinol, 16: 70-84.

61. Noel SD, Keen KL, Baumann DI, Filardo EJ, Terasawa E. (2009) Involvement of G protein-coupled receptor 30 (GPR30) in rapid action of estrogen in primate LHRH neurons. Mol Endocrinol, 23: 349-359.

62. Prossnitz ER, Arterburn JB, Sklar LA. (2007) GPR30: A G protein-coupled receptor for estrogen. Mol Cell Endocrinol, 265-266: 138-142.

63. Brailoiu E, Dun SL, Brailoiu GC, Mizuo K, Sklar LA, Oprea TI, Prossnitz ER, Dun NJ. (2007) Distribution and characterization of estrogen receptor G protein-coupled receptor 30 in the rat central nervous system. J Endocrinol, 193: 311-321.

64. Funakoshi T, Yanai A, Shinoda K, Kawano MM, Mizukami Y. (2006) G protein-coupled receptor 30 is an estrogen receptor in the plasma membrane. Biochem Biophys Res Commun, 346: 904-910.

65. Bologa CG, Revankar CM, Young SM, Edwards BS, Arterburn JB, Kiselyov AS, Parker MA, Tkachenko SE, Savchuck NP, Sklar LA, Oprea TI, Prossnitz ER. (2006) Virtual and biomolecular screening converge on a selective agonist for GPR30. Nat Chem Biol, 2: 207-212.

66. Drummond AE. (2006) The role of steroids in follicular growth. Reprod Biol Endocrinol, 4: 16.

67. Rosenfeld CS, Wagner JS, Roberts RM, Lubahn DB. (2001) Intraovarian actions of oestrogen. Reproduction, 122: 215-226.

68. Groothuis PG, Dassen HH, Romano A, Punyadeera C. (2007) Estrogen and the endometrium: lessons learned from gene expression profiling in rodents and human. Hum Reprod Update, 13: 405-417.

69. Paulson RJ. (2011) Hormonal induction of endometrial receptivity. Fertil Steril, 96: 530-535.

70. Shyamala G. (1997) Roles of estrogen and progesterone in normal mammary gland development insights from progesterone receptor null mutant mice and in situ localization of receptor. Trends Endocrinol Metab, 8: 34-39.

71. McLachlan JA, Newbold RR, Bullock B. (1975) Reproductive tract lesions in male mice exposed prenatally to diethylstilbestrol. Science, 190: 991-992.

72. Carreau S, Genissel C, Bilinska B, Levallet J. (1999) Sources of oestrogen in the testis and reproductive tract of the male. Int J Androl, 22: 211-223.

73. Nitta H, Bunick D, Hess RA, Janulis L, Newton SC, Millette CF, Osawa Y, Shizuta Y, Toda K, Bahr JM. (1993) Germ cells of the mouse testis express P450 aromatase. Endocrinology, 132: 1396-1401.

74. Tsai-Morris CH, Aquilano DR, Dufau ML. (1985) Cellular localization of rat testicular aromatase activity during development. Endocrinology, 116: 38-46.

75. Antal MC, Krust A, Chambon P, Mark M. (2008) Sterility and absence of histopathological defects in nonreproductive organs of a mouse ERbeta-null mutant. Proc Natl Acad Sci U S A, 105: 2433-2438.

76. Korach KS, Couse JF, Curtis SW, Washburn TF, Lindzey J, Kimbro KS, Eddy EM, Migliaccio S, Snedeker SM, Lubahn DB, Schomberg DW, Smith EP. (1996) Estrogen receptor gene disruption: molecular characterization and experimental and clinical phenotypes. Recent Prog Horm Res, 51: 159-186; discussion 186-158.

77. Lopez M, Tena-Sempere M. (2015) Estrogens and the control of energy homeostasis: a brain perspective. Trends Endocrinol Metab, 26: 411-421.

78. Mauvais-Jarvis F, Clegg DJ, Hevener AL. (2013) The role of estrogens in control of energy balance and glucose homeostasis. Endocr Rev, 34: 309-338.

79. Manolagas SC, O'Brien CA, Almeida M. (2013) The role of estrogen and androgen receptors in bone health and disease. Nat Rev Endocrinol, 9: 699-712.

80. Brincat MP, Baron YM, Galea R. (2005) Estrogens and the skin. Climacteric, 8: 110-123.

81. Mendelsohn ME, Karas RH. (1999) The protective effects of estrogen on the cardiovascular system. N Engl J Med, 340: 1801-1811.

82. Goodman RL, Lehman MN, Smith JT, Coolen LM, de Oliveira CV, Jafarzadehshirazi MR, Pereira A, Iqbal J, Caraty A, Ciofi P, Clarke IJ. (2007) Kisspeptin neurons in the arcuate nucleus of the ewe express both dynorphin A and neurokinin B. Endocrinology, 148: 5752-5760.

83. Foradori CD, Amstalden M, Goodman RL, Lehman MN. (2006) Colocalisation of dynorphin a and neurokinin B immunoreactivity in the arcuate nucleus and median eminence of the sheep. J Neuroendocrinol, 18: 534-541.

84. Burke MC, Letts PA, Krajewski SJ, Rance NE. (2006) Coexpression of dynorphin and neurokinin B immunoreactivity in the rat hypothalamus: Morphologic evidence of interrelated function within the arcuate nucleus. J Comp Neurol, 498: 712-726.

85. Cheng G, Coolen LM, Padmanabhan V, Goodman RL, Lehman MN. (2010) The kisspeptin/neurokinin B/dynorphin (KNDy) cell population of the arcuate nucleus: sex differences and effects of prenatal testosterone in sheep. Endocrinology, 151: 301-311.

86. Clarkson J, Han SY, Piet R, McLennan T, Kane GM, Ng J, Porteous RW, Kim JS, Colledge WH, Iremonger KJ, Herbison AE. (2017) Definition of the hypothalamic GnRH pulse generator in mice. Proc Natl Acad Sci U S A, 114: E10216-E10223.

87. Keen KL, Wegner FH, Bloom SR, Ghatei MA, Terasawa E. (2008) An increase in kisspeptin-54 release occurs with the pubertal increase in luteinizing hormone-releasing hormone-1 release in the stalk-median eminence of female rhesus monkeys in vivo. Endocrinology, 149: 4151-4157.

88. Rance NE. (2009) Menopause and the human hypothalamus: evidence for the role of kisspeptin/neurokinin B neurons in the regulation of estrogen negative feedback. Peptides, 30: 111-122.

89. Topaloglu AK, Reimann F, Guclu M, Yalin AS, Kotan LD, Porter KM, Serin A, Mungan NO, Cook JR, Imamoglu S, Akalin NS, Yuksel B, O'Rahilly S, Semple RK. (2009) TAC3 and TACR3 mutations in familial hypogonadotropic hypogonadism reveal a key role for Neurokinin B in the central control of reproduction. Nat Genet, 41: 354-358.

90. Smith JT, Clay CM, Caraty A, Clarke IJ. (2007) KiSS-1 messenger ribonucleic acid expression in the hypothalamus of the ewe is regulated by sex steroids and season. Endocrinology, 148: 1150-1157.

91. Rometo AM, Krajewski SJ, Voytko ML, Rance NE. (2007) Hypertrophy and increased kisspeptin gene expression in the hypothalamic infundibular nucleus of postmenopausal women and ovariectomized monkeys. J Clin Endocrinol Metab, 92: 2744-2750.

92. Smith JT, Cunningham MJ, Rissman EF, Clifton DK, Steiner RA. (2005) Regulation of Kiss1 gene expression in the brain of the female mouse. Endocrinology, 146: 3686-3692.

93. Rometo AM, Rance NE. (2008) Changes in prodynorphin gene expression and neuronal morphology in the hypothalamus of postmenopausal women. J Neuroendocrinol, 20: 1376-1381.

94. Rance NE, Young WS, 3rd. (1991) Hypertrophy and increased gene expression of neurons containing neurokinin-B and substance-P messenger ribonucleic acids in the hypothalami of postmenopausal women. Endocrinology, 128: 2239-2247.

95. Weems P, Smith J, Clarke IJ, Coolen LM, Goodman RL, Lehman MN. (2017) Effects of Season and Estradiol on KNDy Neuron Peptides, Colocalization With D2 Dopamine Receptors, and Dopaminergic Inputs in the Ewe. Endocrinology, 158: 831-841.

96. Gottsch ML, Navarro VM, Zhao Z, Glidewell-Kenney C, Weiss J, Jameson JL, Clifton DK, Levine JE, Steiner RA. (2009) Regulation of Kiss1 and dynorphin gene expression in the murine brain by classical and nonclassical estrogen receptor pathways. J Neurosci, 29: 9390-9395.

97.   Navarro VM, Gottsch ML, Chavkin C, Okamura H, Clifton DK, Steiner RA. (2009) Regulation of gonadotropin-releasing hormone secretion by kisspeptin/dynorphin/neurokinin B neurons in the arcuate nucleus of the mouse. J Neurosci, 29: 11859-11866.

98.   Moore AM, Coolen LM, Porter DT, Goodman RL, Lehman MN. (2018) KNDy Cells Revisited. Endocrinology, 159: 3219-3234.

99.   Wintermantel TM, Campbell RE, Porteous R, Bock D, Grone HJ, Todman MG, Korach KS, Greiner E, Perez CA, Schutz G, Herbison AE. (2006) Definition of estrogen receptor pathway critical for estrogen positive feedback to gonadotropin-releasing hormone neurons and fertility. Neuron, 52: 271-280.

100.   Dorling AA, Todman MG, Korach KS, Herbison AE. (2003) Critical role for estrogen receptor alpha in negative feedback regulation of gonadotropin-releasing hormone mRNA expression in the female mouse. Neuroendocrinology, 78: 204-209.

101.   Dupont S, Krust A, Gansmuller A, Dierich A, Chambon P, Mark M. (2000) Effect of single and compound knockouts of estrogen receptors alpha (ERalpha) and beta (ERbeta) on mouse reproductive phenotypes. Development, 127: 4277-4291.

102.   Yeo SH, Herbison AE. (2014) Estrogen-negative feedback and estrous cyclicity are critically dependent upon estrogen receptor-alpha expression in the arcuate nucleus of adult female mice. Endocrinology, 155: 2986-2995.

103.   Franceschini I, Lomet D, Cateau M, Delsol G, Tillet Y, Caraty A. (2006) Kisspeptin immunoreactive cells of the ovine preoptic area and arcuate nucleus co-express estrogen receptor alpha. Neurosci Lett, 401: 225-230.

104.   Smith JT, Dungan HM, Stoll EA, Gottsch ML, Braun RE, Eacker SM, Clifton DK, Steiner RA. (2005) Differential regulation of KiSS-1 mRNA expression by sex steroids in the brain of the male mouse. Endocrinology, 146: 2976-2984.

105.   Foradori CD, Coolen LM, Fitzgerald ME, Skinner DC, Goodman RL, Lehman MN. (2002) Colocalization of progesterone receptors in parvicellular dynorphin neurons of the ovine preoptic area and hypothalamus. Endocrinology, 143: 4366-4374.

106.   Goubillon ML, Forsdike RA, Robinson JE, Ciofi P, Caraty A, Herbison AE. (2000) Identification of neurokinin B-expressing neurons as an highly estrogen-

receptive, sexually dimorphic cell group in the ovine arcuate nucleus. Endocrinology, 141: 4218-4225.

107. Poling MC, Luo EY, Kauffman AS. (2017) Sex Differences in Steroid Receptor Coexpression and Circadian-Timed Activation of Kisspeptin and RFRP-3 Neurons May Contribute to the Sexually Dimorphic Basis of the LH Surge. Endocrinology, 158: 3565-3578.

108. Adachi S, Yamada S, Takatsu Y, Matsui H, Kinoshita M, Takase K, Sugiura H, Ohtaki T, Matsumoto H, Uenoyama Y, Tsukamura H, Inoue K, Maeda K. (2007) Involvement of anteroventral periventricular metastin/kisspeptin neurons in estrogen positive feedback action on luteinizing hormone release in female rats. J Reprod Dev, 53: 367-378.

109. Clarkson J, d'Anglemont de Tassigny X, Moreno AS, Colledge WH, Herbison AE. (2008) Kisspeptin-GPR54 signaling is essential for preovulatory gonadotropin-releasing hormone neuron activation and the luteinizing hormone surge. J Neurosci, 28: 8691-8697.

110. Smith JT, Popa SM, Clifton DK, Hoffman GE, Steiner RA. (2006) Kiss1 neurons in the forebrain as central processors for generating the preovulatory luteinizing hormone surge. J Neurosci, 26: 6687-6694.

111. Kauffman AS, Gottsch ML, Roa J, Byquist AC, Crown A, Clifton DK, Hoffman GE, Steiner RA, Tena-Sempere M. (2007) Sexual differentiation of Kiss1 gene expression in the brain of the rat. Endocrinology, 148: 1774-1783.

112. Dubois SL, Acosta-Martinez M, DeJoseph MR, Wolfe A, Radovick S, Boehm U, Urban JH, Levine JE. (2015) Positive, but not negative feedback actions of estradiol in adult female mice require estrogen receptor alpha in kisspeptin neurons. Endocrinology, 156: 1111-1120.

113. Wang L, Vanacker C, Burger LL, Barnes T, Shah YM, Myers MG, Moenter SM. (2019) Genetic dissection of the different roles of hypothalamic kisspeptin neurons in regulating female reproduction. Elife, 8.

114. Wang L, DeFazio RA, Moenter SM. (2016) Excitability and Burst Generation of AVPV Kisspeptin Neurons Are Regulated by the Estrous Cycle Via Multiple Conductances Modulated by Estradiol Action. eNeuro, 3.

115. Zhang C, Bosch MA, Qiu J, Ronnekleiv OK, Kelly MJ. (2015) 17beta-Estradiol increases persistent Na(+) current and excitability of AVPV/PeN Kiss1 neurons in female mice. Mol Endocrinol, 29: 518-527.

116. Piet R, Boehm U, Herbison AE. (2013) Estrous cycle plasticity in the hyperpolarization-activated current ih is mediated by circulating 17beta-estradiol in preoptic area kisspeptin neurons. J Neurosci, 33: 10828-10839.

117. Piet R, Kalil B, McLennan T, Porteous R, Czieselsky K, Herbison AE. (2018) Dominant Neuropeptide Cotransmission in Kisspeptin-GABA Regulation of GnRH Neuron Firing Driving Ovulation. J Neurosci, 38: 6310-6322.

118. Hrabovszky E, Steinhauser A, Barabas K, Shughrue PJ, Petersen SL, Merchenthaler I, Liposits Z. (2001) Estrogen receptor-beta immunoreactivity in luteinizing hormone-releasing hormone neurons of the rat brain. Endocrinology, 142: 3261-3264.

119. Hrabovszky E, Shughrue PJ, Merchenthaler I, Hajszan T, Carpenter CD, Liposits Z, Petersen SL. (2000) Detection of estrogen receptor-beta messenger ribonucleic acid and 125I-estrogen binding sites in luteinizing hormone-releasing hormone neurons of the rat brain. Endocrinology, 141: 3506-3509.

120. Hrabovszky E, Kallo I, Szlavik N, Keller E, Merchenthaler I, Liposits Z. (2007) Gonadotropin-releasing hormone neurons express estrogen receptor-beta. J Clin Endocrinol Metab, 92: 2827-2830.

121. Kauffman AS. (2022) Neuroendocrine mechanisms underlying estrogen positive feedback and the LH surge. Front Neurosci, 16: 953252.

122. Seminara SB, Messager S, Chatzidaki EE, Thresher RR, Acierno JS, Jr., Shagoury JK, Bo-Abbas Y, Kuohung W, Schwinof KM, Hendrick AG, Zahn D, Dixon J, Kaiser UB, Slaugenhaupt SA, Gusella JF, O'Rahilly S, Carlton MB, Crowley WF, Jr., Aparicio SA, Colledge WH. (2003) The GPR54 gene as a regulator of puberty. N Engl J Med, 349: 1614-1627.

123. de Roux N, Genin E, Carel JC, Matsuda F, Chaussain JL, Milgrom E. (2003) Hypogonadotropic hypogonadism due to loss of function of the KiSS1-derived peptide receptor GPR54. Proc Natl Acad Sci U S A, 100: 10972-10976.

124. d'Anglemont de Tassigny X, Fagg LA, Dixon JP, Day K, Leitch HG, Hendrick AG, Zahn D, Franceschini I, Caraty A, Carlton MB, Aparicio SA, Colledge WH.

(2007) Hypogonadotropic hypogonadism in mice lacking a functional Kiss1 gene. Proc Natl Acad Sci U S A, 104: 10714-10719.

125. Xie Q, Kang Y, Zhang C, Xie Y, Wang C, Liu J, Yu C, Zhao H, Huang D. (2022) The Role of Kisspeptin in the Control of the Hypothalamic-Pituitary-Gonadal Axis and Reproduction. Front Endocrinol (Lausanne), 13: 925206.

126. West A, Vojta PJ, Welch DR, Weissman BE. (1998) Chromosome localization and genomic structure of the KiSS-1 metastasis suppressor gene (KISS1). Genomics, 54: 145-148.

127. Bilban M, Ghaffari-Tabrizi N, Hintermann E, Bauer S, Molzer S, Zoratti C, Malli R, Sharabi A, Hiden U, Graier W, Knofler M, Andreae F, Wagner O, Quaranta V, Desoye G. (2004) Kisspeptin-10, a KiSS-1/metastin-derived decapeptide, is a physiological invasion inhibitor of primary human trophoblasts. J Cell Sci, 117: 1319-1328.

128. Kotani M, Detheux M, Vandenbogaerde A, Communi D, Vanderwinden JM, Le Poul E, Brezillon S, Tyldesley R, Suarez-Huerta N, Vandeput F, Blanpain C, Schiffmann SN, Vassart G, Parmentier M. (2001) The metastasis suppressor gene KiSS-1 encodes kisspeptins, the natural ligands of the orphan G protein-coupled receptor GPR54. J Biol Chem, 276: 34631-34636.

129. Lee DK, Nguyen T, O'Neill GP, Cheng R, Liu Y, Howard AD, Coulombe N, Tan CP, Tang-Nguyen AT, George SR, O'Dowd BF. (1999) Discovery of a receptor related to the galanin receptors. FEBS Lett, 446: 103-107.

130. Pinilla L, Aguilar E, Dieguez C, Millar RP, Tena-Sempere M. (2012) Kisspeptins and reproduction: physiological roles and regulatory mechanisms. Physiol Rev, 92: 1235-1316.

131. Ohtaki T, Shintani Y, Honda S, Matsumoto H, Hori A, Kanehashi K, Terao Y, Kumano S, Takatsu Y, Masuda Y, Ishibashi Y, Watanabe T, Asada M, Yamada T, Suenaga M, Kitada C, Usuki S, Kurokawa T, Onda H, Nishimura O, Fujino M. (2001) Metastasis suppressor gene KiSS-1 encodes peptide ligand of a G-protein-coupled receptor. Nature, 411: 613-617.

132. Muir AI, Chamberlain L, Elshourbagy NA, Michalovich D, Moore DJ, Calamari A, Szekeres PG, Sarau HM, Chambers JK, Murdock P, Steplewski K, Shabon U, Miller JE, Middleton SE, Darker JG, Larminie CG, Wilson S, Bergsma DJ, Emson

P, Faull R, Philpott KL, Harrison DC. (2001) AXOR12, a novel human G protein-coupled receptor, activated by the peptide KiSS-1. J Biol Chem, 276: 28969-28975.

133. Herbison AE, de Tassigny X, Doran J, Colledge WH. (2010) Distribution and postnatal development of Gpr54 gene expression in mouse brain and gonadotropin-releasing hormone neurons. Endocrinology, 151: 312-321.

134. Han SK, Gottsch ML, Lee KJ, Popa SM, Smith JT, Jakawich SK, Clifton DK, Steiner RA, Herbison AE. (2005) Activation of gonadotropin-releasing hormone neurons by kisspeptin as a neuroendocrine switch for the onset of puberty. J Neurosci, 25: 11349-11356.

135. Babwah AV. (2020) The wonderful and masterful G protein-coupled receptor (GPCR): A focus on signaling mechanisms and the neuroendocrine control of fertility. Mol Cell Endocrinol, 515: 110886.

136. d'Anglemont de Tassigny X, Colledge WH. (2010) The role of kisspeptin signaling in reproduction. Physiology (Bethesda), 25: 207-217.

137. Hu KL, Zhao H, Chang HM, Yu Y, Qiao J. (2017) Kisspeptin/Kisspeptin Receptor System in the Ovary. Front Endocrinol (Lausanne), 8: 365.

138. Castano JP, Martinez-Fuentes AJ, Gutierrez-Pascual E, Vaudry H, Tena-Sempere M, Malagon MM. (2009) Intracellular signaling pathways activated by kisspeptins through GPR54: do multiple signals underlie function diversity? Peptides, 30: 10-15.

139. Liu X, Lee K, Herbison AE. (2008) Kisspeptin excites gonadotropin-releasing hormone neurons through a phospholipase C/calcium-dependent pathway regulating multiple ion channels. Endocrinology, 149: 4605-4614.

140. Kallo I, Vida B, Deli L, Molnar CS, Hrabovszky E, Caraty A, Ciofi P, Coen CW, Liposits Z. (2012) Co-localisation of kisspeptin with galanin or neurokinin B in afferents to mouse GnRH neurones. J Neuroendocrinol, 24: 464-476.

141. Bhattacharya M, Babwah AV. (2015) Kisspeptin: beyond the brain. Endocrinology, 156: 1218-1227.

142. Lehman MN, Hileman SM, Goodman RL. (2013) Neuroanatomy of the kisspeptin signaling system in mammals: comparative and developmental aspects. Adv Exp Med Biol, 784: 27-62.

143. Gocz B, Rumpler E, Sarvari M, Skrapits K, Takacs S, Farkas I, Csillag V, Trinh SH, Bardoczi Z, Ruska Y, Solymosi N, Poliska S, Szoke Z, Bartoloni L, Zouaghi Y, Messina A, Pitteloud N, Anderson RC, Millar RP, Quinton R, Manchishi SM, Colledge WH, Hrabovszky E. (2022) Transcriptome profiling of kisspeptin neurons from the mouse arcuate nucleus reveals new mechanisms in estrogenic control of fertility. Proc Natl Acad Sci U S A, 119: e2113749119.

144. Khodosevich K, Inta D, Seeburg PH, Monyer H. (2007) Gene expression analysis of in vivo fluorescent cells. PLoS One, 2: e1151.

145. Vastagh C, Csillag V, Solymosi N, Farkas I, Liposits Z. (2020) Gonadal Cycle-Dependent Expression of Genes Encoding Peptide-, Growth Factor-, and Orphan G-Protein-Coupled Receptors in Gonadotropin- Releasing Hormone Neurons of Mice. Front Mol Neurosci, 13: 594119.

146. Groelz D, Sobin L, Branton P, Compton C, Wyrich R, Rainen L. (2013) Non-formalin fixative versus formalin-fixed tissue: a comparison of histology and RNA quality. Exp Mol Pathol, 94: 188-194.

147. Adiconis X, Borges-Rivera D, Satija R, DeLuca DS, Busby MA, Berlin AM, Sivachenko A, Thompson DA, Wysoker A, Fennell T, Gnirke A, Pochet N, Regev A, Levin JZ. (2013) Comparative analysis of RNA sequencing methods for degraded or low-input samples. Nat Methods, 10: 623-629.

148. Schuierer S, Carbone W, Knehr J, Petitjean V, Fernandez A, Sultan M, Roma G. (2017) A comprehensive assessment of RNA-seq protocols for degraded and low-quantity samples. BMC Genomics, 18: 442.

149. Skrapits K, Sarvari M, Farkas I, Gocz B, Takacs S, Rumpler E, Vaczi V, Vastagh C, Racz G, Matolcsy A, Solymosi N, Poliska S, Toth B, Erdelyi F, Szabo G, Culler MD, Allet C, Cotellessa L, Prevot V, Giacobini P, Hrabovszky E. (2021) The cryptic gonadotropin-releasing hormone neuronal system of human basal ganglia. Elife, 10.

150. Messager S, Chatzidaki EE, Ma D, Hendrick AG, Zahn D, Dixon J, Thresher RR, Malinge I, Lomet D, Carlton MB, Colledge WH, Caraty A, Aparicio SA. (2005) Kisspeptin directly stimulates gonadotropin-releasing hormone release via G protein-coupled receptor 54. Proc Natl Acad Sci U S A, 102: 1761-1766.

151. Yeo SH, Kyle V, Morris PG, Jackman S, Sinnett-Smith LC, Schacker M, Chen C, Colledge WH. (2016) Visualisation of Kiss1 Neurone Distribution Using a Kiss1-CRE Transgenic Mouse. J Neuroendocrinol, 28.

152. Molnar CS, Kallo I, Liposits Z, Hrabovszky E. (2011) Estradiol down-regulates RF-amide-related peptide (RFRP) expression in the mouse hypothalamus. Endocrinology, 152: 1684-1690.

153. Haisenleder DJ, Schoenfelder AH, Marcinko ES, Geddis LM, Marshall JC. (2011) Estimation of estradiol in mouse serum samples: evaluation of commercial estradiol immunoassays. Endocrinology, 152: 4443-4447.

154. Paxinos G, Franklin KBJ. (szerk.) The mouse brain in stereotaxic coordinates. Academic Press 2001.

155. Dobin A, Davis CA, Schlesinger F, Drenkow J, Zaleski C, Jha S, Batut P, Chaisson M, Gingeras TR. (2013) STAR: ultrafast universal RNA-seq aligner. Bioinformatics, 29: 15-21.

156. Liao Y, Smyth GK, Shi W. (2014) featureCounts: an efficient general purpose program for assigning sequence reads to genomic features. Bioinformatics, 30: 923-930.

157. McCarthy DJ, Chen Y, Smyth GK. (2012) Differential expression analysis of multifactor RNA-Seq experiments with respect to biological variation. Nucleic Acids Res, 40: 4288-4297.

158. Love MI, Huber W, Anders S. (2014) Moderated estimation of fold change and dispersion for RNA-seq data with DESeq2. Genome Biol, 15: 550.

159. Benjamini Y, Drai D, Elmer G, Kafkafi N, Golani I. (2001) Controlling the false discovery rate in behavior genetics research. Behav Brain Res, 125: 279-284.

160. Thomas PD, Campbell MJ, Kejariwal A, Mi H, Karlak B, Daverman R, Diemer K, Muruganujan A, Narechania A. (2003) PANTHER: a library of protein families and subfamilies indexed by function. Genome Res, 13: 2129-2141.

161. Kanehisa M, Goto S. (2000) KEGG: kyoto encyclopedia of genes and genomes. Nucleic Acids Res, 28: 27-30.

162. Tavazoie S, Hughes JD, Campbell MJ, Cho RJ, Church GM. (1999) Systematic determination of genetic network architecture. Nat Genet, 22: 281-285.

163. Tarca AL, Draghici S, Khatri P, Hassan SS, Mittal P, Kim JS, Kim CJ, Kusanovic JP, Romero R. (2009) A novel signaling pathway impact analysis. Bioinformatics, 25: 75-82.

164. Wu T, Hu E, Xu S, Chen M, Guo P, Dai Z, Feng T, Zhou L, Tang W, Zhan L, Fu X, Liu S, Bo X, Yu G. (2021) clusterProfiler 4.0: A universal enrichment tool for interpreting omics data. Innovation (N Y), 2: 100141.

165. Ihnatova I, Budinska E. (2015) ToPASeq: an R package for topology-based pathway analysis of microarray and RNA-Seq data. BMC Bioinformatics, 16: 350.

166. Ensembl Biomart data mining tool. https://www.ensembl.org/biomart/martview/3d4a18a75708600d72c27f17310f9873

167. Neuropeptide database. http://neuropeptides.nl

168. Transcription factor database. http://genome.gsc.riken.jp/TFdb/cdimage/htdocs/tf_list.html

169. Gene Ontology database. http://geneontology.org/

170. Wihan J, Grosch J, Kalinichenko LS, Muller CP, Winkler J, Kohl Z. (2019) Layer-specific axonal degeneration of serotonergic fibers in the prefrontal cortex of aged A53T alpha-synuclein-expressing mice. Neurobiol Aging, 80: 29-37.

171. Hrabovszky E, Molnar CS, Borsay BA, Gergely P, Herczeg L, Liposits Z. (2013) Orexinergic input to dopaminergic neurons of the human ventral tegmental area. PLoS One, 8: e83029.

172. Deurveilher S, Lo H, Murphy JA, Burns J, Semba K. (2006) Differential c-Fos immunoreactivity in arousal-promoting cell groups following systemic administration of caffeine in rats. J Comp Neurol, 498: 667-689.

173. Ciofi P, Leroy D, Tramu G. (2006) Sexual dimorphism in the organization of the rat hypothalamic infundibular area. Neuroscience, 141: 1731-1745.

174. Skrapits K, Borsay BA, Herczeg L, Ciofi P, Liposits Z, Hrabovszky E. (2015) Neuropeptide co-expression in hypothalamic kisspeptin neurons of laboratory animals and the human. Front Neurosci, 9: 29.

175. Wittmann G, Liposits Z, Lechan RM, Fekete C. (2002) Medullary adrenergic neurons contribute to the neuropeptide Y-ergic innervation of hypophysiotropic

thyrotropin-releasing hormone-synthesizing neurons in the rat. Neurosci Lett, 324: 69-73.

176. Turi GF, Liposits Z, Moenter SM, Fekete C, Hrabovszky E. (2003) Origin of neuropeptide Y-containing afferents to gonadotropin-releasing hormone neurons in male mice. Endocrinology, 144: 4967-4974.

177. Varga E, Farkas E, Zseli G, Kadar A, Venczel A, Kovari D, Nemeth D, Mate Z, Erdelyi F, Horvath A, Szenci O, Watanabe M, Lechan RM, Gereben B, Fekete C. (2019) Thyrotropin-Releasing-Hormone-Synthesizing Neurons of the Hypothalamic Paraventricular Nucleus Are Inhibited by Glycinergic Inputs. Thyroid, 29: 1858-1868.

178. Sugiuar T, Bielefeldt K, Gebhart GF. (2004) TRPV1 function in mouse colon sensory neurons is enhanced by metabotropic 5-hydroxytryptamine receptor activation. J Neurosci, 24: 9521-9530.

179. Farkas I, Balint F, Farkas E, Vastagh C, Fekete C, Liposits Z. (2018) Estradiol Increases Glutamate and GABA Neurotransmission into GnRH Neurons via Retrograde NO-Signaling in Proestrous Mice during the Positive Estradiol Feedback Period. eNeuro, 5.

180. Farkas I, Vastagh C, Farkas E, Balint F, Skrapits K, Hrabovszky E, Fekete C, Liposits Z. (2016) Glucagon-Like Peptide-1 Excites Firing and Increases GABAergic Miniature Postsynaptic Currents (mPSCs) in Gonadotropin-Releasing Hormone (GnRH) Neurons of the Male Mice via Activation of Nitric Oxide (NO) and Suppression of Endocannabinoid Signaling Pathways. Front Cell Neurosci, 10: 214.

181. DeFazio RA, Navarro MA, Adams CE, Milescu LS, Moenter SM. (2019) Estradiol Enhances the Depolarizing Response to GABA and AMPA Synaptic Conductances in Arcuate Kisspeptin Neurons by Diminishing Voltage-Gated Potassium Currents. J Neurosci, 39: 9532-9545.

182. Messina A, Pulli K, Santini S, Acierno J, Kansakoski J, Cassatella D, Xu C, Casoni F, Malone SA, Ternier G, Conte D, Sidis Y, Tommiska J, Vaaralahti K, Dwyer A, Gothilf Y, Merlo GR, Santoni F, Niederlander NJ, Giacobini P, Raivio T, Pitteloud N. (2020) Neuron-Derived Neurotrophic Factor Is Mutated in Congenital Hypogonadotropic Hypogonadism. Am J Hum Genet, 106: 58-70.

183. Bouilly J, Messina A, Papadakis G, Cassatella D, Xu C, Acierno JS, Tata B, Sykiotis G, Santini S, Sidis Y, Elowe-Gruau E, Phan-Hug F, Hauschild M, Bouloux PM, Quinton R, Lang-Muritano M, Favre L, Marino L, Giacobini P, Dwyer AA, Niederlander NJ, Pitteloud N. (2018) DCC/NTN1 complex mutations in patients with congenital hypogonadotropic hypogonadism impair GnRH neuron development. Hum Mol Genet, 27: 359-372.

184. Nilsson ME, Vandenput L, Tivesten A, Norlen AK, Lagerquist MK, Windahl SH, Borjesson AE, Farman HH, Poutanen M, Benrick A, Maliqueo M, Stener-Victorin E, Ryberg H, Ohlsson C. (2015) Measurement of a Comprehensive Sex Steroid Profile in Rodent Serum by High-Sensitive Gas Chromatography-Tandem Mass Spectrometry. Endocrinology, 156: 2492-2502.

185. Campbell JN, Macosko EZ, Fenselau H, Pers TH, Lyubetskaya A, Tenen D, Goldman M, Verstegen AM, Resch JM, McCarroll SA, Rosen ED, Lowell BB, Tsai LT. (2017) A molecular census of arcuate hypothalamus and median eminence cell types. Nat Neurosci, 20: 484-496.

186. Chen R, Wu X, Jiang L, Zhang Y. (2017) Single-Cell RNA-Seq Reveals Hypothalamic Cell Diversity. Cell Rep, 18: 3227-3241.

187. Sullivan SD, Howard LC, Clayton AH, Moenter SM. (2002) Serotonergic activation rescues reproductive function in fasted mice: does serotonin mediate the metabolic effects of leptin on reproduction? Biol Reprod, 66: 1702-1706.

188. Vitale ML, Chiocchio SR. (1993) Serotonin, a neurotransmitter involved in the regulation of luteinizing hormone release. Endocr Rev, 14: 480-493.

189. de Croft S, Piet R, Mayer C, Mai O, Boehm U, Herbison AE. (2012) Spontaneous kisspeptin neuron firing in the adult mouse reveals marked sex and brain region differences but no support for a direct role in negative feedback. Endocrinology, 153: 5384-5393.

190. Mammalian Phenotype Browser. http://www.informatics.jax.org/vocab/mp_ontology

191. Human Phenotype Ontology. https://www.ebi.ac.uk/ols/ontologies/hp

192. Bourgon R, Gentleman R, Huber W. (2010) Independent filtering increases detection power for high-throughput experiments. Proc Natl Acad Sci U S A, 107: 9546-9551.

193. Sha Y, Phan JH, Wang MD. (2015) Effect of low-expression gene filtering on detection of differentially expressed genes in RNA-seq data. Annu Int Conf IEEE Eng Med Biol Soc, 2015: 6461-6464.

194. Bi M, Zhang Z, Jiang YZ, Xue P, Wang H, Lai Z, Fu X, De Angelis C, Gong Y, Gao Z, Ruan J, Jin VX, Marangoni E, Montaudon E, Glass CK, Li W, Huang TH, Shao ZM, Schiff R, Chen L, Liu Z. (2020) Enhancer reprogramming driven by high-order assemblies of transcription factors promotes phenotypic plasticity and breast cancer endocrine resistance. Nat Cell Biol, 22: 701-715.

195. Szklarczyk D, Gable AL, Nastou KC, Lyon D, Kirsch R, Pyysalo S, Doncheva NT, Legeay M, Fang T, Bork P, Jensen LJ, von Mering C. (2021) The STRING database in 2021: customizable protein-protein networks, and functional characterization of user-uploaded gene/measurement sets. Nucleic Acids Res, 49: D605-D612.

196. Yang JA, Stires H, Belden WJ, Roepke TA. (2017) The Arcuate Estrogen-Regulated Transcriptome: Estrogen Response Element-Dependent and -Independent Signaling of ERalpha in Female Mice. Endocrinology, 158: 612-626.

197. Mahmoudi F, Haghighat Gollo K. (2020) Influences of Serotonin Hydrochloride on Adiponectin, Ghrelin and KiSS1 Genes Expression. Galen Med J, 9: e1767.

198. Rance NE, Dacks PA, Mittelman-Smith MA, Romanovsky AA, Krajewski-Hall SJ. (2013) Modulation of body temperature and LH secretion by hypothalamic KNDy (kisspeptin, neurokinin B and dynorphin) neurons: a novel hypothesis on the mechanism of hot flushes. Front Neuroendocrinol, 34: 211-227.

199. Nelson HD, Vesco KK, Haney E, Fu R, Nedrow A, Miller J, Nicolaidis C, Walker M, Humphrey L. (2006) Nonhormonal therapies for menopausal hot flashes: systematic review and meta-analysis. JAMA, 295: 2057-2071.

200. Boughton CK, Patel SA, Thompson EL, Patterson M, Curtis AE, Amin A, Chen K, Ghatei MA, Bloom SR, Murphy KG. (2013) Neuromedin B stimulates the hypothalamic-pituitary-gonadal axis in male rats. Regul Pept, 187: 6-11.

201. Todman MG, Han SK, Herbison AE. (2005) Profiling neurotransmitter receptor expression in mouse gonadotropin-releasing hormone neurons using green fluorescent protein-promoter transgenics and microarrays. Neuroscience, 132: 703-712.

202. Dungan Lemko HM, Naderi R, Adjan V, Jennes LH, Navarro VM, Clifton DK, Steiner RA. (2010) Interactions between neurotensin and GnRH neurons in the positive feedback control of GnRH/LH secretion in the mouse. Am J Physiol Endocrinol Metab, 298: E80-88.

203. Porteous R, Petersen SL, Yeo SH, Bhattarai JP, Ciofi P, de Tassigny XD, Colledge WH, Caraty A, Herbison AE. (2011) Kisspeptin neurons co-express met-enkephalin and galanin in the rostral periventricular region of the female mouse hypothalamus. J Comp Neurol, 519: 3456-3469.

204. Kim T, Gondre-Lewis MC, Arnaoutova I, Loh YP. (2006) Dense-core secretory granule biogenesis. Physiology (Bethesda), 21: 124-133.

205. Harashima S, Clark A, Christie MR, Notkins AL. (2005) The dense core transmembrane vesicle protein IA-2 is a regulator of vesicle number and insulin secretion. Proc Natl Acad Sci U S A, 102: 8704-8709.

206. Stephens SBZ, Kauffman AS. (2021) Estrogen Regulation of the Molecular Phenotype and Active Translatome of AVPV Kisspeptin Neurons. Endocrinology, 162.

10. Bibliography of the candidate's

Publications related to the PhD thesis

Journal articles:

1. **Göcz B.**, Rumpler É., Sárvári M., Skrapits K., Takács S., Farkas I., Csillag V., Trinh S.H., Bardóczi Z., Ruska Y., Solymosi N., Póliska S., Szőke Z., Bartoloni L., Zouaghi Y., Messina A., Pitteloud N., Anderson R.C., Millar R.P., Quinton R., Manchishi S.M., Colledge W.H. and Hrabovszky E. (2022) Transcriptome profiling of kisspeptin neurons from the mouse arcuate nucleus reveals new mechanisms in estrogenic control of fertility. Proc Natl Acad Sci U S A 2022 Jul 5;119(27):e2113749119. doi: 10.1073/pnas.2113749119. (**IF.: 12.779**)

2. **Göcz B.**, Takács S., Skrapits K., Rumpler É., Solymosi N., Póliska S., Colledge W.H., Hrabovszky E. and Sárvári M. (2022) Estrogen Differentially Regulates Transcriptional Landscapes of Arcuate and Preoptic Kisspeptin Neuron Populations. Frontiers in Endocrinology: 2022.960769 (**IF.: 6.055**)

Publications not related to the PhD thesis

Journal articles:

1. Takács S., Bardóczi Z., Skrapits K., **Göcz B.**, Váczi V., Maglóczky Z., Szűcs I., Rácz G., Matolcsy A., Dhillo W.S., Watanabe M., Kádár A., Fekete C., Kalló I. and Hrabovszky E (2018) Post mortem single-cell labeling with DiI and immunoelectron microscopy unveil the fine structure of kisspeptin neurons in humans. Brain Structure and Function: 223(5): 2143-2156 (**IF.: 3.622**)

2. Hrabovszky E., Takács S., **Göcz B.**, Skrapits K. (2019) New perspectives for anatomical and molecular studies of kisspeptin neurons in the aging human brain. Neuroendocrinology: 109(3):230-241 (**IF.: 4.271**)

3. Rumpler É., Takács S., **Göcz B.**, Baska F., Szenci O., Horváth A., Ciofi P., Hrabovszky E. and Skrapits K. (2020) Kisspeptin neurons in the infundibular nucleus of ovariectomized cats and dogs exhibit unique anatomical and neurochemical characteristics. Frontiers in Neuroscience doi: 10.3389/fnins.2020.598707 (**IF.: 4.677**)

4. Rumpler É., Skrapits K, Takács S, **Göcz B.**, Trinh S.H., Rácz G., Matolcsy A., Kozma Z., Ciofi P., Dhillo W.S., Hrabovszky E. (2021) Characterization of kisspeptin neurons in the human rostral hypothalamus. Neuroendocrinology: 111(3):249-262. (**IF.: 5.135**)

5. Skrapits K., Sárvári M., Farkas I., **Göcz B.**, Takács S., Rumpler É., Váczi V., Vastagh C., Rácz G., Matolcsy A., Solymosi N., Póliska S., Tóth B., Erdélyi F., Szabó G., Culler, M.D., Allet C., Cotellessa L., Prévot V., Giacobini P. and Hrabovszky E. (2021) The cryptic gonadotropin-releasing hormone neuronal system of human basal ganglia, Elife: 10:e67714 (**IF.: 8.713**)

11. Acknowledgements

First of all, I would like to express my sincere gratitude and deep appreciation to my supervisor, Erik Hrabovszky, for his unwavering support throughout my Ph.D. studies and related research. In addition to my supervisor, I would also like to thank Eva, Rumpler, Katalin Skrapits, and Szabolcs Takács for their invaluable assistance.